RIO

PUC

Tese de Doutorado

Interrelationship among soil organic carbon stock, physicochemical, mineralogical, and hydraulic properties in urban environment

Melissa Casacchi Antunes

Pontifícia Universidade Católica do Rio de Janeiro

Centro Técnico Científico

Departamento de Engenharia Civil e Ambiental

Rio de Janeiro, 24 de setembro de 2025

Pontifícia
Universidade
Católica do
Rio de Janeiro

Interrelationship among soil organic carbon stock, physicochemical, mineralogical and hydraulic properties in urban environment

Melissa Casacchi Antunes

Orientador: Profesor José Tavares Araruna Junior
Co-orientador: Professor Tácio Mauro Pereira de Campos

Tese apresentada como requisito parcial para obtenção do grau de Doutora pelo Programa de Pós-graduação em Engenharia Civil do Departamento de Engenharia Civil e Ambiental da PUC-RIO.

Rio de Janeiro, 24 de setembro de 2025

Pontifícia
Universidade
Católica do
Rio de Janeiro

Interrelationship among soil organic carbon stock, physicochemical, mineralogical and hydraulic properties in urban environment

Melissa Casacchi Antunes

Tese apresentada como requisito parcial para obtenção do grau de Doutora pelo Programa de Pós-graduação em Engenharia Civil do Departamento de Engenharia Civil e Ambiental da PUC-RIO.

Professor Prof. José Tavares Araruna Junior
Orientador
PUC-Rio - Departamento de Engenharia Civil e Ambiental

Professor Tácio Mauro Pereira de Campos
Co-orientador
PUC-Rio - Departamento de Engenharia Civil e Ambiental

Professor Bruna de Carvalho Faria Lima Lopes
PUC-Rio - Departamento de Engenharia Civil e Ambiental

Professor Maria Rafaela Pinheiro Cardoso
ULisboa

Professor Richieri Antônio Sartori
PUC-Rio – Departamento de Biologia

Professor Wenceslau Geraldes Teixeira
Centro Nacional de Pesquisa de Solos

Rio de Janeiro, 24 de setembro de 2025

Pontifícia
Universidade
Católica do
Rio de Janeiro

Melissa Casacchi Antunes
Graduada em Engenharia Civil pela Universidade Estadual de Maringá – Paraná e Mestre em Engenharia Urbana e Ambiental pela Pontifícia Universidade Católica do Rio de Janeiro.

Ficha Catalográfica

Antunes, Melissa Casacchi

Interrelationship among soil organic carbon stock, physicochemical, mineralogical and hydraulic properties in urban environment / Melissa Casacchi Antunes; advisor: José Tavares Araruna Junior; Co-advisor: Tácio Mauro Pereira de Campos. – 2025.
147 f. ; 30 cm

Tese (doutorado)–Pontifícia Universidade Católica do Rio de Janeiro, Departamento de Engenharia Civil e Ambiental, 2025.

Inclui bibliografia

1. Engenharia Civil e Ambiental - Teses. 2. Solos urbanos. 3. Propriedades do solo. 4. Geotecnia. 5. Estabilização da matéria orgânica no solo. 6. Fracionamento da matéria orgânica. I. Araruna Junior, José Tavares. II. Campos, Tácio Mauro Pereira de. III. Pontifícia Universidade Católica do Rio de Janeiro. Departamento de Engenharia Civil e Ambiental. IV. Título.

CDD: 624

To my daughter and my husband, for their encouragement, tolerance and respect.

Acknowledge

This study was financed in part by the Coordenação de Aperfeiçoamento de Pessoal de Nível Superior - Brasil (CAPES) - Finance Code 001.

I want to express my sincere gratitude to Professor Tácio Mauro Pereira de Campos, whose scientific guidance and encouragement during the most challenging phases were truly invaluable.

I would like to thank my advisor, Professor José Arurana, for introducing me to this innovative research topic and for your guidance and contributions throughout the entire study.

I would like to express my heartfelt thanks to the team of the Laboratory of Environment and Geotechnics, Edson, Amaury, Josué, Carlos, Rogério and Sandra, whose support was indispensable to the completion of this work.

I would also like to thank all the staff and professors of the Civil and Environmental Engineering Department, whose support was also fundamental to overcoming this journey.

I would like to acknowledge the partnership and valuable work of the professors and technicians of the Chemistry Laboratory: Renato, Lilian, Fran Godoy, Rodrigo, Maurício, Sonia and Henrique.

I would also like to express my gratitude to my family and friends for their encouragement, patience and support in my personal life.

Special thanks to my dearest colleagues in this journey, Barbara, Alejandra, Lucas, Vitor, Elaine and Talita.

Abstract

Antunes, Melissa Casacchi; Araruna, Junior Jose Tavares (advisor). **Interrelationship among soil organic carbon stock, physicochemical, mineralogical and hydraulic properties in urban environment.** Rio de Janeiro, 2025. 147 p. Doctoral thesis. Postgraduate Program in Civil and Engineering, Pontifical Catholic University of Rio de Janeiro.

Soil is at the center of ecological solutions. Soil organic carbon stock (*Cstock*) is the indicator used to assess soil degradation and to monitor restoration. This study determined the *Cstock* and investigated its interrelations with soil's physicochemical, hydraulic and mineralogical properties across three classes of land use and cover in the city of Rio de Janeiro: non-native vegetation forest (NNF), dense ombrophylous forest in the initial stage (FIS), and bare soil fill (BSF). The investigation was conducted in 20 cm sections of a 1 m deep soil profile.

The *Cstocks* within the 1 m deep profile in the NNF and FIS areas are similar and nearly 38% higher than in the BSF area. In contrast, the BSF presented a higher *Cstock* in the subsoil. However, the NNF area exhibited higher stock in the persistent form of soil organic matter (*MCstock*). The values of soil dry bulk density have a high influence on the *Cstock* and must be carefully determined in highly heterogeneous urban soil profiles. Soil properties presented similarities and dissimilarities between soil profiles; however, statistical analysis revealed significant differences among the three areas studied. Correlations between *Cstock* and geotechnical parameters did not present strong significance when considering all profiles, although they were representative in more homogenous material. Further investigation is required to increase the statistical dataset and confirm correlations. At the end, it is shown that the soil physicochemical, mineralogical and hydraulic characteristics of each land use and cover class in Rio de Janeiro may affect their potential for *Cstock.*

Keywords

Urban soil, soil properties, geotechnics, SOM stabilization, SOM fractions

Resumo

Antunes, Melissa Casacchi; Araruna, Junior José Tavares (orientador). **Interações entre estoque de carbono orgânico, propriedades físico-químicas, mineralógicas e hidráulicas do solo em ambiente urbano.** Rio de Janeiro, 2025. 147 p. Tese de doutorado. Programa de pós-graduação em engenharia civil. Pontifícia Universidade Católica do Rio de Janeiro.

O solo está no centro das soluções ecológicas. O estoque de carbono orgânico do solo (*Cstock*) é um indicador utilizado para investigar solos degradados e monitorar a restauração. Este estudo determinou o *Cstock* e investigou suas interações com propriedades físico-químicas, hidráulicas e mineralógicas do solo em três classes de uso e cobertura do solo na cidade do Rio de Janeiro: floresta com vegetação não nativa (NNF), floresta ombrófila densa em estágio inicial (FIS) e aterro de solo exposto (BSF). As investigações foram realizadas em seções de 20 cm até 1 m de profundidade. Os *Cstocks* nos perfis até 1 metro de profundidade nas áreas NNF e FIS são semelhantes e cerca de 38% maiores do que na área BSF. Em contraste, a área BSF apresentou maior *Cstock* no subsolo. Contudo, a área NNF exibiu maior estoque na forma persistente da matéria orgânica (*MCstock*). A densidade do solo tem grande influência no *Cstock* e deve ser cuidadosamente determinada em perfis de solo urbano altamente heterogêneos. Os perfis de solo apresentaram similaridades e dissimilaridades entre as propriedades do solo, contudo, a análise estatística revelou diferenças significativas entre as três áreas estudadas. As correlações entre o *Cstock* e os parâmetros geotécnicos foram representativas considerando materiais mais homogêneos. No entanto, é necessário ampliar o conjunto de dados estatísticos para confirmar as correlações. Por fim, o estudo mostra que as propriedades do solo de cada classe de uso e cobertura afeta seu potencial para sequestro de carbono.

Palavras-chave

Solos urbanos, propriedades do solo, geotecnia, estabilização da matéria orgânica no solo, fracionamento da matéria orgânica.

Summary

Symbols and Abbreviations

Ac	Activity index
Al	Aluminum
Aw	Tropical with a dry winter climate
Cstock	Soil organic carbon stock
CV	Coefficient of variation
CV_c	Combined coefficient of variation
e	Void ratio
EC	Electrical conductivity
Fe	Iron
Fsp	Feldspar
IP	Plasticity Index
K	Potassium
Kln	Kaolinite
MCstock	Carbon stock in the mineral-associated organic matter fraction
MAOM	Mineral-associated organic matter
MOC	Soil organic carbon in the mineral-associated organic matter
Mg	Magnesium
Mn	Manganese
OC	Organic carbon
OxOH	Oxy hydroxides
PCstock	Carbon stock in the particulate organic matter fraction
POC	Soil organic carbon in the particulate organic matter
POM	Particulate organic matter
Qz	Quartz
TC	Total carbon
SOC	Soil organic carbon
SOM	Soil organic matter
w	Gravimetric moisture
w_L	Liquid limit
w_p	Plasticity limit
ρ_d	Soil dry density
ρ_{dfe}	Soil dry density in the fine earth ($\phi < 2mm$)
ρ_s	Specific mass of solids
ρ_t	Soil total density

List of Figures

List of Tables

1. Introduction

The impact of anthropic activities on the environment is an urgent issue in science. The damage to natural ecosystems and the greenhouse gas emissions (GHG) have a detrimental effect on the balance of the Carbon (C) biogeochemical cycle (IPCC, 2023).

Carbon is divided into five carbon planet pools: oceanic, geologic, atmospheric, biotic and pedologic, which exchange C between them through balanced C fluxes (Friedlingstein et al., 2020). The depletion of certain sinks causes an increase in concentration in others. It is the case of the high concentrations of carbon dioxide ($CO_{2)}$ in the atmosphere caused by the depletion of C in the biotic and pedologic pools.

For instance, it is estimated that between the years 1850 and 1998, 136 Pg of C were released from the pedological reservoir due to land use changes (Albritton et al., 2001). It is also estimated that 1.66 Pg of C per year are being transferred to the atmosphere as a result of deforestation, erosion, and soil respiration (Lal, 2008a). One of the emerging sustainable solutions for mitigating this ecological issue is soil carbon sequestration (SCS) (Granja Dorilêo Leite et al., 2025a; Pereira et al., 2024; C. L. Xiao et al., 2025), which may be measured by the SOC stocks indicator (Lorenz et al., 2019).

SCS may be defined as "*the process of transferring C from the atmosphere into the soil through plants or other organisms, which is retained as SOC, resulting in a global C stock increase in the soil*" (Don et al., 2024). It is measured by the soil organic carbon (SOC) stock, which is usually expressed as Mg SOC ha^{-1} at a given soil depth and restricted to the soil fraction < 2mm (FAO, 2019)

SOC is formed through the deposition-decomposition of organic matter (OM). It is a source for soil biota and has low density and high reactivity. The SOC pool is extremely dynamic; gains and losses of SOC can be expressed through a balance between biomass-C inputs I and outputs or losses, L. Part of SOC can be easily removed from soil, while part of it may stabilize for a long time throughout the soil profile (3000 Pg C below 1m) (Köchy et al., 2015). If, in a period, I > L, an accrual of SOC indicates SCS (Lal et al., 2015).

It is known that 50 % of the organic carbon in the soil is chemically or physically associated with soil minerals (mineral-associated organic carbon – MAOM), which creates a stable form of organic C through physical mineral protection and influences the dynamics of long-term C storage in soil. Studies indicate that such an association depends on soil structure, mineralogical characteristics and environmental conditions (Georgiou et al., 2022). Arias Estévez et al. (2016) pointed out that soils rich in iron and aluminum oxides have a greater capacity for carbon association.

Concerns about the effects of extreme climate events and atmospheric carbon concentration have increased interest in quantifying SOC stocks. Efforts to understand SOC dynamics have mainly been applied to investigate natural and agricultural soils (e.g., Huang et al., 2020; Minasny et al., 2017; Yu et al., 2024). However, soil under urban areas also has the potential to store carbon (Lorenz & Lal, 2015; Pouyat et al., 2006).

Despite urban areas occupying only 0.5% of terrestrial land, they are responsible for 70% of the planet's greenhouse gas (GHG) emissions and house more than fifty percent of the global population (United Nations, 2019). Although the useful and comfortable conditions that those artificial lands provide for citizens, the urbanization impacts on soils influence the capacity of soils to provide essential ecosystem services.

The expansion of urban areas highlights the importance of soils in supporting sustainable cities through a range of regulating soil ecosystem services, like air purification, climate regulation, runoff reduction and soil organic carbon sequestration (O'Riordan et al., 2021). In this sense, the interest in investigating SOC stock in urban soils has been enhanced (Cambou et al., 2018; H. Guo et al., 2024; Y. Guo et al., 2024; Pouyat et al., 2002a, 2006; Tagiverdiev et al., 2020; V. I. Vasenev et al., 2018; Zhang et al., 2021).

However, assessing SOC stocks in urban areas is a complicated task due to spatial-temporal variability resulting from bioclimatic conditions, local urban factors and management. The urban SOC stock is highly heterogeneous and drives a fragmented spatial distribution. It is also correlated with functional zones (recreational, industrial, and residential) and so with surface features (sealed or open) and anthropic disturbances (pseudo-natural or engineered) (Morel et al.,

2015). In this sense, as observed by Vasenev et al. (2018), analysis of urban SOC stock must consider soil types, biomes, climates and urbanization scenarios.

In addition, as noted by Scharenbroch et al. (2018), there is a lack of standards for investigating urban soils, including sampling procedures, soil profile depth definitions, and specifications regarding soil-forming factors. Indeed, it is still a new discipline compared to others in soil science.

Although urban soil seems to have a small contribution to mitigating climate change on a global scale, it is highly relevant to minimizing city vulnerability. Reliable data can be crucial for the development of public policies that stimulate citizens and governments to invest in nature-based solutions that include aspects of soil restoration and conservation (Bispo et al., 2017).

In this context, this study aims to evaluate C-Stock, physicochemical, mineralogical and physical-hydric properties in the soil profile of three different classes of land use and cover in the urban area of the Rio de Janeiro city to understand the interactions between land use and cover characterization with soil profiles.

To do so, it was determined soil organic carbon stocks in the total soil (*Cstock*) and the soil organic matter fractions (particulate organic matter, POM – *PCstock* - and mineral-associated organic matter, MAOM – *MCstock*), and measured physico-chemical, mineralogical, and physical-hydric (pore size distribution and soil-water retention) properties to characterize the soil profiles under the land and use classes of: non-native vegetation forest (NNF), dense ombrophylous forest in the initial stage (FIS), and bare soil fill (BSF). The study undertook soil sections of 20 cm (0 - 0.2 m, 0.2 - 0.4 m, 0.4 - 0.6 m, 0.6 - 0.8 m, and 0.8 - 1.0 m) to a depth of 1 m in the soil profile (Appendix 1).

Soil physical-chemical and mineralogical characterization comprised the determination of the specific mass of grains, particle size distribution curve, consistency limits, gravimetric moisture content, total soil densities, electrical conductivity, pH, metal elements, organic matter (*OM*), soil organic matter physical fractionation, total carbon (*TC*), total nitrogen (*TN*), organic carbon (*OC*), stable isotope ^{13}C ($\delta^{13}C$) and ^{15}N ($\delta^{15}N$), X-ray diffraction (XRD) analysis, soil water retention curve, and pore-size distribution. Details on the methodology employed in the development of these analyses and specific results are included in Appendix 2.

Research laboratory analyses were performed at the Laboratory of Geotechnics and Environment (LGMA) of the Civil and Environmental Engineering Department, at the Laboratory of Marine and Environmental Studies (LabMAM) and the Laboratory of Atomic Spectrometry (LABSPECTRO) of the Department of Chemistry, at the X-Ray Diffraction and Scattering Laboratory (Lab DRX) of the Department of Chemical and Materials Engineering (DEQM) at the Pontifical Catholic University of Rio de Janeiro (PUC-Rio), and also, at the São Carlos Physics Institute of the University of São Paulo (USP).

This thesis is organized into five sections, in addition to this one. Chapter 2 presents a critical literature review based on a multidisciplinary approach to consolidate concepts and definitions encompassed in the SOC dynamics. It also includes aspects of the applicability of the SOC stock in engineering projects. The content is part of the article titled “Soil carbon storage and retention: a critical synthesis on concepts, research opportunities and environmental engineering sustainable application,” which was published (October 2025) in the Brazilian Journal of Environmental Sciences (e-ISSN 1806-9657, Qualis A3).

Chapter 3, named SOC stock and physico-chemical analysis, is presented by the article: “Soil organic carbon stock: a case study under different land-use and cover classes in Rio de Janeiro, Brazil,” written according to the standards of the Brazilian Journal of Soil Science. It describes the study area, the methodology applied for physico-chemical and mineralogical laboratory tests, and for carbon stock quantification. It also brings the results and discussion of the obtained soil parameters and the correlation analyses between them.

Chapter 4, called SOC stock and physical-hydric analysis, addresses the investigation of the physical-hydric properties (soil-water retention curves and the soil-pore distribution) and their correlations with C stocks in the three soil profiles. It describes the methodology employed for pore-size distribution and water-retention curve tests and presents and discusses the obtained results.

Chapter 5 delivers a synthesis of the content presented previously and provides an integrated discussion of the results, while Chapter 6 contains conclusions and recommendations for future work.

The literature references that are not listed in the papers in Chapters 2 and 3 are shown in Chapter 7. Finally, Appendices 1 and 2 include the description of the

study areas, the laboratory methodologies, and supplementary data of the experimental testing results.

The main contributions of the research are as follows:

1. Advances the comprehension of processes related to SOC stock by surpassing domain-specific knowledge and adopting a multidisciplinary approach.
2. Points out interactions between SOC stock research gaps and geotechnical investigation methods responses.
3. Sheds light on the potential for applying SOC stock as an indicator of decarbonization performance in engineering projects.
4. Adopts a geoenvironmental sampling methodology to investigate SOC stock and soil properties along the soil profile in an urban environment.
5. Provides soil organic carbon stock (*Cstock; PCstock; MCstock*) quantifications and soil properties data in three typologies of land use and cover in the city of Rio de Janeiro.
6. Provides linear regression equations to correlate soil physical parameters and carbon stocks.

2. Soil carbon storage and retention: a critical literature review

Soil functions have been threatened by anthropic activities, comprising ecosystem services and unbalancing the carbon biogeochemical cycle. Soil carbon sequestration (SCS) is an emergent solution for mitigating climate change and restoring degraded soils. Soil organic carbon stock (SOC stock) plays a relevant role in measuring ecosystem restoration projects. Nevertheless, soil is complex and heterogeneous. It is subjected to the soil-plant-atmosphere system interaction and is controlled by many multidisciplinary processes in the C cycle, from C air sequestration to C soil retention. There are still a series of uncertainties around concepts, mechanisms and methodological protocols to assess SOC stock. Throughout a critical literature review, this paper aims to synthesize concepts under a cross-disciplinary approach, analyze research opportunities and examine sustainable applications underneath environmental engineering. Results point out the conceptual advances in organic matter stabilization in soil and highlight the research gap on the dynamics of the SOC and soil water flux within structured soil profiles, which may be explained through geotechnical engineering concepts. It also observed the need for a multidisciplinary framework of variables that may clarify the transdisciplinary contributions in this field. Finally, the SOC stock is an index that may be employed as an indicator of ecosystem restoration results in C-based engineering solutions.

Keywords: carbon sequestration mechanisms, soil organic matter stabilization, soil hydrodynamics, ecosystem restoration, geotechnics.

2.1. Introduction

The impact of anthropic activities on the environment is an urgent issue in science. Damage to ecosystems and greenhouse gas emissions (GHG) have a detrimental effect on the balance of biogeochemical cycles (IPCC, 2023). An agreed parameter for monitoring this issue is the concentration of carbon dioxide (CO_2) in the atmosphere (Friedlingstein et al., 2020).

Besides the atmosphere, the carbon in the planet is divided into four other pools: oceanic, geologic, biotic and pedologic. The carbon depletion caused by land use changes in the latest pool (soil) is a relevant factor in the increase of the carbon concentration in the atmosphere (Lal et al., 2015). As a solution, strategies of soil carbon sequestration (SCS) contribute to soil carbon storage, which has multiple benefits on ecosystem restoration and climate mitigation (Granja Dorilêo Leite et al., 2025b; C. L. Xiao et al., 2025).

The soil pool comprises soil organic carbon (SOC), of the order of 1.550 Pg C (10^{15}), and soil inorganic carbon (SIC), of circa 950 Pg C, up to 1m depth (Batjes, 1996; Lal, 2008). As put forward by Sharififar et al. (2023), SIC occurs as primary carbonates derived from lithogenic processes (geogenic - alteration of primary carbonate, and biogenic - accumulation of residues of animals and plants) or secondary carbonates (pedogenic - formed on site as a result of recrystallization of pre-existing carbonates. SIC is also found in solutions as dissolved ions (DIC). Precipitation of carbonate requires the availability of Ca^{2+} or Mg^{2+} ions and CO_2 in the soil. Because of the long turnover time of SIC sequestration, it has been overlooked. Nevertheless, recently, SIC has gained attention for its potential for carbon storage, especially in arid regions (Dina Ebouel et al., 2024). On the other hand, SOC is formed through the deposition-decomposition of organic matter (OM) (Muhammad et al., 2025). This is a resource for soil biota and has low density and high reactivity. The SOC pool is extremely dynamic; gains and losses of SOC can be expressed through a balance between biomass-C inputs, I (natural or managed aboveground biomass, root C and exudates and C sediments) and outputs or losses, L (oxidation, mineralization, erosion and leaching). Part of SOC can be easily removed, while part of it may stabilize for a long time along the soil profile (3000 Pg C below 1m) (Köchy et al., 2015). If, in a period, I > L, an accrual of SOC indicates SCS (Lal et al., 2015).

C sequestration was previously defined as the uptake of a C substance from one reservoir to another pool (IPCC, 2001). According to FAO (2019), in the lens of soil, carbon sequestration *"corresponds to an increase in the stock of soil carbon that can be measured or estimated in different ways from balances of carbon fluxes"*. Despite the relevance of SIC in the carbon cycle, SCS has been focused only on SOC stock (expressed as Mg SOC ha^{-1} at a given soil depth and restricted to the fraction < 2mm). Recently, Don et al. (2024) proposed the following

definition for SCS: "*the process of transferring C from the atmosphere into the soil through plants or other organisms, which is retained as SOC, resulting in a global C stock increase in the soil*". It has to be noted that SOC storage and stock have the same meaning, while SOC accrual is the difference between the initial and SOC stock in a unit area in a period that characterizes SCS. On the other hand, SOC content is the amount of carbon in a soil sample relative to the total mineral content (expressed in percentage of mass) and SOC retention concerns the stabilization of SOC stock over time.

SCS became a financial product to stimulate sustainable land management. Carbon credits can be traded if quantified and monitored (Dupla et al., 2024). Nonetheless, inventories of SOC stock hold uncertainties and there is a lack of knowledge on SOC dynamics and an absence of consensus on methods of measuring and monitoring soil-based strategies (Paustian et al., 2016). In addition, the soil has an interdisciplinary nature (Brevik et al., 2015). It is complex, heterogeneous and dynamic, dependent on anthropogenic perturbance and climate conditions (Mitchell and Soga, 2005).

In this context, comprehension of SOC dynamics requires the integration of different areas of knowledge. Only a multidisciplinary framework may allow advances in research through disciplinary connections and cooperation among teams. Bearing in mind that, this literature review aims to identify the recurrent research themes linked to SOC dynamics, synthesize the most significant conceptual contributions and analyze research opportunities and sustainable application through the lens of environmental engineering. To do so, the literature review followed the methodology proposed by Boell & Cecez-Kecmanovic (2014) based on a multidisciplinary search framework starting from the carbon biogeochemical cycle (soil-plant-atmosphere) and constrained by soil properties and structure, soil organic carbon dynamics and soil organic carbon stock. Environmental engineering aspects delimited research on sustainable application. References were obtained in web-based bibliographic databases such as Brazilian Portal of Scientific Journals (CAPES Periódicos), Google Scholar, ScienceDirect and Scopus.

2.2. Concepts and definitions

2.2.1. Soil as an Ecosystem

Soil is a complex, particulate, multiphase system in which the solid phase forms a matrix or skeleton containing interconnected or not connected pores (Figure 1). The solid matrix is composed of primary minerals, which are those inherited from the weathered parent rock (typically, siliceous minerals such as quartz, feldspar, and mica); noncrystalline or amorphous solids, which are silica-rich mineral-like solids such as obsidian, opal, geyserite, and biogenic silica); secondary minerals such as those called clay minerals, originate from bio-physical-chemical weathering of primary minerals (belonging to the families of kaolinite, illite, and montmorillonite); oxides and hydroxides (comprising bonding elements to primary minerals and amorphous solids, typically originated from leaching of iron and aluminum from upper soil layers); and OM (typically labile and recalcitrant plant litter residues).

Soil pores can be filled by fluids or gases (originating from the atmosphere and/or resulting from microorganisms' action). The liquid phase is a soil solution of water containing dissolved electrolytes and organic and/or inorganic substances, dissolved or in the form of colloids.

Soil structure, as herein considered, includes a combination of the soil matrix arrangement, comprising the distribution, size and interconnections of the solid particles; pores arrangement, which includes the distribution, size and interconnections of the void’s spaces, and interaction effects among the solids of the matrix and the fluids within the pores (essentially, the water), which may change over time particularly due to human interferences. Furthermore, the soil is home to billions of organisms responsible for biocenosis, a term that better represents the soil community (Primavesi, 2018).

From the viewpoint of environmental engineering, the grain size of the particles (ϕ) composing the soil matrix constitutes a divisor to be considered as, in most cases, individual particles of size greater than sand ($\phi > 0.075$ mm), typically encompassing primary minerals, do not show any relevant aspect related to carbon storage or retention (CS/R). On the other hand, particles comprising the fine soil fraction (silt fraction, ϕ ranging from 0.075 mm to 0.002 mm, and clay fraction, with $\phi < 0.002$ mm), play a relevant role in CS/R, either acting individually or in

the form of clusters or aggregates (ASTM – American Society for Testing and Materials, 2025).

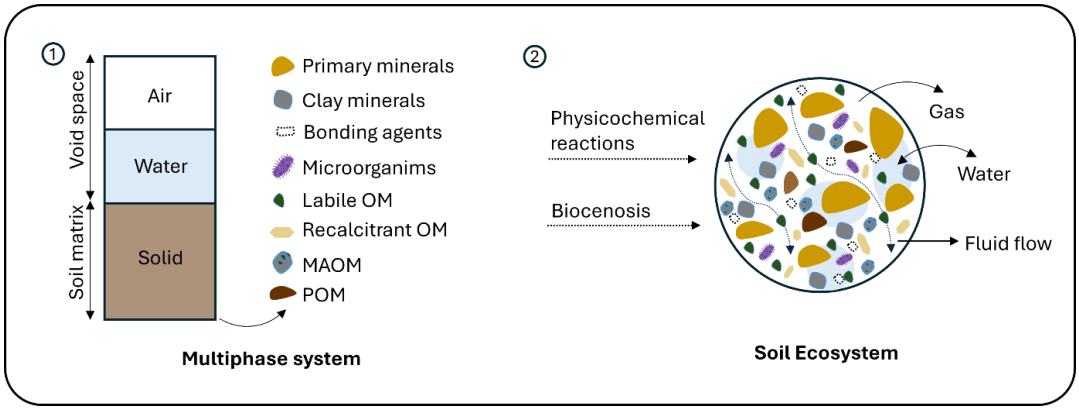

Figure 1. The soil multiphase ecosystem. (1) Distinct phases encountered in the soil structure are delimited by the pore spaces and the solid matrix in which the solid phase exceeds mineral particles. (2) The physicochemical weathering reactions and the bioactivity affect the interaction among soil solids in the presence of air and water in the pore spaces. This combination of phases, reactions and living organisms turns the soil into an ecosystem.

Soil clusters comprise an assemblage of interconnected fine soil particles with complex aggregation formation. According to Bronick & Lal (2005), aggregates result from the rearrangement, flocculation, and cementation of mineral particles with organic and inorganic substances. The hierarchical aggregation dynamic is based on the attachment of bonding agents (organic molecules, clay, and polyvalent cations) to form micro-aggregates (< 250 µm), which progressively join other particles to form macroaggregates (> 250 µm). A discussion on cluster formation, including the presence of OC input, is provided by Denef et al. (2002). The experimental results put forward by these authors indicated that fine fraction soil mineralogy has an important role in soil cluster formation in the presence of OC.

It is interesting to note here that such mineralogy is directly related to the specific surface area (SSA) of clay minerals, defined as the area of the surface of the particle divided by its mass or volume (Table 1). The SSA of clay minerals comprises a good indicator of their potential to store or retain, besides water, organic or inorganic substances in their diffused or double-layer (Mitchell and Soga, 2005). This double layer is inherent to a clay mineral, which presents unbalanced negative electric charges on its surface and positive electric charges at its corners. To balance that, based on their cation exchange capacity (CEC), cations and anions are attracted to the clay surface, including polarized water molecules, which is limited by the

hydrated interlayer surface (basal space). Thus, dissolved organic matter (DOM) can be adsorbed in the clay mineral double layer. (Kleber et al., 2015; Six, 2002).

Table 1. Clay minerals properties (Grim, 1968; Mitchell and Soga, 2005).

Mineral	SSA (m^2 g^{-1})	CEC (cmol kg^{-1})	Basal space (Å)
Kaolinite	7 - 30	3 - 15	7.2
Illite	65 - 100	10 - 40	10.0
Montmorillonite	50 - 840	80 - 150	9.6

It is also interesting to note that DOM can be transported with water as it flows through the pores of the soil, either as a result of rainwater infiltration in an unsaturated soil profile or through water percolation in the saturated soil below the local water table.

The degree of soil saturation (S) is defined by the ratio between its void ratio and its total volume. If the soil is saturated, S = 1. Saturated and unsaturated water flow rates in soils strongly depend on hydraulic soil properties, which are highly dependent on the soil structure (Fredlund et al., 2012).

2.3. SOC storage

SOC is a result of the soil organic matter (SOM). It is continuously changing, varying in depth and space and it is dependent on the broken-down plant metabolism, which is regulated by bioactivity and water (Lal, 2004). SOC storage and retention depend on the deposition and degradation of OM and its interactions with the soil matrix. Thus, a comprehensible understanding of SOM is necessary to assess SOC dynamics (Cotrufo et al., 2019).

2.3.1. Soil organic matter

As put forward by Tan (2003), SOM is derived from the deposition of residues of plant inputs or animals into the soil. Bio-physical-chemical transformation converts this dead material into organic compounds at various degrees of decomposition. On the surface, it is called litter. Downwards, it is broken down into simple molecules (e.g. monomeric sugars, amino acids), polymeric molecules (e.g., cellulose, lignin, and protein), and a highly stable black-brown substance called humic substances.

Such substances comprise a mixture of amorphous, polydisperse organic colloids with electrochemical properties such as those associated with clay minerals (e.g. adsorption).

SOM has a diversity of physical forms and molecular structures that can be identified by its biological stability, decomposition rate and turnover time. This allows a better understanding of the OM dynamics in soils (Prescott & Vesterdal, 2021). Most of the SOM is found in two fractions (Lavallee et al., 2019; S. J. Leuthold et al., 2022): a lower density (< 1.60 to 1.85 g/cm^3) and larger size (> 53 µm) particulate organic matter (POM) and a higher density (>1.85 g/cm^3) and smaller size (< 53 µm) mineral-associated organic matter (MAOM). These fractions hold different physical and chemical properties, persistence and vulnerability to land use changes. POM is largely composed of plant-derived matter found in the organic soil horizons (horizons O and A) and of rhizosphere fragmentation, which are partially decomposed/depolymerized and insoluble. It may be physically protected against degradation by occlusion within aggregates. On the other hand, MAOM is mostly formed by thermolabile compounds of microbial origin in the form of microscopic molecules of OM leached directly from litter or chemically transformed by soil fauna associated with mineral surfaces by adsorption (Figure 2).

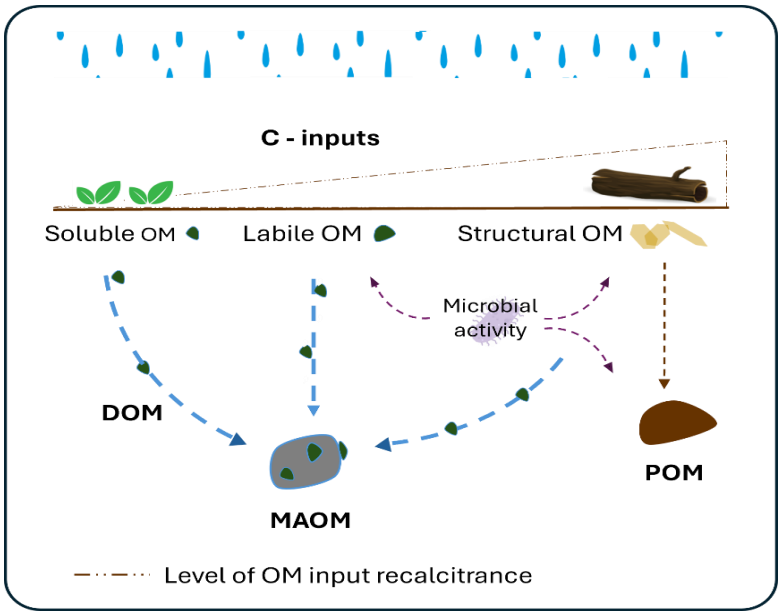

Figure 2. SOM fractions transformation pathways. The OM placed on the soil surface presents molecular diversity structures and different levels of recalcitrance. Bio-physical-chemical transformation also begins at the surface level and OM has already entered soils with distinct biological stability and electrochemical properties. DOM, POM and MAOM may be formed and encountered along the profile.

Despite the large proportion of POM and MAOM in soils, a third fraction of the OM, the dissolved one (DOM), is considered the mobile fraction. It is responsible for the C transport through soil water; it is highly reactive and plays a critical role in C-stabilization as it may reach almost all soil compartments by advection and diffusion (von Lützow et al., 2007). This fraction may also contribute to aggregation and the formation of MAOM under adsorption mechanisms (e.g. Gmach et al., 2020).

2.4. SOC retention

Part of the C input in the soil is mineralized, and part remains stabilized for a different mean residence time (Lal et al., 2015). SOM stabilization mechanisms protect organic molecules against mineralization and oxidation. The two main physical protection mechanisms occur through organo-mineral association and aggregation (Figure 3) (Lützow et al., 2006; Schmidt et al., 2011; Six, 2002). The mineral association mechanism is an interaction between organic matter and the mineral surface and metal ions (Lützow et al., 2006). MAOM refers to OM encapsulated in micropores or micro-aggregates in the soil matrix directly associated with the mineral surface (organo-mineral) or through organo-organic and organo-metal-oxide interactions (Possinger et al., 2020). These associations are regulated by multimodal sorption mechanisms and by coprecipitation (Kleber et al., 2015). They are controlled by three key elements: aqueous species (DOM), microbial metabolism, and clay mineral surface (Dwivedi et al., 2019). In this sense, organo-mineral interactions may be constrained by the percentage of fine particles in soil (< 2 µm), setting a soil carbon saturation potential (Hassink, 1997). OM sorbed in clay particles may partially or fully cover their SSA, modifying its C-saturation capacity (Kaiser and Guggenberger, 2003). As put forward by Six et al. (2024), the maximum C stabilization in 2:1 clay-dominated soils may be ~ 42 % higher than the stabilization in 1:1 clay-dominated soils.

Physical aggregation consists of the occlusion of OM compounds via micro-aggregation within macroaggregates (clusters) and intra-aggregates (Bronick & Lal, 2005). Aggregation restricts the decomposition of OM by microbes and fauna. Molecular C compounds stay spatially isolated (Six, 2002). SOM is the primary binding agent for aggregation, and POM can also act as a nucleus for macro-

aggregation, which results in an arrangement of low-density POM fragments protected by intra-aggregation (Lavallee et al., 2019). Occlusion processes are also guided by organo-mineral interactions as a prior process of aggregation (Lehmann et al., 2007).

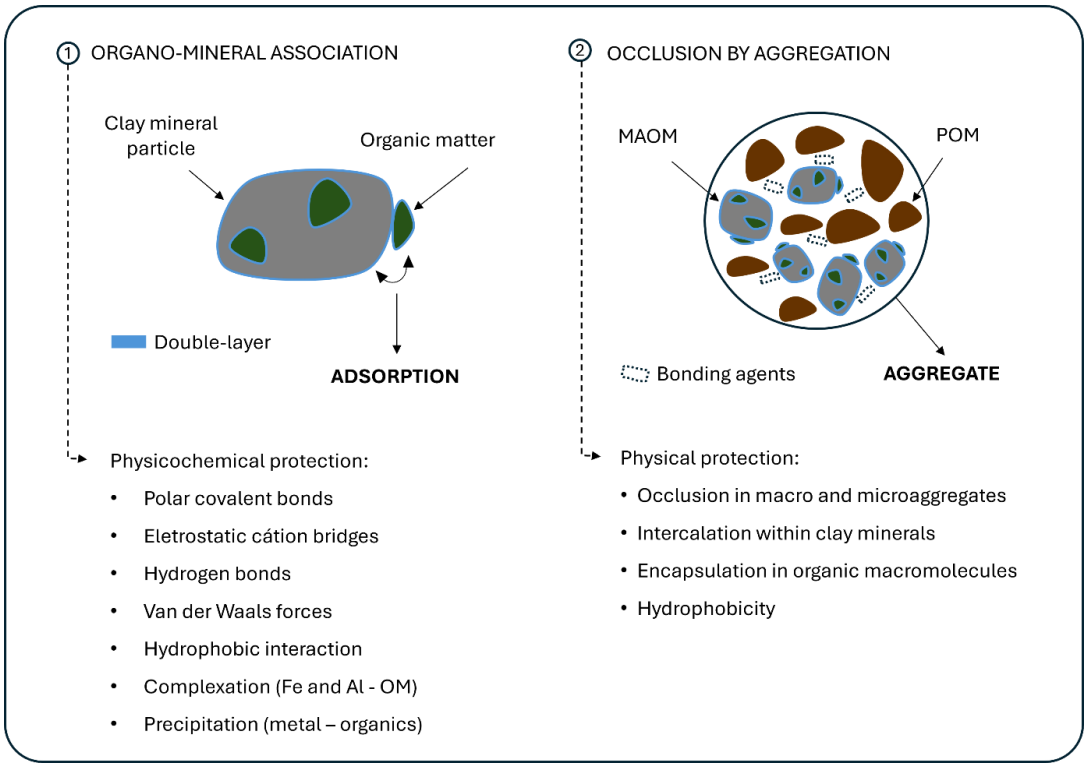

Figure 3. SOC protection mechanisms. (1) Process of organic matter association with the clay mineral particle through the adsorption that occurs in the hydration interlayer. (2) Protection of the SOC through the occlusion into the aggregates. Physicochemical and physical interacting processes were compiled based on Mitchell and Soga (2005), Lützow et al. (2006) and Kleber et al. (2015).

In this context, the occurrence of stabilization mechanisms depends on the soil structure in each horizon, as well as on the chemical structure of organic molecules. The complexity of clarifying SOM stabilization stems from the simultaneous occurrence of variable mechanisms (Lützow et al., 2006).

2.5. SOC stock

Soil carbon stock involves SOC and SIC. Although SIC represents a significant portion of C in some types of soil, it is considered a static pool and is excluded from SCS strategy measurements (FAO, 2019). Considering the bulk density of the soil at a given depth, the SOC stock can be evaluated through Equation 1. Usually, it is measured in one layer or multiple layers to 30 cm depth.

$$SOC_i\ stock\ =\ OC_i\ x\ BD_i\ x\ (1-G_i)x\ t_i\ x\ 0{,}1 \qquad \text{Eq. (1)}$$

where SOC_i is the SOC stock of the soil layer (Mg C ha^{-1}); OC_i is the SOC content of the fine fraction in the layer (g kg^{-1}), BD_i is the bulk density of the soil layer (g cm^{-3}), G_i is the percentage of coarse particles of the layer (g g^{-1}), t_i is the thickness of the layer (cm) and 0.1 is a unit converter factor. POM and MAOM fractions have also been used, separately, in the evaluation of SOC stocks (e.g. Souza Medeiros et al., 2022).

Different methodologies and assessment protocols can be employed to obtain the SOC stock parameters, leading to largely differing results (e.g. Poeplau et al., 2017; Dupla et al., 2024). For example, Peoplau et al. (2020) showed that comparison results between a default modeling reference of SOC stock and in situ measurements may be overestimated by 71 % in depleted soils and underestimated by 549% in carbon-rich soils. Despite uncertainties of modeling results, the adoption of remote sensing technologies, such as spectroscopy imaging (hyperspectral), has promised effectiveness in SOC prediction (e.g., Guo et al., 2021; Roy et al., 2024).

Finally, Bispo et al. (2017) state that the use of international standards may contribute to improving the reliability of the measure, report and verification (MRV) protocols on soil C quantification, mainly when it is applied to the carbon market.

2.6. Soil Storage and Retention

Research into soil carbon dynamics highlights the concept of soil as a multiphase ecosystem that contains biotic and abiotic compounds. Even though soil structure (e.g., skeleton, pore-distribution, mineralogy) regulates the transport, storage and retention of water, gas and OM, most of the interactions in the processes and mechanisms of carbon storage and retention require bioproducts. (Figure 4).

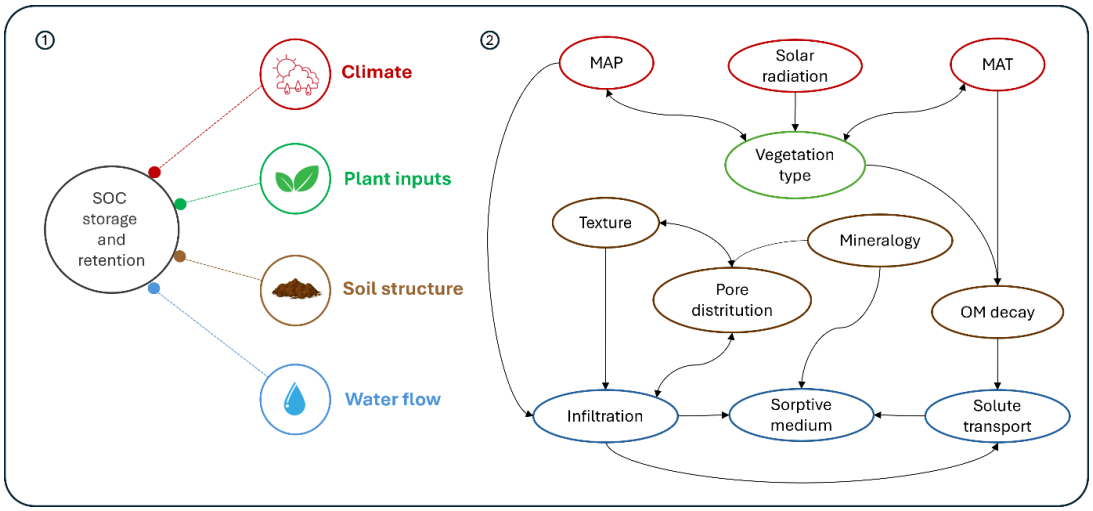

Figure 4. SOC influence factors and variables interactions. (1) The formation and stabilization of SOC encompass elements from the atmosphere, biota and pedosphere and depend on the water dynamics within the soil. (2) In this sense, several phenomena occur simultaneously, with the interaction among variables resulting in complex cause-and-effect relationships. The picture also illustrates the multidisciplinarity in the field

Additionally, soil C sequestration science goes beyond the boundaries of a single scientific area or a specific problem statement. It embraces several research areas such as environmental, soil and plant science, microbiology, atmosphere, and hydrology, among others (Possinger et al., 2020; Verma and Ghosh, 2024) with a myriad of research questions concerning, for instance, food security, climate mitigation, and soil and ecosystem restoration. Moreover, it is a relatively young area of knowledge (Dina Ebouel et al., 2024). Since there is no specified research framework for each science area, interconnected knowledge is needed to investigate any individual phenomenon on soil C storage and retention. It comprises divergences in vocabulary and concept description (Don et al., 2024), as well as in measurement standards and quantification methods, which are further applied to carbon credit protocols (Dupla et al., 2024).

In this context, concepts on soil C storage and retention can be synthesized through the lens of carbon pools (atmospheric-biotic-pedologic) to provide an overview of concepts and mechanisms associated with soil C, and the research boundary areas are referred to in Table 2.

Table 2. Literature references on SOC through carbon pools.

Carbon pool	Thematic	Key factors	References
Atmospheric	MAP and MAT	Wetting and drying cycles	Galluzzi et al., 2024; Heckman et al., 2023; Kramer & Chadwick, 2018
	Climate change	Warming	Georgiou et al., 2024; Rocci et al., 2021; Wang et al., 2024; Wei et al., 2024
Biotic	SOM input	Vegetation input	Cotrufo et al., 2022; Paltineanu et al., 2024; Y. Sun et al., 2024
		Roots metabolism	Dijkstra et al., 2021; Gross & Harrison, 2019
Pedologic	Soil structure	Physical-chemical properties	Fukumasu et al., 2022; Luo et al., 2021; Luo and Viscarra-Rossel, 2020
		Hydrodynamic	Lal, 2020; Védère et al., 2022
		C- saturation	Georgiou et al., 2022; Rodríguez-Albarracín et al., 2023; Six et al., 2024
	SOC storage	SOM decay	Cotrufo et al., 2015; Lehmann & Kleber, 2015; Prescott and Vesterdal, 2021; Smith et al., 2018
		SOM fractions	Angst et al., 2023; Cotrufo et al., 2019; Lavallee et al., 2019; Poeplau et al., 2018
	SOC retention	Stabilization concepts	Cotrufo and Lavallee, 2022; Lehmann et al., 2020; Schmidt et al., 2011
		Physical protection	Chi et al., 2022; Scartazza et al., 2023; van den Bergh et al., 2024
		Mineral association	Hemingway et al., 2019; Kleber et al., 2015; Kopittke et al., 2020; Possinger et al.,2020

2.7. Soil hydrodynamics on SOC mobility

The hydroclimatic regime influences soil C dynamics in multiple ways. As put forward by Védère et al. (2022) in the macroscale, mean annual precipitation (MAP) affects soil surface conditions, plant inputs, runoff and water infiltration and evapotranspiration (Figures 5.1 and 5.2). In the soil profile, water flows and transports soluble matter and controls biological dynamics (SOM production). At the microscale, water influences soil C stabilization mechanisms (Figure 5.3).

The dynamic movement of water may establish layers of variable saturated conditions with distinct decomposition rates and nutrient dynamics that affect several carbon stabilization and destabilization mechanisms (Yusuf et al., 2024).

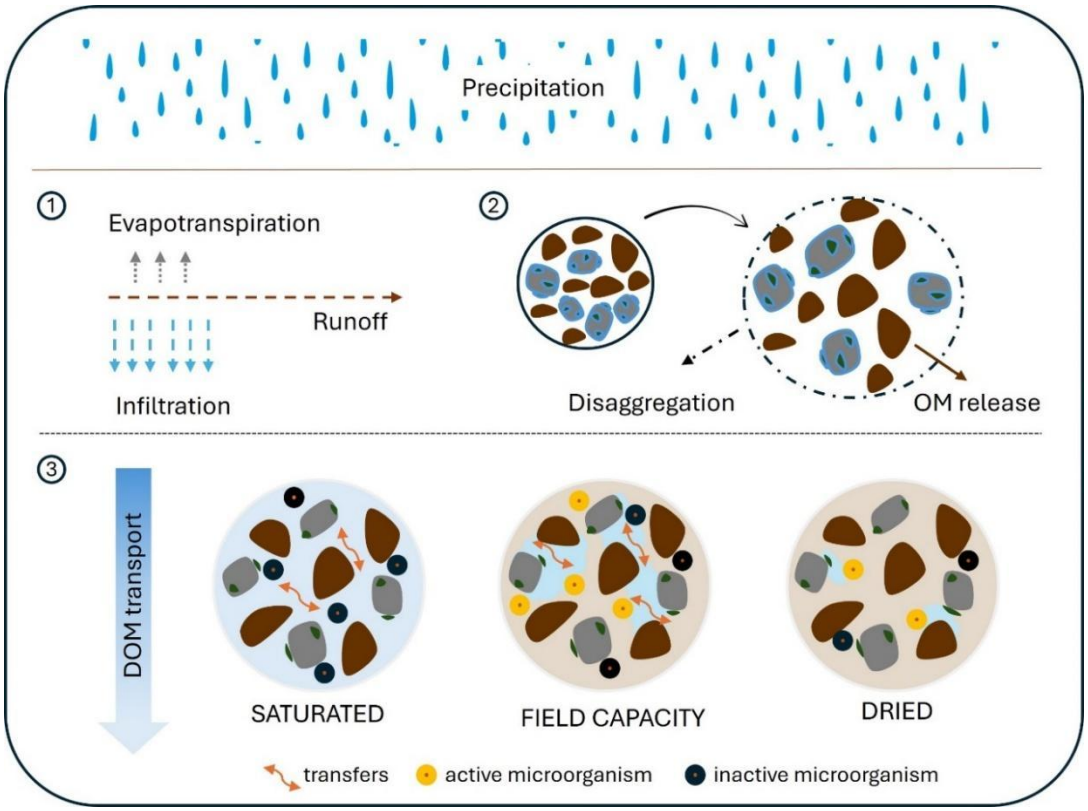

Figure 5. Water effect on SOM: (1) Precipitation generates horizontal (runoff) and vertical (infiltration) transport of particles and soluble OM depending on soil surface conditions (saturation and/or crust formation). Infiltration results in the leaching and integration of OM along the soil profile. Part of the water can be released as vapor. (2) Raindrops can induce aggregate destabilization. Detached OM may be transported by erosion and accumulated along the pathway. (3) Water content induces a gradient of soluble organic molecules, transfers of microorganisms and nutrients (advection and/or diffusion) and affects oxygen supply. Microbial-substrate accessibility (biodegradation) performs mineralization or stabilization of OM according to the degree of saturation.

Moisture also drives differences in soil factors regulating MAOM concentration and persistence. It depicts a clear divergence in the total organic carbon retained in reactive minerals between climate types of soil (humid and arid soils) according to the water balance (Heckman et al., 2023). Additionally, soil moisture regulates the leaching of OM and, in intermediate moisture conditions, the translocation of Ca-carbonate polymerization and the flocculation process of Fe-Al and colloids adsorption (Kramer and Chadwick, 2018).

SOM affects the field capacity (FC). As mentioned by Lal (2020) and Santos Brito et al. (2011), it may increase water retention (WR), likewise, FC condition is favorable for bioactivity and SOM retention (Védère et al., 2022). Wetting and drying cycles strongly affect soil properties and soil aggregate stability; therefore, the capacity of soil to physically protect OM (Jesús Melej et al., 2024). On the other hand, close to saturation conditions, water encounters flow paths in aggregated

media according to aggregate roughness and size of pores, which settle preferential flows that by-pass the aggregate matrix (Carminati et al., 2008).

Water is in the center of the SOM formation, in its vertical distribution and in the retention in each soil structure. Water flows through soil-void spaces, transporting matter - ions and suspended solids - and interacts with clay minerals (e.g. Mitchell and Soga, 2005). Physical and bio-physical-chemical processes are involved in OM transport in soil and can control SOC stock (Figure 5). DOM transport is correlated to the soil hydraulic conductivity (K) and its retention to the type of minerals present in the soil.

Researchers have observed the complexity of examining soil C mobility in soil profiles. For instance, Fukumasu et al. (2024) mention the influence of aggregation aspects on SOC transport and Si et al. (2018) observed the relationship between DOC vertical movement, soil sorptive capability and sorption/desorption dynamics with SOC allocation along the soil profile. Considering agricultural practices, Jephita et al. (2023) attempt to correlate hydrodynamic parameters such as the saturated hydraulic conductivity (Ks), steady state infiltration rates (is) and soil sorptivities (Sp) with soil parameters such as BD, SOC content and aggregate stability.

Indeed, there is a consensus on the lack of information on correlating soil hydrodynamic-SOM transport and C retention in the subsoil (Falloon et al., 2011; Sun and Mu, 2022; F. Yu et al., 2023).

Despite progress in descriptions of hydrological processes in numerical simulations, knowledge is still required of hydrological parameters and solute migration in the context of organic carbon. Hydraulic conductivity, degree of saturation, fluid temperature and viscosity are some of the hydrodynamic soil parameters that require further investigation in response to soil C sequestration. In addition, responses of soil C stabilization dynamics may be correlated to soil-water retention curves (Fredlund et al., 2012), which comprise a sort of soil DNA (Ibañez, 2008) Moreover, the migration of ions in soil water that are controlled by advection, molecular diffusion and mechanical dispersion (Figure 6) is subject to its capacitance (Mitchell and Soga, 2005). All these aspects may strongly affect the SOC vertical distribution and stabilization mechanisms. To overcome the complexity of such interactions, numerical programs like Hydrus-1D, which allow

simulating water flux and solute transport in variably saturated media, may be useful to the comprehension of the SOC-water dynamics (e.g. Biesek et al., 2024).

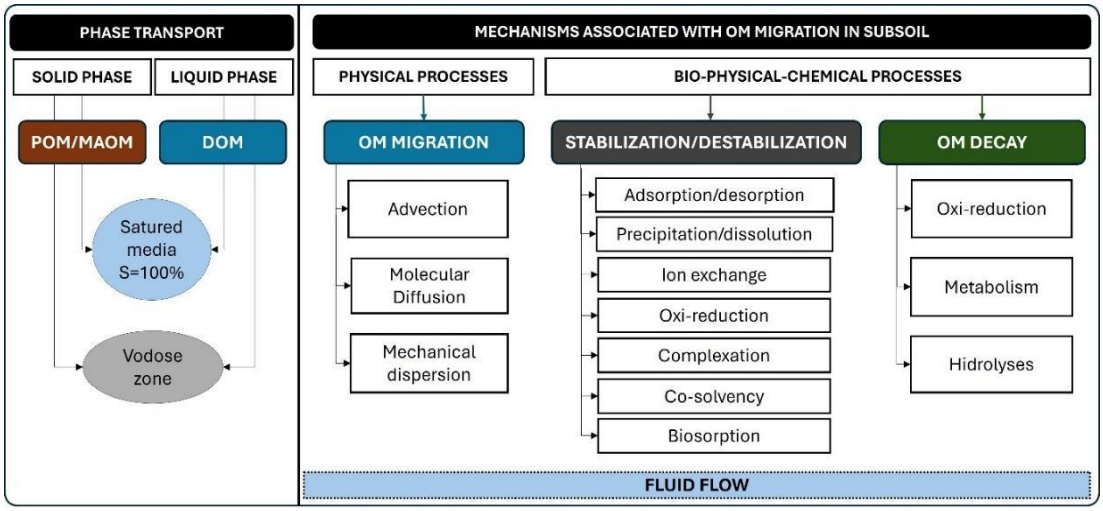

Figure 6. Diagram of OM phases and transport mechanisms in the subsoil.

2.8. Soil assessment and SOC stock

Soil multifunctionality supports planet life, provides food, water, and energy, protects biodiversity and mitigates climate (Kopittke et al., 2022). Soil degradation caused by land-use change, industrialization and urbanization raised concerns about the preservation and restoration of soil functions and services in a holistic view beyond previous concerns only referred to food security (Bünemann et al., 2018). In this context, evaluating SOC losses and storage potential becomes crucial to establishing recovery strategies.

Soil quality index (SQI) (e.g., Guo et al., 2024), soil security (SS) multidimensional concept (e.g., Evangelista et al., 2023) and soil ecosystem services (SES) (e.g., Latawiec et al., 2022) are some of the relevant frameworks employed to evaluate vital soil functions and services.

SQI encompasses soil properties and soil functions, being related to its capacity to perform the ecosystem functions to sustain life and environmental balance (Bünemann et al., 2018). However, soil physical, chemical and biological attributes selected for SQI are not standardized (Li et al., 2023; Raiesi, 2017) and links between soil quality and soil socio-ecological functions are not well-established (J. Guo et al., 2024).

On the other hand, the multidimensional concept of SS consists of five soil dimensions: capability, condition, capital, connectivity and codification – that can be understood, quantified and managed through soil functions, services and threats (McBratney et al., 2014). A proposed SS assessment framework based on soil functions (properties and processes) is being discussed (Evangelista et al., 2024). Moreover, SES also falls into four service categories: provisional, regulatory, cultural and supporting (Baer and Birgé, 2018). It is derived from the concept of ecosystem services (ES), which are the direct or indirect benefits that ecosystems provide to people (MEA, 2003). SES is directly linked to sustainability. The type, quantity and quality of SES depend on edaphic properties and soil functions. The valuation of SES is linked to natural features and land management (Pereira et al., 2018).

Besides this framework assessment, other efforts have been made to link soil structural properties to soil functions (e.g., Orlova & Savin, 2024; Rabot et al., 2018; Séré et al., 2024). However, the lack of clear interpretation schemes has limited the opportunities to support decision-makers and public policies (Bünemann et al., 2018; Rodrigues et al., 2021) as well as constrained the quantification of functions and services for monetary valuation (Baveye et al., 2016).

Notwithstanding, SOC stock is an indicator that exhibits soil functions and quality (Kopittke et al., 2022). Indeed, SOC has been taken as a planetary resource to support ES (Lorenz et al., 2019) and has been used to boost comprehension of changes in the soil surface and subsurface under degradation (Blanco-Canqui, 2024; De Laurentiis et al., 2024; Kavukattu Sreekumar et al., 2024). In addition, advances in new technologies such as the hybrid modeling approach and machine learning have enhanced the SOC prediction to support restoration management practices (Ding et al., 2025). However, further investigation is needed to correlate SOC stock to SES.

Moreover, an indicator based on the organic carbon-to-clay ratio (SOC:Clay) has been admitted specifying levels of soil structural degradation (Dexter et al., 2008; Johannes et al., 2017; Prout et al., 2021). However, owing to the variability of soil types, there are uncertainties on threshold values to adopt SOC:Clay on a large scale (Feeney et al., 2024; Mäkipää et al., 2024).

Despite the “in progress” development of accurate methods to quantify SOC stock, SOC represents a reliable index to express soil multifunctionalities and services.

Indeed, it is guiding national and global public policies on soil restoration (European Commission, 2023; FAO, 2019; IPCC, 2019).

2.9. Sustainable applications

Environmental engineering provides solutions for environmental sanitation – delivery of proper disposal of wastewater and solid waste, drainage of rural and urban areas and control of water, soil and atmospheric pollution – considering the socio-environmental impacts of these solutions (Davis and Cornwell, 1991). Most environmental technologies are based on soil functions or aim to restore it. To ensure the provision of ecosystem services and increase multiple soil functions, mainly in degraded urban areas, technical and conceptual solutions, such as climate-smart soils (Paustian et al., 2016), manufactured soils or technosols (Deeb et al., 2020), sustainable remediation (Ridsdale & Noble, 2016), carbon footprint calculation (Cappuyns, 2024) and incorporation of ES in the remediation process for contaminated sites (Harwell et al., 2021) have been considered. In most cases, SOC stock has been used as an indicator of ecosystem restoration (Sims et al., 2020).

For instance, Chen et al. (2021) applied the SOC stock in two types of restoration strategies. The study pointed out that the two rehabilitated sites had different development trajectories for SOC sequestration and different performances of ecosystem carbon sequestration. Bucka et al. (2024) utilized total organic carbon to assess soil function deliverables in manufactured soil (rock mining waste and soil). The authors observed the potential of the waste and soil mixture to enhance carbon storage due to the abundance of OC-free mineral surfaces. In this case, besides recycling mining waste, the manufactured soil enhances soil carbon sequestration. Thus, restoration strategy choices may define future ecosystem performance.

In addition, changes in urban soil may promote soil degradation and loss of its functions (Pouyat et al., 2002b). Reintegrating the ability of an area to absorb carbon from the atmosphere and store it in the form of SOC is crucial for air purification, climate regulation, runoff reduction and the development of sustainable cities (O'Riordan et al., 2021).

In this context, as illustrated in Figure 7, civil and environmental engineering solutions can employ SOC stock as a metric to express the ecological performance

of a rehabilitated or constructed site. It may also be an opportunity to monetize the SCS as carbon credits if the challenges of policy integration for carbon markets, such as differences in the use of methodologies and protocols and the definition of the minimum monitoring period, are overcome (Batjes et al., 2024).

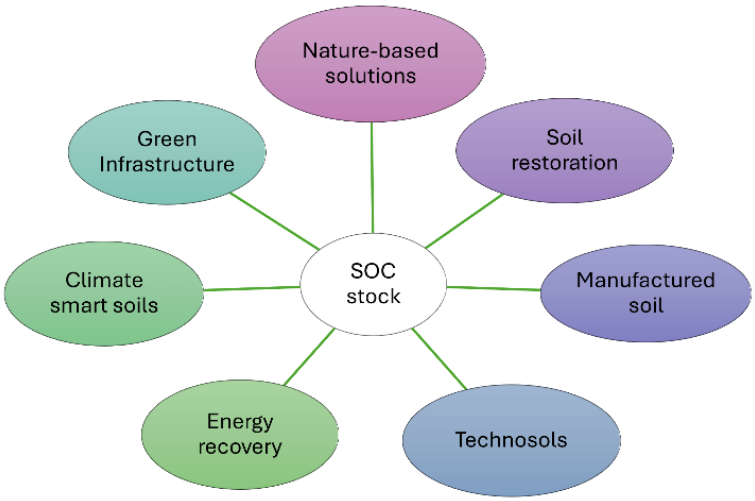

Figure 7. C-based engineering applications. The SOC stock indicator may be used to monitor advances in soil restoration and express the potential of the project to mitigate climate and restore ecosystem services.

2.10. Conclusion

Research on SOC sequestration has been advanced, driven by climate mitigation and soil restoration. Nevertheless, as soil carbon dynamics is a multidisciplinary science, it requires transdisciplinary analysis considering the interaction of biophysical-chemical variables derived from the carbon pools (atmospheric-biotic-pedologic), which vary according to soil structure - water dynamics. To do so, it is required a standardization of definitions, concepts and protocols. A guiding multidisciplinary framework of biophysical-chemical variables correlations would overcome the challenges related to SOC transdisciplinary research.

In addition, research opportunities dwell on data acquisition of SOC and SIC in soil profile, mainly in tropical and subtropical areas where water flux may potentialize SOC storage and retention in depth. Other aspects to be investigated through the lens of environmental engineering include the behavior of SOC storage and retention under the effects of soil hydrodynamics considering hydraulic conductivity, degree of saturation and soil-water retention curve.

The emergency to ecosystem restoration and climate regulation highlights the role of SOC stock as an index that reflects the integral capacity of the land to provide ecosystem services. Despite discrepancies in MRV protocols, the additionality of SOC in restored soils may generate soil carbon credits (SCC) for a monetary carbon market.

Advances in SOC storage and retention research will contribute to minimizing discrepancies in MRV protocols. In this sense, the development of decision-support systems integrating SOC, hydrology and land-use data would be useful to endorse the elaboration of public policies to incentivize the restoration of degraded areas other than agricultural ones. For instance, restoring degraded soils in urban areas, rehabilitating green spaces and building nature-based solutions and green infrastructure through C-based engineering solutions.

2.11. References

Angst, G.; Mueller, K. E.; Castellano, M. J.; Vogel, C.; Wiesmeier, M.; Mueller, C. W., 2023. Unlocking complex soil systems as carbon sinks: multi-pool management as the key. Nature Communications, v.14 (1). https://doi.org/10.1038/s41467-023-38700-5.

ASTM – American Society for Testing and Materials, 2023. ASTM D6282/D6282M-14 Standard guide for direct push soil sampling for environmental site characterizations (Withdrawn 2023)

ASTM – American Society for Testing and Materials, 2025. ASTM D2487-17(2025): Standard Practice for Classification of Soils for Engineering Purposes (Unified Soil Classification System).

Baer, S. G.; Birgé, H. E., 2018. Soil ecosystem services: an overview, 17-38. https://doi.org/10.19103/as.2017.0033.02.

Batjes, N. H., 1996. Total carbon and nitrogen in the soils of the world. European Journal of Soil Science, v. 47 (2), 151-163. https://doi.org/10.1111/j.1365-2389.1996.tb01386.x.

Batjes, N. H.; Ceschia, E.; Heuvelink, G. B. M.; Demenois, J.; le Maire, G.; Cardinael, R.; Arias-Navarro, C.; van Egmond, F., 2024. Towards a modular, multi-ecosystem monitoring, reporting and verification (MRV) framework for soil organic carbon stock change assessment. Carbon Management; v. 15(1). https://doi.org/10.1080/17583004.2024.2410812.

Baveye, P. C.; Baveye, J.; Gowdy, J., 2016. Soil “ecosystem” services and natural capital: Critical appraisal of research on uncertain ground. Frontiers in Environmental Science, v. 4, 1-49. https://doi.org/10.3389/fenvs.2016.00041.

Biesek, B. J.; Szymkiewicz, A.; Šimůnek, J.; Gumuła-Kawęcka, A.; Jaworska-Szulc, B., 2024.Numerical modeling of PFAS movement through the vadose zone: Influence of plant water uptake and soil organic carbon distribution. Science of the Total Environment.; v. 935. https://doi.org/10.1016/j.scitotenv.2024.173252.

Bispo, A.; Andersen, L.; Angers, D. A.; Bernoux, M.; Brossard, M.; Cécillon, L.; Comans, R. N. J.; Harmsen, J.; Jonassen, K.; Lamé, F.; Lhuillery, C.; Maly, S.; Martin, E.; Mcelnea, A. E.; Sakai, H.; Watabe, Y.; Eglin, T. K., 2017. Accounting for carbon stocks in soils and measuring GHGs emission fluxes from soils: Do we have the necessary standards? Frontiers in Environmental Science, v. 5, 1-12. https://doi.org/10.3389/fenvs.2017.00041.

Blanco-Canqui, H., 2024. Assessing the potential of nature-based solutions for restoring soil ecosystem services in croplands. In Science of the Total Environment, v. 921. https://doi.org/10.1016/j.scitotenv.2024.170854.

Boell, S. K.; Cecez-Kecmanovic, D., 2014. A Hermeneutic Approach for Conducting Literature Reviews and Literature Searches. In Communications of the Association for Information Systems, v. 34. http://aisel.aisnet.org/cais/vol34/iss1/12.

Brevik, E. C.; Cerdà, A.; Mataix-Solera, J.; Pereg, L.; Quinton, J. N.; Six, J.; Van Oost, K., 2015. The interdisciplinary nature of SOIL. SOIL, v. 1, 117-129. https://doi.org/10.5194/soil-1-117-2015.

Bronick, C. J.; Lal, R., 2005. Soil structure and management: A review. Geoderma, v. 124, 3-22. https://doi.org/10.1016/j.geoderma.2004.03.005.

Bucka, F. B.; Guigue, J.; Reifschneider, L.; Pihlap, E.; Garcia-Franco, N.; Kühnel, A.; Kögel-Knabner, I.; Vidal, A., 2024. From waste to soil: Can we create functioning manufactured soils by recycling rock processing waste? Soil Use and Management, v. 40. https://doi.org/10.1111/sum.13094.

Bünemann, E. K.; Bongiorno, G.; Bai, Z.; Creamer, R. E.; De Deyn, G.; de Goede, R.; Fleskens, L.; Geissen, V.; Kuyper, T. W.; Mäder, P.; Pulleman, M.; Sukkel, W.; van Groenigen, J. W.; Brussaard, L., 2018. Soil quality – A critical review. In Soil Biology and Biochemistry, v. 120, 105-125. Elsevier Ltd. https://doi.org/10.1016/j.soilbio.2018.01.030.

Cappuyns, V., 2024. Carbon footprint calculations in the soil remediation sector: A comparative analysis. Science of the Total Environment, v. 915. https://doi.org/10.1016/j.scitotenv.2024.170100.

Carminati, A.; Kaestner, A.; Lehmann, P.; Flühler, H., 2008. Unsaturated water flow across soil aggregate contacts. Advances in Water Resources, v.31 (9),1221–1232. https://doi.org/10.1016/j.advwatres.2008.01.008

Chen, S.; Chen, B.; Chen, G.; Ji, J.; Yu, W.; Liao, J.; Chen, G., 2021. Higher soil organic carbon sequestration potential at a rehabilitated mangrove comprised of Aegiceras corniculatum compared to Kandelia obovata. Science of the Total Environment, v. 752, 142279. https://doi.org/10.1016/j.scitotenv.2020.142279.

Chi, J.; Fan, Y.; Wang, L.; Putnis, C. V.; Zhang, W., 2022. Retention of soil organic matter by occlusion within soil minerals. In Reviews in Environmental Science and Biotechnology, v. 21 (3), 727–746. https://doi.org/10.1007/s11157-022-09628-x.

Costa, J.; Furquim, S., 2025. Aggregation of tropical urban soils in the metropolis of São Paulo, southern Brazil. Catena, v. 249, p. https://doi.org/10.1016/j.catena.2024.108681

Cotrufo, M. F.; Haddix, M. L.; Kroeger, M. E.; Stewart, C. E., 2022. The role of plant input physical-chemical properties, and microbial and soil chemical diversity on the formation of particulate and mineral-associated organic matter. Soil Biology and Biochemistry, v. 168. https://doi.org/10.1016/j.soilbio.2022.108648.

Cotrufo, M. F.; Lavallee, J. M., 2022. Soil organic matter formation, persistence, and functioning: A synthesis of current understanding to inform its conservation and regeneration. In Advances in Agronomy, v. 172, 1-66. Academic Press Inc. https://doi.org/10.1016/bs.agron.2021.11.002.

Cotrufo, M. F.; Ranalli, M. G.; Haddix, M. L.; Six, J.; Lugato, E., 2019. Soil carbon storage informed by particulate and mineral-associated organic matter. Nature Geoscience, v. 12 (12), 989-994. https://doi.org/10.1038/s41561-019-0484-6.

Cotrufo, M. F.; Soong, J. L.; Horton, A. J.; Campbell, E. E.; Haddix, M. L.; Wall, D. H.; Parton, W. J., 2015. Formation of soil organic matter via biochemical and physical pathways of litter mass loss. Nature Geoscience, v. 8 (10), 776-779. https://doi.org/10.1038/ngeo2520.

Davis, M. L.; Cornwell, D. A, 1991. Introduction to environmental engineering. McGraw-Hill, New York, 822 p.

De Laurentiis, V.; Maier, S.; Horn, R.; Uusitalo, V.; Hiederer, R.; Chéron-Bessou, C.; Morais, T.; Grant, T.; Milà i Canals, L.; Sala, S., 2024. Soil organic carbon as an indicator of land use impacts in life cycle assessment. International Journal of Life Cycle Assessment, v. 29 (7), 1190-1208. https://doi.org/10.1007/s11367-024-02307-9.

Deeb, M.; Groffman, P.; Blouin, M.; Perl Egendorf, S.; Vergnes, A.; Vasenev, V.; Cao, D.; Walsh, D.; Morin, T.; Séré, G., 2020. Using constructed soils for green infrastructure - Challenges and limitations. SOIL, v. 6 (2), 413-434. https://doi.org/10.5194/soil-6-413-2020.

Denef, K.; Six, J.; Merckx, R.; Paustian, K., 2002. Short-term effects of biological and physical forces on aggregate formation in soils with different clay mineralogy. In Plant and Soil, v. 246.

Dexter, A. R.; Richard, G.; Arrouays, D.; Czyz, E. A.; Jolivet, C.; Duval, O., 2008. Complexed organic matter controls soil physical properties. Geoderma, v. 144 (3-4), 620-627. https://doi.org/10.1016/j.geoderma.2008.01.022.

Dijkstra, F. A.; Zhu, B.; Cheng, W., 2021. Root effects on soil organic carbon: a double-edged sword. In New Phytologist, v. 230 (1), 60-65. https://doi.org/10.1111/nph.17082.

Dina Ebouel, F. J.; Betsi, T. B.; Eze, P. N., 2024. Soil inorganic carbon: A review of global research trends, analytical techniques, ecosystem functions and critical knowledge gaps. In Catena, v. 242. https://doi.org/10.1016/j.catena.2024.108112.

Ding, Z.; Liu, K.; Grunwald, S.; Smith, P.; Ciais, P.; Wang, B.; Wadoux, A.M.J.C.; Ferreira, C.; Karunaratne, S.; Shurpali, N.; Yin, X.; Roberts, D.; Madgett, O.; Duncan, S.; Zhou, M.; Liu, Z.; Harrison, M. T., 2025. Advancing Soil Organic Carbon Prediction: A Comprehensive Review of Technologies, AI, Process-Based and Hybrid Modelling Approaches. Advanced Science. https://doi.org/10.1002/advs.202504152

Don, A.; Seidel, F.; Leifeld, J.; Kätterer, T.; Martin, M.; Pellerin, S.; Emde, D.; Seitz, D.; Chenu, C., 2024. Carbon sequestration in soils and climate change mitigation—Definitions and pitfalls. In Global Change Biology, v. 30 (1). https://doi.org/10.1111/gcb.16983.

Dupla, X.; Bonvin, E.; Deluz, C.; Lugassy, L.; Verrecchia, E.; Baveye, P. C.; Grand, S.; Boivin, P., 2024. Are soil carbon credits empty promises? Shortcomings of current soil carbon quantification methodologies and improvement avenues. Soil Use and Management, v. 40. https://doi.org/10.1111/sum.13092.

Dwivedi, D.; Tang, J.; Bouskill, N.; Ge0orgiou, K.; Chacon, S. S.; Riley, W. J., 2019. Abiotic and biotic controls on soil organo mineral interactions: Developing model structures to analyze why soil organic matter persists. Reviews in Mineralogy and Geochemistry, v. 85 (1), 329-348. https://doi.org/10.2138/rmg.2019.85.11.

EUROPEAN COMMISSION. Directive of the European Parliament and the Council on Soil Monitoring and Resilience: Soil Monitoring Law, 2023. Issue 416 final. https://doi.org/10.2777/821504.

Evangelista, S. J.; Field, D. J.; McBratney, A. B.; Minasny, B.; Ng, W.; Padarian, J.; Román Dobarco, M.; Wadoux, A. M. J. C., 2023. A proposal for the assessment of soil security: Soil functions, soil services and threats to soil. Soil Security, v.10. https://doi.org/10.1016/j.soisec.2023.100086.

Evangelista, S. J.; Field, D. J.; McBratney, A. B.; Minasny, B.; Wartini Ng; Padarian, J.; Dobarco, M. R.; Wadoux, A. M. J.C., 2024. Soil security - Strategizing a sustainable future for soil. Advances in Agronomy, v. 183.

Falloon, P.; Jones, C. D.; Ades, M.; Paul, K., 2011. Direct soil moisture controls of future global soil carbon changes: An important source of uncertainty. Global Biogeochemical Cycles, v. 25 (3). https://doi.org/10.1029/2010GB003938.

FAO, 2019. Measuring and modelling soil carbon stocks and stock changes in livestock production systems: guidelines for assessment: version 1, 170 p., Rome. http://www.fao.org/partnerships/leap/publications/en/.

Feeney, C. J.; Bentley, L.; De Rosa, D.; Panagos, P.; Emmett, B. A.; Thomas, A.; Robinson, D. A., 2024. Benchmarking soil organic carbon (SOC) concentration provides more robust soil health assessment than the SOC/clay ratio at European scale. Science of the Total Environment, v. 951. https://doi.org/10.1016/j.scitotenv.2024.175642.

Fredlund, D. G., Rahardjo, H., Fredlund, M. D., 2012. Unsaturated Soil Mechanics in Engineering Practice. John Wiley & Sons, Inc. New Jersey. 939 p.

Friedlingstein, P.; O'Sullivan, M.; Jones, M. W.; Andrew, R. M.; Hauck, J.; Olsen, A.; Peters, G. P.; Peters, W.; Pongratz, J.; Sitch, S.; Le Quéré, C.; Canadell, J. G.; Ciais, P.; Jackson, R. B.; Alin, S.; Aragão, L. E. O. C.; Arneth, A.; Arora, V.; Bates, N. R.; … Zaehle, S., 2020. Global Carbon Budget 2020. Earth System Science Data, v. 12 (4), 3269-3340. https://doi.org/10.5194/ESSD-12-3269-2020.

Fukumasu, J.; Jarvis, N.; Koestel, J.; Kätterer, T.; Larsbo, M., 2022. Relations between soil organic carbon content and the pore size distribution for an arable topsoil with large variations in soil properties. European Journal of Soil Science, v. 73 (1). https://doi.org/10.1111/ejss.13212.

Fukumasu, J.; Jarvis, N.; Koestel, J.; Larsbo, M., 2024. Links between soil pore structure, water flow and solute transport in the topsoil of an arable field: Does soil organic carbon matter? Geoderma, v. 449. https://doi.org/10.1016/j.geoderma.2024.117001.

Galluzzi, G.; Plaza, C.; Priori, S.; Giannetta, B.; Zaccone, C., 2024. Soil organic matter dynamics and stability: Climate vs. time. Science of the Total Environment, v. 929. https://doi.org/10.1016/j.scitotenv.2024.172441.

Georgiou, K.; Jackson, R. B.; Vindušková, O.; Abramoff, R. Z.; Ahlström, A.; Feng, W.; Harden, J. W.; Pellegrini, A. F. A.; Polley, H. W.; Soong, J. L.; Riley, W. J.; Torn, M. S., 2022. Global stocks and capacity of mineral-associated soil organic carbon. Nature Communications, v. 13 (1). https://doi.org/10.1038/s41467-022-31540-9.

Georgiou, K.; Koven, C. D.; Wieder, W. R.; Hartman, M. D.; Riley, W. J.; Pett-Ridge, J.; Bouskill, N. J.; Abramoff, R. Z.; Slessarev, E. W.; Ahlström, A.; Parton, W. J.; Pellegrini, A. F. A.; Pierson, D.; Sulman, B. N.; Zhu, Q.; Jackson, R. B., 2024. Emergent temperature sensitivity of soil organic carbon driven by mineral associations. Nature Geoscience, v. 17 (3), 205-212. https://doi.org/10.1038/s41561-024-01384-7.

Gmach, M. R.; Cherubin, M. R.; Kaiser, K.; Cerri, C. E. P., 2020. Processes that influence dissolved organic matter in the soil: A review. Scientia Agricola, v. 77 (3). https://doi.org/10.1590/1678-992x-2018-0164.

Granja Dorilêo Leite, F. F.; Fontana, A.; Nóbrega, G. N.; Santos, F. M.; Rodrigues Alves, B. J.; da Silveira, J. G.; Cordeiro, R. C.; Cerri, C. E. P.; Firmino dos Santos, R. A.; Ribeiro Rodrigues, R. de A., 2025. Land use change effect on organic matter dynamics and soil carbon sequestration in the Brazilian Cerrado: A study case in Mato Grosso do Sul state (Midwest-Brazil). Catena, v. 249. https://doi.org/10.1016/j.catena.2024.108670.

Grim, R. E., 1968. Clay Mineralogy. Second edition. McGraw-Hill, New York, 596 p.

Gross, C. D.; Harrison, R. B., 2019. The case for digging deeper: Soil organic carbon storage, dynamics, and controls in our changing world. Soil Systems, v. 3, Issue 2, 1-24. https://doi.org/10.3390/soilsystems3020028.

Guo, J.; Li, G.; Zhu, Q.; Jiang, Y.; Guo, X.; Ding, L.; Zhao, X., 2024. Exploring the spatial relationship between soil quality index and soil ecosystem services driven by social-ecological factors: A peri-urban case study in central China. Catena, v. 245. https://doi.org/10.1016/j.catena.2024.108350.

Guo, L.; Sun, X.; Fu, P.; Shi, T.; Dang, L.; Chen, Y.; Linderman, M.; Zhang, G.; Zhang, Y.; Jiang, Q.; Zhang, H.; Zeng, C., 2021. Mapping soil organic carbon stock by hyperspectral and time-series multispectral remote sensing images in low-relief agricultural areas. Geoderma, 398:115-118. https://doi.org/10.1016/j.geoderma.2021.115118

Harwell, M. C.; Jackson, C.; Kravitz, M.; Lynch, K.; Tomasula, J.; Neale, A.; Mahoney, M.; Pachon, C.; Scheuermann, K.; Grissom, G.; Parry, K., 2021. Ecosystem services consideration in the remediation process for contaminated sites. Journal of Environmental Management, v. 285. https://doi.org/10.1016/j.jenvman.2021.112102.

Hassink, J., 1997. The capacity of soils to preserve organic C and N by their association with clay and silt particles. Plant and Soil, v. 191.

Heckman, K. A.; Possinger, A. R.; Badgley, B. D.; Bowman, M. M.; Gallo, A. C.; Hatten, J. A.; Nave, L. E.; SanClements, M. D.; Swanston, C. W.; Weiglein, T. L.; Wieder, W. R.; Strahm, B. D., 2023. Moisture-driven divergence in mineral-associated soil carbon persistence. Proceedings of the National Academy of Sciences of the United States of America, v. 120 (7). https://doi.org/10.1073/pnas.2210044120.

Hemingway, J. D.; Rothman, D. H.; Grant, K. E.; Rosengard, S. Z.; Eglinton, T. I.; Derry, L. A.; Galy, V. V., 2019. Mineral protection regulates long-term global preservation of natural organic carbon. Nature, v. 570, 228-231. https://doi.org/10.1038/s41586-019-1280-6.

Huat, B. B. K.; Toll, D. G.; Prasad, A., 2012. Handbook of Tropical Residual Soils Engineering. Taylor & Francis, London.

Ibañez, J. P., 2008. Modelagem micro-mecânica discreta de solos residuais. Doctoral Thesis, Pontifical Catholic University of Rio de Janeiro (PUC-Rio), Rio de Janeiro. Biblioteca Central – PUC-Rio.

IPCC. Intergovernmental Panel on Climate Change, 2001. Climate Change 2001: The Scientific Bases. Contribution of Working Group I to the Third Assessment Report of the Intergovernmental Panel on Climate Change https://doi.org/10.1016/S1058-2746(02)86826-4.

IPCC. Intergovernmental Panel on Climate Change, 2019. 2019 Refinement to the 2006 IPCC Guidelines for National Greenhouse Gas Inventories. Chapter 2: Generic Methodologies applicable to multiple land-use categories. https://www.ipcc.ch/report/2019-refinement-to-the-2006-ipcc-guidelines-for-national-greenhouse-gas-inventories/

IPCC. Intergovernmental Panel on Climate Change, 2023. Summary for Policymakers. In: Climate Change 2023: Synthesis Report. Contribution of Working Groups I, II and III to the Sixth Assessment Report of the Intergovernmental Panel on Climate Change. https://doi.org/10.59327/IPCC/AR6-9789291691647.001.

Jephita, G.; Jefline, K.; Willis, G.; Justice, N., 2023. Carbon stock, aggregate stability and hydraulic properties of soils under tillage, crop rotation and mineral fertiliser application in sub-humid Zimbabwe. Heliyon, v. 9 (5). https://doi.org/10.1016/j.heliyon.2023.e15846.

Jesús Melej, M.; Acevedo, S. E.; Contreras, C. P.; Giraldo, C. V.; Maurer, T.; Calderón, F. J.; Bonilla, C. A., 2024. Changes in macroaggregate stability as a result of wetting/drying cycles of soils with different organic matter and clay contents. Geoderma, v. 448. https://doi.org/10.1016/j.geoderma.2024.116965.

Jobbágy, E. G.; Jackson, R. B., 2000. The vertical distribution of soil organic carbon and its relation to climate and vegetation. Ecological Applications, v. 10 (2), 423-436. https://doi.org/10.1890/1051-0761(2000)010[0423:TVDOSO]2.0.CO;2.

Johannes, A.; Matter, A.; Schulin, R.; Weisskopf, P.; Baveye, P. C.; Boivin, P., 2017. Optimal organic carbon values for soil structure quality of arable soils. Does clay content matter? Geoderma, v. 302, 14-21. https://doi.org/10.1016/j.geoderma.2017.04.021.

Kaiser, K.; Guggenberger, G., 2003. Mineral surfaces and soil organic matter. European Journal of Soil Science, v. 54 (2), 219-236. https://doi.org/10.1046/j.1365-2389.2003.00544.x.

Kavukattu Sreekumar, K.; Anil Kumar, K. S.; Madhusoodanan Nair, K. P.; Beeman, K.; Manickam, L.; Sreekumar, P.; Ramamurthy, V., 2024. Assessing changes in soil organic carbon stocks and vulnerability to land degradation in

Western Ghats, South India: Is it restorative enough? Soil Use and Management, v. 40 (2). https://doi.org/10.1111/sum.13056.

Kleber, M.; Eusterhues, K.; Keiluweit, M.; Mikutta, C.; Mikutta, R.; Nico, P. S., 2015. Mineral-Organic Associations: Formation, Properties, and Relevance in Soil Environments. Advances in Agronomy, v. 130, 1-140. https://doi.org/10.1016/bs.agron.2014.10.005.

Köchy, M.; Hiederer, R.; Freibauer, A., 2015. Global distribution of soil organic carbon – Part 1: Masses and frequency distributions of SOC stocks for the tropics, permafrost regions, wetlands, and the world. SOIL, v. 1 (1), 351-365. https://doi.org/10.5194/soil-1-351-2015.

Kopittke, P. M.; Berhe, A. A.; Carrillo, Y.; Cavagnaro, T. R.; Chen, D.; Chen, Q. L.; Román Dobarco, M.; Dijkstra, F. A.; Field, D. J.; Grundy, M. J.; He, J. Z.; Hoyle, F. C.; Kögel-Knabner, I.; Lam, S. K.; Marschner, P.; Martinez, C.; McBratney, A. B.; McDonald-Madden, E.; Menzies, N. W.; Minasny, B., 2022. Ensuring planetary survival: the centrality of organic carbon in balancing the multifunctional nature of soils. In Critical Reviews in Environmental Science and Technology, v. 52 (23), 4308-4324). Taylor and Francis Ltd. https://doi.org/10.1080/10643389.2021.2024484.

Kopittke, P. M.; Dalal, R. C.; Hoeschen, C.; Li, C.; Menzies, N. W.; Mueller, C. W., 2020. Soil organic matter is stabilized by organo-mineral associations through two key processes: The role of the carbon to nitrogen ratio. Geoderma, v. 357. https://doi.org/10.1016/j.geoderma.2019.113974.

Kramer, M. G.; Chadwick, O. A., 2018. Climate-driven thresholds in reactive mineral retention of soil carbon at the global scale. Nature Climate Change, v.8 (12), 1104-1108. https://doi.org/10.1038/s41558-018-0341-4.

Krug, T.; Kurz, W. A.; Lasco, R. D.; Martino, D. L.; McConkey, B. G., 2006. Volume 4: Agriculture, Forestry and Other Land Use 2.2, 2006. IPCC Guidelines for National Greenhouse Gas Inventories.

Lal, R., 2004a. Soil carbon sequestration impacts on global climate change and food security. Science, v. 304, 1623-1627. https://doi.org/10.1126/science.1097396.

Lal, R., 2004b. Soil carbon sequestration to mitigate climate change. Geoderma, v. 123(1-2), 1-22. https://doi.org/10.1016/j.geoderma.2004.01.032.

Lal, R., 2008. Sequestration of atmospheric CO2 in global carbon pools. Energy and Environmental Science, v.1 (1), 86-100. https://doi.org/10.1039/b809492f.

Lal, R., 2020. Soil organic matter and water retention. Agronomy Journal, v. 112 (5), 3265-3277. https://doi.org/10.1002/agj2.20282.

Lal, R.; Negassa, W.; Lorenz, K., 2015. Carbon sequestration in soil. Current Opinion in Environmental Sustainability, v. 15, 79-86. https://doi.org/10.1016/j.cosust.2015.09.002.

Latawiec, A. E.; Rodrigues, A.; Korys, K. A.; Medeiros, B., 2022. Methodical Aspects of Soil Ecosystem Services Valuation. Agricultural Engineering, v. 26 (1), 39-49. https://doi.org/10.2478/agriceng-2022-0004.

Lavallee, J. M.; Soong, J. L.; Cotrufo, M. F., 2019. Conceptualizing soil organic matter into particulate and mineral-associated forms to address global change in the 21st century. Global Change Biology, v. 26 (1), 261-273. https://doi.org/10.1111/gcb.14859.

Lehmann, J.; Hansel, C. M.; Kaiser, C.; Kleber, M.; Maher, K.; Manzoni, S.; Nunan, N.; Reichstein, M.; Schimel, J. P.; Torn, M. S.; Wieder, W. R.; Kögel-Knabner, I., 2020. Persistence of soil organic carbon caused by functional complexity. Nature Geoscience, v. 13 (8), 529-534. https://doi.org/10.1038/s41561-020-0612-3.

Lehmann, J.; Kinyangi, J.; Solomon, D., 2007. Organic matter stabilization in soil microaggregates: Implications from spatial heterogeneity of organic carbon contents and carbon forms. Biogeochemistry, v. 85 (1), 45-57. https://doi.org/10.1007/s10533-007-9105-

Lehmann, J.; Kleber, M., 2015. The contentious nature of soil organic matter. Nature v. 528 (7580), 60-68). https://doi.org/10.1038/nature16069.

Leuthold, S. J.; Haddix, M. L.; Lavallee, J.; Cotrufo, M. F., 2022. Physical fractionation techniques. Reference Module in Earth Systems and Environmental Sciences. https://doi.org/10.1016/b978-0-12-822974-3.00067-7.

Li, F.; Zhang, X.; Zhao, Y.; Song, M.; Liang, J., 2023. Soil quality assessment of reclaimed land in the urban-rural fringe. Catena, v. 220. https://doi.org/10.1016/j.catena.2022.106692.

Lorenz, K.; Lal, R.; Ehlers, K., 2019. Soil organic carbon stock as an indicator for monitoring land and soil degradation in relation to United Nations' Sustainable Development Goals. Land Degradation and Development, v. 30 (7), 824-838. https://doi.org/10.1002/ldr.3270.

Luo, Z.; Viscarra-Rossel, R., 2020. Soil properties override climate controls on global soil organic carbon stocks. https://doi.org/10.5194/bg-2020-298.

Luo, Z.; Viscarra-Rossel, R. A.; Qian, T., 2021. Similar importance of edaphic and climatic factors for controlling soil organic carbon stocks of the world. Biogeosciences, v. 18 (6), 2063-2073. https://doi.org/10.5194/bg-18-2063-2021.

Lützow, M. V.; Kögel-Knabner, I.; Ekschmitt, K.; Matzner, E.; Guggenberger, G.; Marschner, B.; Flessa, H., 2006. Stabilization of organic matter in temperate soils: Mechanisms and their relevance under different soil conditions - A review. European Journal of Soil Science, v. 57 (4), 426-445. https://doi.org/10.1111/j.1365-2389.2006.00809.x.

Mäkipää, R.; Menichetti, L.; Martínez-García, E.; Törmänen, T.; Lehtonen, A., 2024. Is the organic carbon-to-clay ratio a reliable indicator of soil health? Geoderma, v. 444. https://doi.org/10.1016/j.geoderma.2024.116862.

McBratney, A.; Field, D. J.; Koch, A., 2014. The dimensions of soil security. Geoderma, v. 213, 203-213. https://doi.org/10.1016/j.geoderma.2013.08.013.

MEA., 2003. Millennium Ecosystem Assessment. Ecosystems and Human Well-Being: a Framework for Assessment.

Mitchell, J. K., Soga, K., 2005. Fundamentals of soil behavior. Third edition. John Wiley & Sons, New Jersey, 522 p.

Muhammad, M.; Wahab, A.; Waheed, A.; Hakeem, K. R.; Mohamed, H. I.; Basit, A.; Toor, M. D.; Liu, Y. H.; Li, L.; Li, W. J., 2025. Navigating Climate Change: Exploring the Dynamics Between Plant–Soil Microbiomes and Their Impact on Plant Growth and Productivity. Global Change Biology, v. 31(2). https://doi.org/10.1111/gcb.70057.

Olson, K. R.; Al-Kaisi, M. M.; Lal, R.; Lowery, B., 2014. Experimental Consideration, Treatments, and Methods in Determining Soil Organic Carbon Sequestration Rates. Soil Science Society of America Journal, v. 78 (2), 348-360. https://doi.org/10.2136/sssaj2013.09.0412.

O'Riordan, R.; Davies, J.; Stevens, C.; Quinton, J. N.; Boyko, C., 2021. The ecosystem services of urban soils: A review. Geoderma, v. 395 (115076). https://doi.org/10.1016/J.GEODERMA.2021.115076.

Orlova, K. S.; Savin, I. Y., 2024. Ecosystem Services Provided by Urban Soils and Their Assessment: A Review. Eurasian Soil Science, v. 57 (6), 1072-1083. https://doi.org/10.1134/S1064229324600155.

Paltineanu, C.; Dumitru, S.; Vizitiu, O.; Mocanu, V.; Lăcătusu, A. R.; Ion, S.; Domnariu, H., 2024. Soil organic carbon and total nitrogen stocks related to land use and basic environmental properties − assessment of soil carbon sequestration potential in different ecosystems. Catena, v. 246. https://doi.org/10.1016/j.catena.2024.108435.

Paustian, K.; Lehmann, J.; Ogle, S.; Reay, D.; Robertson, G. P.; Smith, P., 2016. Climate-smart soils. Nature, v. 532 (7597), 49-57. https://doi.org/10.1038/nature17174.

Pereira, P.; Bogunovic, I.; Muñoz-Rojas, M.; Brevik, E. C., 2018. Soil ecosystem services, sustainability, valuation and management. Current Opinion in Environmental Science and Health, v. 5, 7-13https://doi.org/10.1016/j.coesh.2017.12.003.

Poeplau, C.; Don, A.; Six, J.; Kaiser, M.; Benbi, D.; Chenu, C.; Cotrufo, M. F.; Derrien, D.; Gioacchini, P.; Grand, S.; Gregorich, E.; Griepentrog, M.; Gunina, A.; Haddix, M.; Kuzyakov, Y.; Kühnel, A.; Macdonald, L. M.; Soong, J.; Trigalet, S.; Nieder, R., 2018. Isolating organic carbon fractions with varying turnover rates in

temperate agricultural soils – A comprehensive method comparison. Soil Biology and Biochemistry, v. 125, 10-26. https://doi.org/10.1016/j.soilbio.2018.06.025.

Poeplau, C.; Gregorich, E., 2022. Advances in measuring soil organic carbon stocks and dynamics at the profile scale, 323–350. https://doi.org/10.19103/as.2022.0106.10.

Poeplau, C.; Vos, C.; Don, A., 2017. Soil organic carbon stocks are systematically overestimated by misuse of the parameters bulk density and rock fragment content. SOIL, v. 3 (1), 61-66. https://doi.org/10.5194/SOIL-3-61-2017.

Poeplau, C.; Jacobs, A.; Don, A.; Vos, C.; Schneider, F.; Wittnebel, M.; Tiemeyer, B.; Heidkamp, A.; Prietz, R.; Flessa, H., 2020. Stocks of organic carbon in German agricultural soils: Key results of the first comprehensive inventory. Journal of Plant Nutrition and Soil Science, 183(6), 665–681. https:// doi. org/ 10.1002/ jpln. 20200 0113

Possinger, A. R.; Zachman, M. J.; Enders, A.; Levin, B. D. A.; Muller, D. A.; Kourkoutis, L. F.; Lehmann, J., 2020. Organo–organic and organo–mineral interfaces in soil at the nanometer scale. Nature Communications, v. 11 (1). https://doi.org/10.1038/s41467-020-19792-9.

Pouyat, R.; Groffman, P.; Yesilonis, I.; Hernandez, L., 2002. Soil carbon pools and fluxes in urban ecosystems. Environmental Pollution, v. 116 (1), 107-118. https://doi.org/10.1016/S0269-7491(01)00263-9.

Prescott, C. E.; Vesterdal, L., 2021. Decomposition and transformations along the continuum from litter to soil organic matter in forest soils. Forest Ecology and Management, v. 498. https://doi.org/10.1016/j.foreco.2021.119522.

Primavesi, A. M, 2018. A biocenose do solo na produção vegetal e deficiências minerais em culturas: nutrição e produção vegetal. Primeira ed., Expressão Popular, São Paulo, 608 p.

Prout, J. M.; Shepherd, K. D.; McGrath, S. P.; Kirk, G. J. D.; Haefele, S. M., 2021. What is a good level of soil organic matter? An index based on organic carbon to clay ratio. European Journal of Soil Science, v. 72 (6), 2493-2503. https://doi.org/10.1111/ejss.13012.

Rabot, E.; Wiesmeier, M.; Schlüter, S.; Vogel, H. J., 2018. Soil structure as an indicator of soil functions: A review. Geoderma, v. 314, 122-137. https://doi.org/10.1016/j.geoderma.2017.11.009.

Raiesi, F., 2017. A minimum data set and soil quality index to quantify the effect of land use conversion on soil quality and degradation in native rangelands of upland arid and semiarid regions. Ecological Indicators, v. 75, 307-320. https://doi.org/10.1016/j.ecolind.2016.12.049.

Ridsdale, D. R.; Noble, B. F., 2016. Assessing sustainable remediation frameworks using sustainability principles. Journal of Environmental Management, v. 184 (3644). https://doi.org/10.1016/j.jenvman.2016.09.015.

Rocci, K. S.; Lavallee, J. M.; Stewart, C. E.; Cotrufo, M. F., 2021. Soil organic carbon response to global environmental change depends on its distribution between mineral-associated and particulate organic matter: A meta-analysis. Science of the Total Environment, v. 793. https://doi.org/10.1016/j.scitotenv.2021.148569.

Rodrigues, A. F.; Latawiec, A. E.; Reid, B. J.; Solórzano, A.; Schuler, A. E.; Lacerda, C.; Fidalgo, E. C. C.; Scarano, F. R.; Tubenchlak, F.; Pena, I.; Vicente-Vicente, J. L.; Korys, K. A.; Cooper, M.; Fernandes, N. F.; Prado, R. B.; Maioli, V.; Dib, V.; Teixeira, W. G., 2021. Systematic review of soil ecosystem services in tropical regions. Royal Society Open Science, v. 8 (3). https://doi.org/10.1098/rsos.201584.

Rodríguez-Albarracín, H. S.; Demattê, J. A. M.; Rosin, N. A.; Contreras, A. E. D.; Silvero, N. E. Q.; Cerri, C. E. P.; Mendes, W. de S.; Tayebi, M., 2023. Potential of soil minerals to sequester soil organic carbon. Geoderma, v. 436. https://doi.org/10.1016/j.geoderma.2023.116549.

Roy, B.; Sagan, V.; Alifu, H.; Saxton, J.; Ghoreishi, D.; Shakoor, N., 2024. Soil Carbon Estimation From Hyperspectral Imagery With Wavelet Decomposition and Frame Theory. IEEE Trans Geosci Remote Sens, v. 62. https://doi.org/10.1109/TGRS.2024.3461628

Santos Brito, A.; Libardi, P. L.; Mota, J. C. A.; Moraes, S. O., 2011. Estimativa da capacidade de campo pela curva de retenção e pela densidade de fluxo da água. Rev. Bras. Ciênc. Solo, v. 35 (6). https://doi.org/10.1590/S0100-06832011000600010.

Scartazza, A.; Gavrichkova, O.; Pini, R.; D'Acqui, L. P., 2023. Physically protected organic matter drives soil carbon sequestration potential of a managed grassland ecosystem in Italian Alps. Geoderma Regional, v. 34. https://doi.org/10.1016/j.geodrs.2023.e00686.

Schmidt, M. W. I.; Torn, M. S.; Abiven, S.; Dittmar, T.; Guggenberger, G.; Janssens, I. A.; Kleber, M.; Kögel-Knabner, I.; Lehmann, J.; Manning, D. A. C.; Nannipieri, P.; Rasse, D. P.; Weiner, S.; Trumbore, S. E., 2011. Persistence of soil organic matter as an ecosystem property. Nature v. 478 (7367), 49-56. https://doi.org/10.1038/nature10386.

Séré, G.; Lothode, M.; Blanchart, A.; Chirol, C.; Tribotte, A.; Schwartz, C., 2024. Destisol: A decision-support tool to assess the ecosystem services provided by urban soils for better urban planning. European Journal of Soil Science, v. 75 (5). https://doi.org/10.1111/ejss.13557.

Six, J.; Doetterl, S.; Laub, M.; Müller, C. R.; Van De Broek, M., 2024. The six rights of how and when to test for soil C saturation. SOIL; v. 10 (1), 275–279. https://doi.org/10.5194/soil-10-275-2024

Sharififar, A.; Minasny, B.; Arrouays, D.; Boulonne, L.; Chevallier, T.; van Deventer, P.; Field, D. J.; Gomez, C.; Jang, H.; Jeon, S.; Koch, J.; McBratney, A. B.; Malone, B. P.; Marchant, B. P; Martin, M. P.; Monger, C.; Munera-Echeverri, J.L.; Padarian,J.; Pfeiffer, M.; Richer-de-Forges, A. C.; Saby, N. P. A.; Singh,K.; Song, X.; Zamanian, K.; Zhang, G.; van Zijl, G., 2023. Soil inorganic carbon, the other and equally important soil carbon pool: distribution, controlling factors, and the impact of climate change. Advances in Agronomy, v. 178, 165-231. https://doi.org/10.1016/bs.agron.2022.11.005.

Si, Y.; Xiong, L.; Chen, Y.; Zhu, J.; Xie, J.; Gao, R.; Yang, Y., 2018. Contribution of the vertical movement of dissolved organic carbon to carbon allocation in two distinct soil types under Castanopsis fargesii Franch. and C. carlesii (Hemsl.) Hayata forests. Annals of Forest Science, v. 75 (3). https://doi.org/10.1007/s13595-018-0756-0.

Sims, N. C.; Barger, N. N.; Metternicht, G. I.; England, J. R., 2020. A land degradation interpretation matrix for reporting on UN SDG indicator 15.3.1 and land degradation neutrality. Environmental Science and Policy, v. 114, 1-6. https://doi.org/10.1016/j.envsci.2020.07.015.

Six, J.; Conant. R. T.; Paul, E. A.; Paustian, K., 2002. Stabilization mechanisms of soil organic matter: implications for C- saturation of soils, 2002. Plant and Soil, v. 241, 155-176. https://doi.org/10.1023/A:1016125726789.

Six, J.; Doetterl, S.; Laub, M.; Müller, C. R.; Van De Broek, M., 2024. The six rights of how and when to test for soil C saturation. SOIL, v. 10 (1), 275-279. https://doi.org/10.5194/soil-10-275-2024.

Smith, P.; Lutfalla, S.; Riley, W. J.; Torn, M. S.; Schmidt, M. W. I.; Soussana, J. F., 2018. The changing faces of soil organic matter research. European Journal of Soil Science, v. 69 (1), 23-30. https://doi.org/10.1111/ejss.12500.

Souza Medeiros, A. DE; Silva Soares, A. A.; Ferreira Maia, S. M., 2022. Soil carbon stocks and compartments of organic matter under conventional systems in Brazilian semi-arid region. Revista Caatinga, v. 35 (3), 697-710. https://doi.org/10.1590/1983-21252022v35n321rc.

Sun, G.; Mu, M., 2022. Role of hydrological parameters in the uncertainty in modeled soil organic carbon using a coupled water-carbon cycle model. Ecological Complexity, v. 50. https://doi.org/10.1016/j.ecocom.2022.100986.

Sun, Y.; Wang, X.; Zhang, Y.; Duan, W.; Xia, J.; Wu, J.; Deng, T., 2024. Vegetation types can affect soil organic carbon and δ13C by influencing plant inputs in topsoil and microbial residue carbon composition in subsoil. Sustainability v. 16 (11). https://doi.org/10.3390/su16114538.

Tan, K. H., 2003. Humic Matter in Soil and the Environment: Principles and Controversies. Marcel Dekker, New York, 408 p.

van den Bergh, S. G.; Chardon, I.; Leite, M. F. A.; Korthals, G. W.; Mayer, J.; Cougnon, M.; Reheul, D.; de Boer, W.; Bodelier, P. L. E., 2024. Soil aggregate stability governs field greenhouse gas fluxes in agricultural soils. Soil Biology and Biochemistry, v. 191. https://doi.org/10.1016/j.soilbio.2024.109354.

Védère, C.; Lebrun, M.; Honvault, N.; Aubertin, M. L.; Girardin, C.; Garnier, P.; Dignac, M. F.; Houben, D.; Rumpel, C., 2022. How does soil water status influence the fate of soil organic matter? A review of processes across scales. Earth-Science Reviews, v. 234. https://doi.org/10.1016/j.earscirev.2022.104214.

Verma, P.; Ghosh, P. K., 2024. The economics of forest carbon sequestration: a bibliometric analysis. Environment, Development and Sustainability, v. 26 (2), 2989-3019. https://doi.org/10.1007/s10668-023-02922-w.

von Lützow, M.; Kögel-Knabner, I.; Ekschmitt, K.; Flessa, H.; Guggenberger, G.; Matzner, E.; Marschner, B., 2007. SOM fractionation methods: Relevance to functional pools and to stabilization mechanisms. Soil Biology and Biochemistry, v. 39 (9), 2183-2207. https://doi.org/10.1016/j.soilbio.2007.03.007.

Xiao, C. L.; Ji, N. H.; Wang, P.; He, J. R.; Wang, X.; Li, L., 2025. Crop diversity significantly enhances soil carbon sequestration via alleviating soil inorganic carbon decline caused by rhizobium inoculation. Soil Tillage Res, v. 245. https://doi.org/10.1016/j.still.2024.106286

Wang, M.; Zhang, S.; Guo, X.; Xiao, L.; Yang, Y.; Luo, Y.; Mishra, U.; Luo, Z., 2024. Responses of soil organic carbon to climate extremes under warming across global biomes. Nature Climate Change, v. 14 (1), 98-105. https://doi.org/10.1038/s41558-023-01874-3.

Wei, Y.; Wang, M.; Viscarra Rossel, R. A.; Chen, H.; Luo, Z., 2024. Extreme climate as the primary control of global soil organic carbon across spatial scales. Global Biogeochemical Cycles, v. 38 (11). https://doi.org/10.1029/2024GB008200.

Yu, F.; Liu, Q.; Fan, C.; Li, S., 2023. Modeling the vertical distribution of soil organic carbon in temperate forest soils on the basis of solute transport. Frontiers in Forests and Global Change, v. 6. https://doi.org/10.3389/ffgc.2023.1228145.

Yusuf, A. Y.; Silvester, E.; Brkljaca, R.; Birnbaum, C.; Chapman, J.; Grover, S., 2024. Peatland carbon chemistry, amino acids and protein preservation in biogeochemically distinct ecohydrologic layers. European Journal of Soil Science, v. 75 (3). https://doi.org/10.1111/ejss.1351

3. SOC stock and physico-chemical analysis

Soil is at the center of ecological solutions. In cities, it supports infrastructure and provides fundamental ecosystem services (*ES*) that contribute to human well-being and climate regulation. Sustainable cities require functional soils to perform green solutions. This study investigates physical-chemical and mineralogical properties of three classes of land use and cover soil profiles in the city of Rio de Janeiro, Brazil, and quantifies the soil organic carbon stock in the total soil (*Cstock*) and in the soil organic matter (SOM) fractions: particulate organic matter (*PCstock*) and mineral-associated organic matter (*MCstock*). Soil profiles in the areas of non-native vegetation forest (NNF), dense ombrophylous forest in the initial stage (FIS), and bare soil fill (BSF) were investigated up to a depth of 1 m, divided into five sections of 20 cm. The results revealed that C*stock* within the 1 m deep profile in the vegetated areas (NNF and FIS) are similar and nearly 38% higher than in the landfilled area (BSF) due to the deposition of organic matter in their surface. In contrast, the Technosol profile (BSF) presented a higher *Cstock* in the subsoil due to the organic matter added into the landfilled material.
The preserved green-cover class (NNF) exhibited a natural soil profile with a higher stock in the persistent form of SOM (MCstock). It is confirmed that the soil dry density has a high influence on the Cstock and must be carefully determined in highly heterogeneous urban soil profiles. The physicochemical and mineralogical soil properties showed similarities and dissimilarities between soil profiles; however, statistical analysis revealed significant differences among the three studied areas. Correlations between Cstock and geotechnical parameters did not present strong significance when considering the three profiles as a whole, although they were representative when considering only the more homogenous material.
Further urban soil investigation in similar areas is required to increase the statistical dataset and confirm correlations. At the end, it is shown that soil physicochemical and mineralogical characteristics of each land use and cover class in Rio de Janeiro may affect their potential for carbon storage and sequestration.

Keywords: urban soil, soil properties, geotechnics, SOM stabilization, SOM fractions.

3.1. Introduction

Soil holds two and a half times the amount of carbon in the atmosphere. It is a fundamental sink in the global carbon cycle to restore ecosystems and climate change adaptation in the face of ecological crises caused by human activities (Batjes, 1998; Lal et al., 2015). In addition, soil is the basis of essential ecosystem services (ES) for life (e.g., Baer & Birgé, 2018).

Recent anthropogenic activities have increased greenhouse gas emissions (GHG) more than before, impacting global warming and ecosystem functions (Friedlingstein et al., 2020). Part of the problem stems from soil conversion resulting from agricultural, forestry, and other land-use transformations (IPCC, 2023; Sanderman et al., 2017). Then, soil conservation and restoration strategies appear as mitigation and adaptation solutions across systems (Janzen, 2004; Lal, 2004). In this context, soil organic carbon stock (*C stock*) is the indicator to assess soil quality, levels of restoration and ES potential (Kopittke et al., 2022; Lorenz et al., 2019; MEA, 2003).

SOC results from the deposition and degradation of organic matter (OM) on the soil surface and subsurface (Jobbágy & Jackson, 2000). Its dynamics are complex, and depend on plant inputs, soil structure, water flux and microbiological metabolism (Lehmann & Kleber, 2015). SOM occurs in various sizes and shapes during different stages of decomposition. Most of them are encountered in two soil fractions: the particulate organic matter (POM), which presents a lower density (<1.60 to 1.85 g cm^{-3}) and larger size (0,053 < ϕ < 2mm), and the mineral-associated organic matter (MAOM), which has higher density (>1.85 g cm^{-3}) and smaller size (< 53 µm). While POM may be free in soil pores or physically protected in soil clusters, MAOM is typically adsorbed in clay minerals (Lavallee et al., 2019).

SOM fractions are regulated by edaphic factors that impact SOC storage (Cotrufo et al., 2019). Efforts to understand SOC dynamics have mainly been applied to investigate natural and cultivated soils (e.g., Huang et al., 2020; Minasny et al., 2017; Yu et al., 2024). However, soil under urban areas also has the potential to store carbon (Lorenz & Lal, 2015; Pouyat et al., 2002a, 2006). Besides climate mitigation, the restoration of urban soil can enhance soil, air and water quality by providing ecosystem services derived from soils (O'Riordan et al., 2021; Orlova & Savin, 2024).

According to Zhao M et al. (2022), 0.68 % of the total global surface is urbanized. However, despite the small relative area, approximately 57.0 % of the global population lives in cities (UN Population Division, 2025). Moreover, there is a prediction of urban land expansion, which will reduce urban system stability and resilience, leaving people exposed to extreme heat events, floods and air pollution (Hu et al., 2025). These trends have sparked interest in urban SOC management, highlighting the importance of balancing urban expansion, ecosystem protection, and human well-being (Feng et al., 2025; V. I. Vasenev et al., 2018).

Soil is a complex, particulate, and multiphase system. Its structure comprises a combination of the soil matrix and pore arrangements (void spaces) that can be filled with different types of fluids, and as pointed out by Primavesi (2018), where microorganisms perform biocenoses. Furthermore, soil carbon dynamics vary according to soil structure, and it is subject to the soil-plant-atmosphere interaction. Urban soils undergo several anthropogenic disturbances, such as transport and deposition, mixing and sealing, that may result in short cycles of soil formation, primarily in the topsoil. Anthrosols (soils under strong human influence) and Technosols (soils containing significant amounts of artifacts) are two general classifications of disturbed soils, also used for soils in urban areas (IUSS Working Group WRB, 2015). Nonetheless, classification taxonomies for soils of urban, industrial, traffic, mining and military areas (SUITMA) are still being studied (Charzynski et al., 2017; Costa et al., 2019). For instance, in Brazil, Furquim and Almeida (2022) pointed out the need to incorporate anthropic soils in the Brazilian Soil Classification System.

In general, urban soil is characterized by higher spatial heterogeneity, both horizontally and vertically (Zhang et al., 2021); it is subject to (i) functional zones such as recreational, industrial, and residential, (ii) surface features: sealed or open; and (iii) pseudo-natural or engineered disturbances (Morel et al., 2015). In addition, indirect anthropic disturbances (climate, chemical pollutants, biome, and invasive species) and direct human-made conversions, such as land-use and cover changes, physical compaction, and management practices (fertilization, composting, or soil organic matter removal), affect carbon storage in urban soils (Trammell et al., 2018).

Research on soil characterization and SOC dynamics in urban ecosystems has gained attention in recent years (Burghardt et al., 2015; Burgos Hernández et al.,

2019; Cambou et al., 2018, 2023; Chien & Krumins, 2022; Feng et al., 2025; H. Guo et al., 2024; Y. Guo et al., 2024; Tagiverdiev et al., 2020; Tiema & Gasiorek, 2024; V. I. Vasenev et al., 2018). However, the investigation of urban soil still embraces several challenges.

Sampling is constrained by soil variation and limited access, such as sealing, ownership permission and community approval (Legg & Hodges, 2024; Stevenson & Hartemink, 2024). There is a lack of standard methods for specific urban soil investigation, particularly at depth (Burghardt et al., 2015) and there are still divergences in methods (e.g., Dupla et al., 2024) and equations employed to calculate the SOC stock (e.g., Poeplau et al., 2017). Indeed, it is a new discipline compared to others in soil science (Scharenbroch et al., 2018).

In this context, this study evaluated profiles of three classes of land use and cover of unsealed soils in Rio de Janeiro, Brazil. Initially, the physical, chemical, and mineralogical characteristics of the soil profile to a depth of 1 m in the classes were evaluated. Then, the soil organic carbon stock in the total soil (Cstock) and the soil organic matter fractions POM and MAOM (*PCstock* and *MCstock*) were quantified in the soil profiles at a given point in time. Following, correlations between soil geotechnical indexes and physical-chemical and mineralogical variables with SOC content and Cstock in the areas were developed. Finally, statistical similarities and dissimilarities between classes are pointed out.

3.2. Materials and Methods

3.2.1. Study area

The study was conducted in Rio de Janeiro city at the Pontifical Catholic University of Rio de Janeiro (PUC-Rio) campus in the Gávea district. The campus is located at a low elevation of the Tijuca Massif, within coordinates 22°58’70” S and 43°14’00’’ W. According to the Köppen classification system, the climate in the region is tropical with a dry winter (Aw) (Alvares et al., 2013). The mean annual temperature is 23.6 °C, and the mean annual precipitation is 1,252 mm, with the rainy period concentrated in the summer (December to March) (https://clima.inmet.gov.br).

Locally, the geology is quite complex, comprising granitic-gneissic bedrock located some 14 to 27 meters below the ground surface. The soil profile in the region may

present sedimentary (colluvial and alluvial soils), residual (mature and young or saprolitic soils) and landfill soil with variable thickness (De Campos, 2020).

3.2.2. Land use and change

According to Drummond (1997), the documented history of land use in the Tijuca Massif dates back to Brazil's colonization in the 16th century. Until 1817, the land was used for summer residences, orchards and farming (mainly sugar cane and coffee plantations) under an intense deforestation process that caused water scarcity in the watershed. From the mid-19th century onward (1845 - 1848), a reforestation project was established on the massif's slopes, resulting in the existing conservation area of the National Park of the Tijuca Forest (PNT). Simultaneously, urbanization advanced in the lower lands.

The university campus was established in the area in 1945. Nowadays, it comprises constructed areas, pavements, and unsealed soil, as well as fragments of non-native and native forest species.

Rio de Janeiro holds twenty-four classes of land use and cover (SIG Floresta, 2018). At the site (see Figures 8a and 8b), the following classes were identified (Figure 8c):

(i) Bare Soil Fill (BSF): uncover soil fill comprising grains of variable sizes (from clay to gravel), construction and demolition debris, organic matter and rock blocks.

(ii) Dense Ombrophylous Forest in the Initial Stage (FIS): soil under herbaceous and shrubby physiognomy with open or closed cover. Woody plants have an average diameter of 5 cm (breast height), a height of up to 5 meters, and an age of up to 10 years.

(iii) Non-Native Forest (NNF): soil covered with fragments of forest composed of non-native species. It occurs in residential, industrial, unoccupied, or abandoned public and private plots and urban parks.

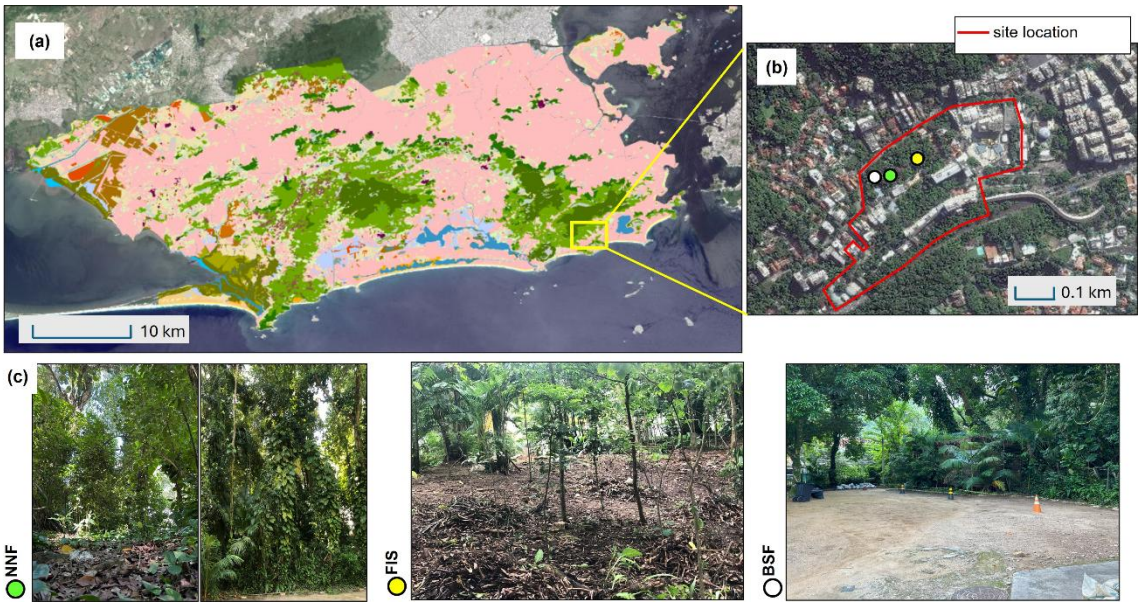

Figure 8. Study area. a) Land use and cover map of the Rio de Janeiro city; b) Site location map, and c) Research plots of NNF, FIS and BSF areas.

3.2.3. Soil sampling and characterization

Remolded and undisturbed samples were collected randomly in 5 x 5 m plots, extending up to 1 m depth in each experimental area. Remolded sampling was done manually with an electrical helical auger. Undisturbed sampling was performed using Geoprobe's Direct Push Subsurface Sampling technology, which utilizes dual tube sampling composed of a soil probe rod (1.75" OD) and a clear PVC liner (1.25" OD). Colored caps were used on the liner ends to differentiate the top and bottom. Physical-chemical-mineralogical soil characterization tests were performed in the laboratory on specimens retrieved from investigated layers corresponding to the topsoil (0 – 20 cm) and the subsoil (20 to 40 cm; 40 to 60 cm; 60 to 80 cm and 80 to 100 cm) nominated in here as layer 1, 2, 3, 4 and 5 from top to bottom.

3.2.4. Physical analysis

Comprised the determination of the specific mass of grains, particle size distribution curve, consistency limits, gravimetric water content, total and dry soil densities and electrical conductivity. Grain size distribution was performed by sieving and sedimentation techniques following the Brazilian standard, NBR 7181: Soil-granulometric analysis *(*ABNT,2025a). Grain sizes were defined according to ABNT (2022a) as gravel (60 – 2.0 mm), sand (2.0 – 0.06 mm), silt (0.06 – 0.002 mm), and clay (< 0.002 mm). Determination of the consistency or Atterberg limits – liquid (w_L) and plasticity (w_P) limits – followed the ABNT (2016a) and ABNT

(2016b), respectively. It was also computed the Skempton clay activity index, *Ac*, given by the ratio between the plasticity index, $PI = w_L - w_P$, and the percentage by weight of clay (Skempton, 1953). Soil classification and content of fines were performed according to the Unified Soil Classification System - USCS (ASTM, 2025).

The specific mass of grains (ρ_s) and gravimetric moisture content (w) were determined according to the ABNT (2025b) and ABNT (2024), respectively. Total density, ρ_t, (ratio between the total soil mass, M, and its total volume, V, and dry soil density, ρ_d, (ratio between the oven dried soil mass or mass of solids, M_s, and the total volume of the specimen, V), were determined in three replicates of undisturbed specimens retrieved from the liner using a volumetric ring (approximately 11 cm³) with an area ratio of circa of 15 % (Clayton et al., 1995). Knowing ρ_s, w and ρ_t, the physical index voids ratio, e, given by V_v/V_s (V_v = volume of voids and V_s = volume of solids) was computed (e.g., Lambe & Whitman, 1969). Electrical conductivity, *EC*, was determined in soil solution with a conductivity meter, Hanna model HI763100, according to FAO (2021a).

3.2.5. Chemical analysis

Comprised the determination of pH, metal elements, organic matter (*OM*), total carbon (*TC*), organic carbon (*OC*), and stable isotope ^{13}C ($\delta^{13}C$).

The pH was measured under a 1:25 suspension of soil: water (*m:v*) using a pHmetro EDGE HI2002-02 from Hanna Instruments, on air-dried and sieved (< 2 mm) specimens, according to FAO (2021b). Samples for heavy metals were treated according to USEPA (1996) in air-dried and sieved (< 2 mm) samples, grounded with a mortar and pestle, and sieved to get a fine powder texture (< 0,15mm). The quantification was performed by inductively coupled plasma optical emission spectrometry (ICP-OES) with Optima DV 4300 (Perkin Elmer, EUA). Both measurements, pH and metal elements, were done in duplicates.

Organic matter (*OM*) determination proceeded according to ABNT (2022b) in triplicate. *TC, OC*, and stable isotope $\delta^{13}C$ determinations were performed in the bulk soil samples (air-dried and sieved < 2 mm) and in the SOM fractions POM (*POC*) and MAOM (*MOC*), which were obtained using the physical size fractionation method suggested by Cotrufo et al. (2019). To do this, bulk soil samples were dispersed in a shaker with glass beads (18 h; ~120 rpm) in a 5 g L^{-1}

sodium hexametaphosphate solution. Fractions were separated by sieving and oven-dried (40 ºC). A fine powder texture was obtained for the bulk soil and SOM fractions (FAO, 2019). The samples for *OC* quantification were acid-washed with 1 M HCl (hydrochloric acid) to remove inorganic carbon.

Carbon analysis was performed by dry combustion in the Elemental Analyzer coupled to Isotope Ratio Mass Spectrometer (EA-IRMS), model Focus-Delta V Plus by Thermo Scientific, with a C limit of detection (LOD) of 3 µg. Carbon determinations were performed in the bulk soil sample in quadruplicate, while the SOM fractions (POM and MAOM) were measured in triplicate.

3.2.6. Mineralogical analysis

Mineralogical analysis patterns were carried out with X-ray diffraction by the powder method in air-dried and sieved samples (< 0.053 mm) with a D8 Advance Bruker XRD diffractometer. Qualitative analysis applies Profex and the EVA program by Bruker, and quantitative analysis follows Doebelin & Kleeberg (2015).

3.2.7. SOC stock quantification

Soil organic carbon stock was calculated in each 20 cm soil layer for the total soil and the SOM fractions, applying Equation 2, proposed by Poeplau et al. (2017) and FAO (2019).

$$Cstock_i(kg\ C\ m^{-2}) = OC_{fine\ earth_i}\ x\ \rho_{dfine\ earth_i}\ x\ depth_i \quad \text{(Eq. 2)}$$

where $Cstock_i$ is the SOC stock in the investigated soil layer (i); $OC_{fines\ earth_i}$ is the soil organic carbon content in the fine earth (< 2 mm) in the layer (g kg^{-1}), $depth_i$ is the thickness of the respective layer (m) and $\rho_{dfines\ earth_i}$ is the dry density of the fine soil fraction, given by Equation 3.

$$\rho_{dfines\ earth_i}\ (g\ cm^{-3}) = \frac{mass_{fine\ earth\ soil}}{volume_{sample}} \quad \text{(Eq. 3)}$$

For each soil layer, the mass of fine soil was obtained by the product of the dry density, ρ_d, by the percentage of soil mass with less than 2 mm (obtained from the respective particle size distribution curve). Equation 2 was also applied to determine the SOC stock for the POM fraction (*PCstock*) and the MAOM fraction

(*MCstock*). To do so, $OC_{fines\ earth_i}$ was obtained by the OC content in the POM fraction (POC_i) and the MAOM fraction (MOC_i).

POC and *MOC* contents were computed considering the percentage in mass of the respective grain size range - POM (2 mm < ϕ > 0.053 mm) and MAOM (ϕ < 0.053 mm) - obtained from the particle size distribution curves of each soil with less than 2mm (see Figure 9).

3.2.8. Statistical analysis

Descriptive data analysis was performed to interpret the mean, standard deviation (*SD*), and the coefficient of variation (*CV*) for each area along the profile. For particle size distribution, the combined coefficient of variation (*CV_c*) was also calculated.

Mean values of variables selected for statistical analysis were tested for normality using the Shapiro-Wilk test. Depending on the outcome, either a parametric (ANOVA) or non-parametric (Kruskal-Wallis) analysis of variance was conducted to assess statistically significant differences among land-use and land-cover classes. When significant differences were detected, post hoc tests (Tukey and Dunnett) were applied.

Statistical differences are indicated by different letters (e.g., a, b, c) in the results. The significance level is represented by *p*-values, with thresholds defined as follows: $p \leq 0.05$ (*), $p \leq 0.01$ (**), and $p \leq 0.001$ (***). Alternatively, significance is discussed in terms of probability values lower than 5%.

Spearman's rank correlation was used to evaluate the relationship (*r*) between physicochemical and mineralogical variables and soil organic carbon (*OC*) and carbon SOC stock (*Cstock*) in the whole soil ($n = 15$) and in the subsoil ($n = 12$), given that the topsoil data were non-parametric. This approach is based on the principle that variables may vary together without a strictly linear relationship (Gauthier, 2001).

Finally, parametric and non-collinear variables were used in a Linear Discriminant Analysis (LDA). All statistical analyses were performed in R software using the RStudio interface (R Core Team, 2024).

3.3. Results

3.3.1. Physical characterization

The soil particle size distribution of the three profiles is shown in Figure 9. The BSF area consists primarily of coarse particles (sand + gravel), while the FIS and the NNF areas present a larger proportion of fines (silt + clay), particularly in the subsoil layers. The topsoil of the FIS and NNF areas displays distributions distinct from those of the subsoil. Along the subsoil, FIS exhibits more variable particle size curves, with a 16.4% combined coefficient of variation (*CV_c*), and NNF preserves more uniformity (*CV_c* = 7.4%).

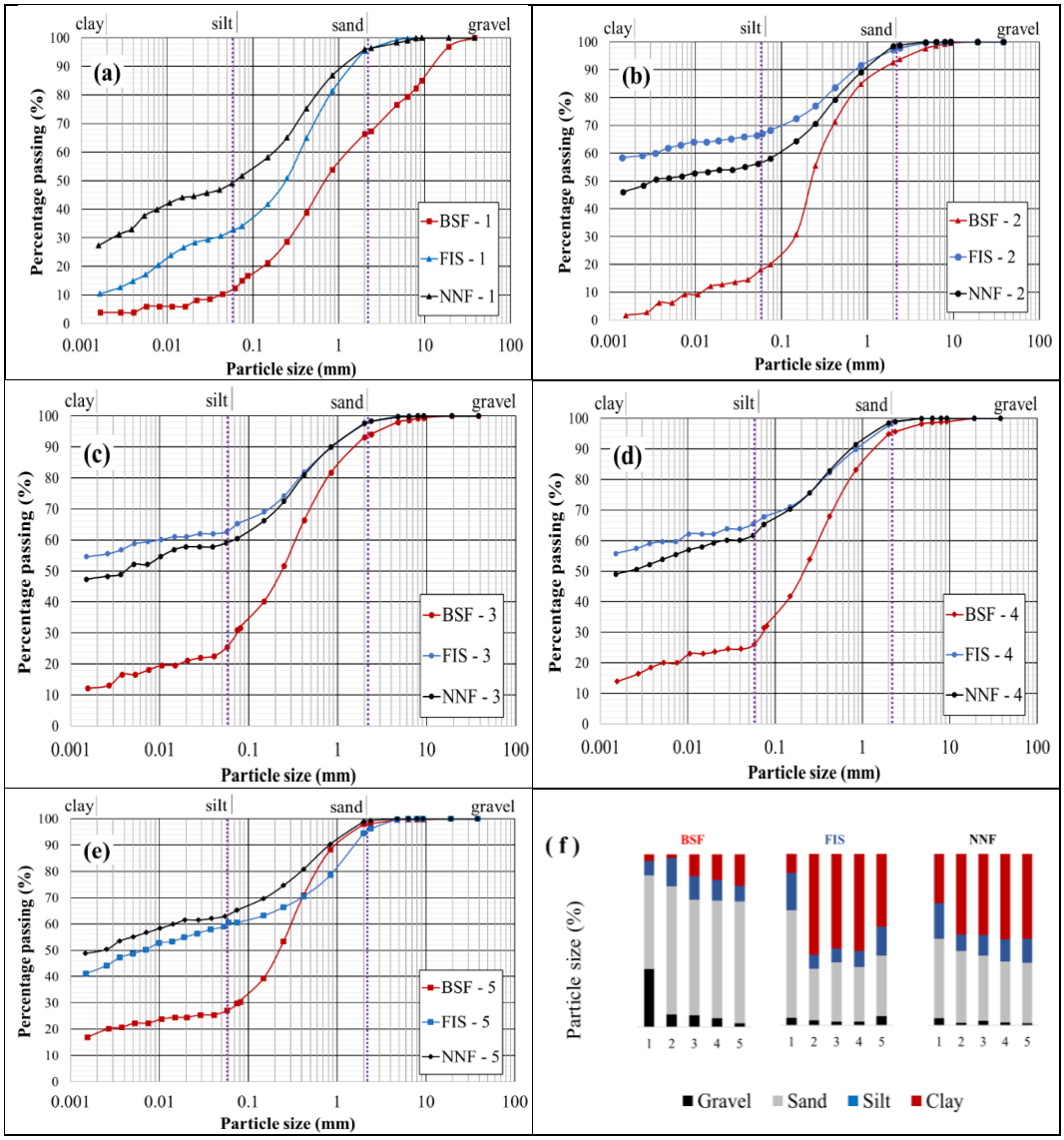

Figure 9. Soil granulometry. Particle size distribution curves of the area BSF, FIS and NNF from layers 1 to 5 in the figures a) to e), respectively. Dashed lines in the graphs indicate particle size limits for SOM fractions POM (2 < φ > 0,053 mm) and MAOM (φ < 0,053 mm); f) Percentage of the grain size content in each layer (1 to 5) in the three areas.

Figure 10 shows the consistency limits for each layer in each area. Note that the BSF 1 specimen is non-plastic, so it was plotted at the chart origin. Figure 10 also includes the soil classification according to the USCS. In this system, the topsoil from the NNF area is classified as high-plasticity silt (MH), while that from the BSF and FIS areas is classified as silty sand (SM). For topsoil, organic classification was excluded by testing the liquid limit values after oven drying (ASTM, 2025).

On the other hand, the subsoil from the NNF and FIS areas is classified as high plasticity clay (CH) and that from the BSF as clayey sand (SC). From the viewpoint of Soil Science, the BSF area is classified as Technosol, while the FIS and the NNF areas are classified as Acrisols (Santos et al., 2025; Lumbreras and Gomes, 2004).

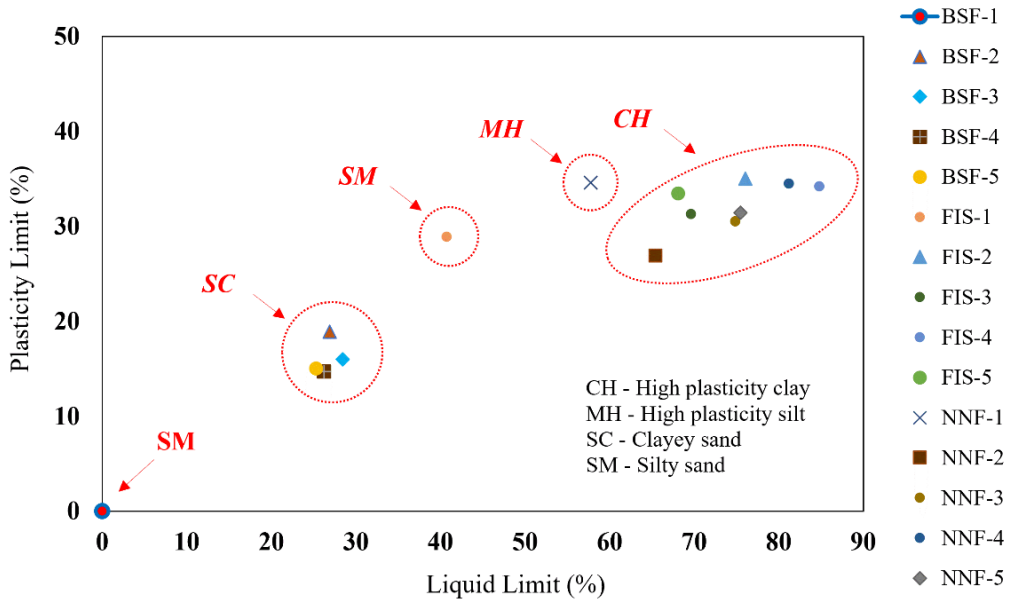

Figure 10. Soil classification and consistency limits by area and depth (layers 1 to 5).

Results of the specific mass of grains (ρ_s), dry soil density (ρ_d), void ratio (e), fines content (%), activity index *(Ac)* and electrical conductivity (EC) are shown in Figure 11.

The BSF area takes the highest ρ_s, which varies little with depth (CV = 0.65 %). The lowest values of ρ_s are found in the upper layer of the FIS and NNF areas, indicating the presence of OM. Dry soil density (ρ_d) - and total density (ρ_t), not shown in Figure 11 - follow similar patterns, while the void ratio (e) presents

opposite patterns, considering differences between topsoil and subsoil. It is interesting to note that the mirrored pattern between ρ_d and e results from the inverse relationship between these two physical soil indices, as shown by Equation 4.

$$e = \frac{\rho_s}{\rho_d} - 1 \qquad \text{(Eq. 4)}$$

The fine content varies considerably between the backfilled (BSF) and the vegetated areas (FIS and NNF), ranging, on average, from ~ 25% to ~ 60% respectively. However, while the content of fines in the FIS reduces in the subsoil, it increases in the BSF and NNF areas.

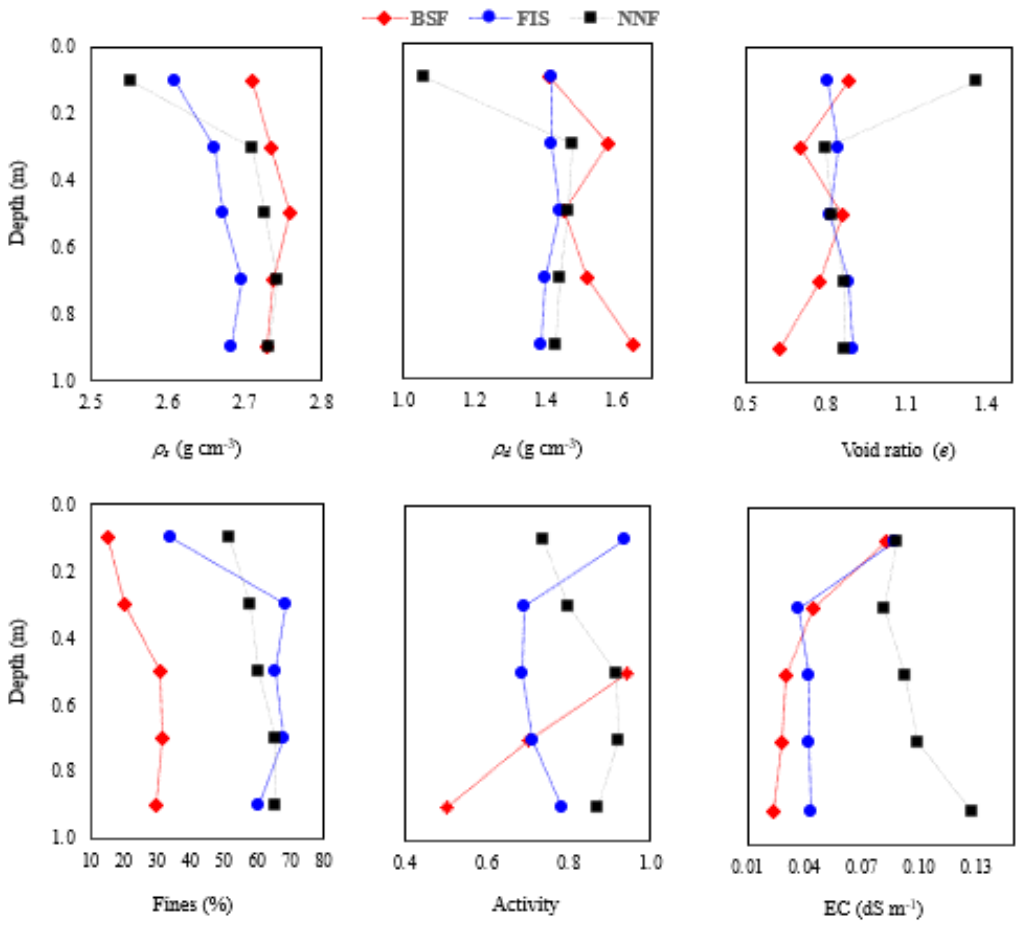

Figure 11. Physical index results per area along the profile: (a) specific mass of grains (ρ_s), (b) dry soil density (ρ_d), (c) void ratio (e), (d) content of fines (%), (e) Activity index (Ac) and (f) electrical conductivity (EC).

Owing to its definition, the activity index (Ac) reflects the variation of both the plasticity index and the clay content. Bearing in mind that this index is

undefined in the non-plastic layers 1 and 2 of the BSF area, decreasing from layer 3 to 5. However, it must be considered that the use of such an index, which reflects the potential reactivity of a given soil (e.g., Mitchel and Soga, 2005), may be seen with care in the case of such a type of soil profile (cohesionless, sandy soil layers). The silty soils from layer 1 of the FIS and NNF profiles provide *Ac* differing from those of the respective subsoil clayey layers. As these subsoil layers present similar plasticity indexes, observed variations reflect differences in clay contents.

Electrical conductivity (*EC*) is about the same in layer 1 (top layer) of all areas, probably reflecting the influence of the temperature and rainfall precipitation on the soil surface (Corwin and Lesch, 2005). In the subsoil, *EC* tends to increase with depth in the NNF area and to become constant with depth in the FIS and BSF areas.

As indicated in Table 3, physical variables (fines, ρ_d and *e*) present statistical differences between the BSF area and the FIS and NNF areas; EC, between the NNF and the BSF and FIS areas, while *Ac* does not present a statistical difference between areas.

Table 3. Statistical tests. Fine content (%), Activity (Ac), Dry soil density (g cm-3), void ratio (e) and Electrical Conductivity (dS m-1) with their respective variance test and significance level (p).

Variable	*n*	Land-use and cover			Teste	*p*	
		BSF	FIS	NNF			
Fines (%)	5	25.44 ± 7.51^{a}	59.19 ± 14.37^{b}	60.14 ± 5.67^{b}	Kruskal-Wallis	0.02	**
Ac	3, 5, 5	0.72 ± 0.22^{a}	0.76 ± 0.11^{a}	0.85 ± 0.08^{a}	Anova	0.178	ns
ρ_d (g cm^{-3})	5	1.52 ± 0.09^{a}	1.41 ± 0.02^{b}	1.37 ± 0.18^{b}	Anova	> 0,001	***
e	5	0.77 ± 0.11^{a}	0.85 ± 0.04^{b}	0.95 ± 0.23^{b}	Anova	0.005	***
EC (dS m^{-1})	5	0.04 ± 0.02^{a}	0.05 ± 0.02^{a}	0.10 ± 0.02^{b}	Kruskal-Wallis	0.02	**

Note: Values are expressed as mean + SD. Different letters denote statistical differences (Tukey or Dunn).

3.3.2. Chemical and mineralogical characterization

The results of pH, total concentration of metal elements and the percentage of the predominant minerals encountered in the profile are presented in Table 4.

The pH gradually changes from slightly alkaline in the BSF area to acidic in the bottom layer of the other two areas. These results reflect the occurrence of construction and demolition waste (CDW) in the BSF area, in contrast with the acidity of the soils resulting from weathering of granite-gneissic rocks in the FIS

and NNF areas. In terms of metal elements, the concentrations of Mn, Mg and K are higher in BSF than in the other areas, probably due to the presence of CDW.

They are also higher in the upper layer of all areas. Fe and Al do not present regular patterns throughout the profiles but show lower concentrations in the topsoil and higher in the subsoil in all areas. Regarding primary minerals, quartz is present in all layers of the three areas, while feldspar occurs in the whole BSF profile and layer 1 of the FIS area. Mica is also present in layers 1 (~ 13.6%) and 3 (~ 8%) of the BSF profile. The clay mineral Kaolinite is present in all layers of the three areas, while Illite was encountered in layer 1 of the BSF profile (~ 18%). The occurrence of oxy-hydroxides is variable in all the profiles.

Table 4. Chemical and mineralogical results: pH, concentration of the Manganese (Mn), Magnesium (Mg), Potassium (K), Iron (Fe) and Aluminum (Al), minerals Kaolinite (Kln), Quartz (Qz), Feldspar (Fsp), and Oxy hydroxides (OxOH) for BSF, FIS and NNF profile, in layers 1 to 5.

Area -Layer	pH	Metal elements					Mineralogy			
		Mn	Mg	K	Fe	Al	Kln	Qz	Fsp	OxOH
		mg kg^{-1}					*wt* (%)			
BSF 1	8.2	342	4011	5752	30495	26230	29.2	18.0	21.0	0.0
BSF 2	7.7	223	2236	3575	33405	27220	69.5	13.1	13.0	2.2
BSF 3	7.8	206	948	775	33405	25710	16.2	23.3	51.9	0.0
BSF 4	8.0	246	567	548	31920	21960	67.7	22.8	5.2	4.4
BSF 5	7.9	204	257	220	26915	19485	38.7	41.9	9.7	5.1
mean	*7.9*	*244*	*1604*	*2174*	*31228*	*24121*	*44.3*	*23.8*	*20.1*	*2.3*
SD	*0.2*	*57*	*1542*	*2407*	*2697*	*3269*	*23.6*	*10.9*	*18.7*	*2.4*
CV	*2.5*	*23.4*	*96.2*	*110.7*	*8.6*	*13.6*	*53.4*	*45.9*	*92.8*	*102.4*
FIS 1	7.5	100	976	489	28185	27030	73.5	14.3	4.3	7.9
FIS 2	6.7	27	249	189	37910	32580	92.5	3.5	0.0	3.5
FIS 3	6.0	18	128	147	36830	30735	92.1	3.7	0.0	4.3
FIS 4	5.0	14	65	140	39675	26535	94.7	2.9	0.0	2.4
FIS 5	4.7	15	65	150	40640	25070	87.8	1.3	0.0	10.9
mean	*6.0*	*35*	*297*	*223*	*36648*	*28390*	*88.1*	*5.1*	*0.9*	*5.8*
SD	*1.1*	*37*	*387*	*150*	*4959*	*3137*	*8.6*	*5.2*	*1.9*	*3.5*
CV	*19.2*	*105.7*	*130.5*	*67.2*	*13.5*	*11.1*	*9.7*	*101.4*	*223.6*	*60.6*
NNF 1	6.4	100	758	405	37670	20060	86.7	9.4	0.0	3.9
NNF 2	4.4	32	165	161	55835	27710	85.0	15.0	0.0	0.0
NNF 3	4.4	29	151	159	55080	27180	89.9	5.8	0.0	4.4
NNF 4	3.9	39	125	160	60110	27475	93.1	3.6	0.0	1.8
NNF 5	3.8	75	128	147	57485	24620	93.2	1.7	0.0	2.1
mean	*4.6*	*55*	*265*	*206*	*53236*	*25409*	*89.6*	*7.1*	*0.0*	*2.4*
SD	*1.1*	*31*	*276*	*111*	*8913*	*3238*	*3.7*	*5.3*	*0.0*	*1.8*
CV	*23.2*	*56.3*	*104.0*	*53.8*	*16.7*	*12.7*	*4.1*	*74.2*	-	*72.8*

3.3.3. Carbon analysis

The contents of organic matter (*OM*), total carbon (*TC*) and soil organic carbon (g kg^{-1}) in the total soil (*OC*) and in the SOM fractions - POM (*POC*) and MAOM (*MOC*) - are displayed in Table 5.

Table 5. Soil carbon parameters results: Organic Matter (OM), total carbon (TC), soil organic carbon in total soil (OC) and in the POM (POC) and MAOM fraction (MOC) for the three land cover classes and layers (n = sample's number).

Class	Layer	*OM*	*TC*	*OC*	*POC*	*MOC*
		%		g kg^{-1}		
		n = 3 / 2*	*n* = 4		*n* = 3	
BSF	1	1.72 ± 0.57	18.00 ± 5.14	16.28 ± 4.71	5.17 ± 0.67	5.02 ± 0.10
	2	1.45 ± 0.28	12.44 ± 1.82	10.92 ± 1.51	7.60 ± 0.97	3.05 ± 0.03
	3	2.75 ± 0.54	11.73 ± 0.64	11.01 ± 0.10	1.93 ± 0.13	4.59 ± 0.08
	4	2.00 ± 0.30	10.08 ± 0.69	9.72 ± 0.76	2.09 ± 0.22	4.03 ± 0.07
	5	1.80 ± 0.11	7.82 ± 0.56	7.05 ± 0.39	0.90 ± 0.05	3.61 ± 0.05
	mean	1.94 ± 0.49[a]	12.014 ± 1.77	11.00 ± 3.36[a]	3.54 ± 2.78	4.06 ± 0.78
	CV (%)	25.30	31.54	30.55	78.44	16.16
FIS	1	7.43 ± 1.00	55.79 ± 14.32	51.06 ± 18.58	16.06 ± 0.31	26.86 ± 0.74
	2	5.10 ± 0.29	14.18 ± 0.46	13.01 ± 1.07	1.65 ± 0.05	10.26 ± 0.55
	3	4.48 ± 0.87	9.34 ± 0.69	8.55 ± 1.29	1.07 ± 0.10	6.01 ± 0.33
	4	4.28 ± 0.39	7.50 ± 0.63	6.65 ± 1.12	0.81 ± 0.06	5.46 ± 0.02
	5	3.45 ± 0.63	5.61 ± 0.27	5.42 ± 0.13	0.87 ± 0.06	3.71 ± 0.07
	mean	4.95 ± 1.51[b]	18.48 ± 3.27	16.94 ± 19.29[b]	4.09 ± 6.70	10.46 ± 9.48
	CV (%)	30.47	114.13	113.89	163.70	90.62
NNF	1	10.57 ± 0.04	85.13 ± 1.77	70.4 ± 15.19	17.52 ± 2.67	49.91 ± 0.24
	2	4.42 ± 0.58	9.90 ± 0.51	8.94 ± 0.78	1.55 ± 0.13	6.65 ± 0.37
	3	3.89 ± 0.25	7.78 ± 0.34	7.37 ± 0.34	1.48 ± 0.09	4.76 ± 0.07
	4	3.46 ± 0.28	7.41 ± 0.10	6.94 ± 0.40	2.74 ± 0.12	4.55 ± 0.05
	5	4.13 ± 0.19	6.84 ± 1.41	6.48 ± 1.51	2.2 ± 0.12	5.44 ± 0.07
	mean	5.23 ± 2.97[b]	23.41 ± 0.83	20.03 ± 28.18[b]	5.1 ± 6.96	14.26 ± 19.94
	CV (%)	56.11	147.45	140.69	136.59	139.84

Note*: m*: mean; *SD*: standard deviation; *CV*: coefficient of variation (%); Letters indicate statistical differences (Tukey or Dunn test, $p < 0.05$). The * in the number of samples (*n*) of the OM indicates a difference between areas: BSF and FIS areas have *n* =3, while the NNF area has *n* = 2.

The amount of *OM* in bulk soil is the smallest in the BSF area. Average values in FIS and NNF profiles present similar magnitudes; however, the variation of *OM* is lower in FIS (*CV* = 30.47 %) than in NNF (*CV* = 56.11%) due to the higher contents of *OM* in the topsoil.

TC and *OC* follow a similar average pattern along the profile in the three areas. In layer 1, the NNF presents the highest concentration of *TC* and *OC*, while in layer 2, this is in the FIS area. Considering layers 3 to 5, these are slightly higher

in the sandy soil of the BSF area than in the clayey soils of the FIS and NNF. As expected, these variables show little difference in the acid subsoil (Gozukara et al., 2025).

The average *POC* and *MOC* in the three areas increases from the backfilled (BSF) area to the FIS and NNF areas. However, it has to be noted that the large difference between the topsoil and the subsoil concentration increases the *CV* in these last two areas.

The average *OC* recovery from the total *OC* in the *POC* and *MOC* in the BSF, FIS and NNF areas was 69.26 %, 87.47%, and 98.99%, respectively.

Figure 12 presents the isotopic composition ($\delta^{13}C$) of the organic carbon in total soil and the SOM fractions POM and MAOM. In the green-covered areas, FIS and NNF, there is an enrichment of $\delta^{13}C$ along the profile in *OC* and *MOC*, indicating distinct levels of organic carbon mineralization in the topsoil and subsoil.

In the BSF area, the *OC* and *MOC* also exhibit an enrichment throughout the profile down to layer 4, whereas in layer 5, depletion occurs. The isotopic signature in *POC* displays less variation along the profile and, as expected, is less enriched in $\delta^{13}C$ on average for all areas (S. Leuthold et al., 2024).

All $\delta^{13}C$ results are in the range of -29.62 ‰ to -22.78 ‰, indicating that the predominant vegetation in the SOM composition originates from C3 plants, which are characterized by forest vegetation (Martinelli et al., 2018).

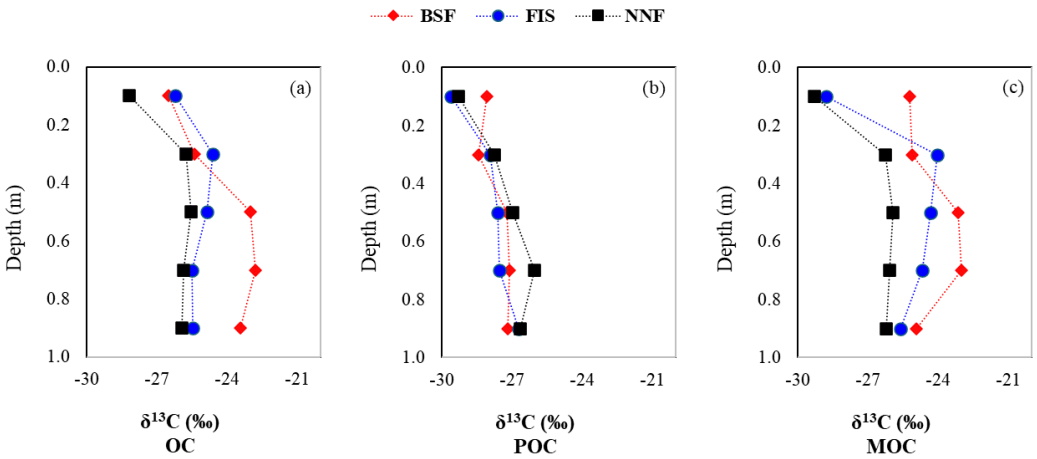

Figure 12. Stable isotope results: δ13C (‰) of organic carbon in the (a) total soil (OC), (b) in the POC fraction and (c) in the MOC fraction in the areas BSF, FIS and NNF along the soil profile.

3.3.4. SOC stock

Figure 13 shows the *Cstock* in each layer of each area. As indicated in Figure 13a, the larger *Cstock* occurs in layer 1 of the NNF area (14.30 kg C m^{-2}) and of the FIS area (13.83 kg C m^{-2}). However, in layer 2, the *Cstock* is larger in the FIS area (3.58 kg C m^{-2}) than that in the NNF (2.60 kg C m^{-2}). From layers 3 to 5, the BSF area presents the highest amounts of *Cstock* compared to the FIS and NNF areas.

Unlike the green areas, the absence of OM inputs in the bare soil of the BSF area implies a uniform *Cstock* along the profile, with an average of 2.86 kg C m^{-2} (*SD* = 0.35). The total *Cstock* in 1 m depth in the BSF, FIS and NNF areas is 14.29 kg C m^{-2}, 23.07 kg C m^{-2} and 22.83 kg C m^{-2}, respectively. The contribution of topsoil *Cstock* is lower in the BSF area (~ 20 %), while it is approximately 60 % in the FIS and NNF areas due to the enriched OM topsoil (Figure 13b). Nonetheless, the *MCstock* contribution in the three areas is higher than the *PCStock,* in a proportion of 54 % and 46 % respectively in the BSF area, and of ~ 72 % and ~ 28 % respectively in the FIS and NNF areas (Figure 13c).

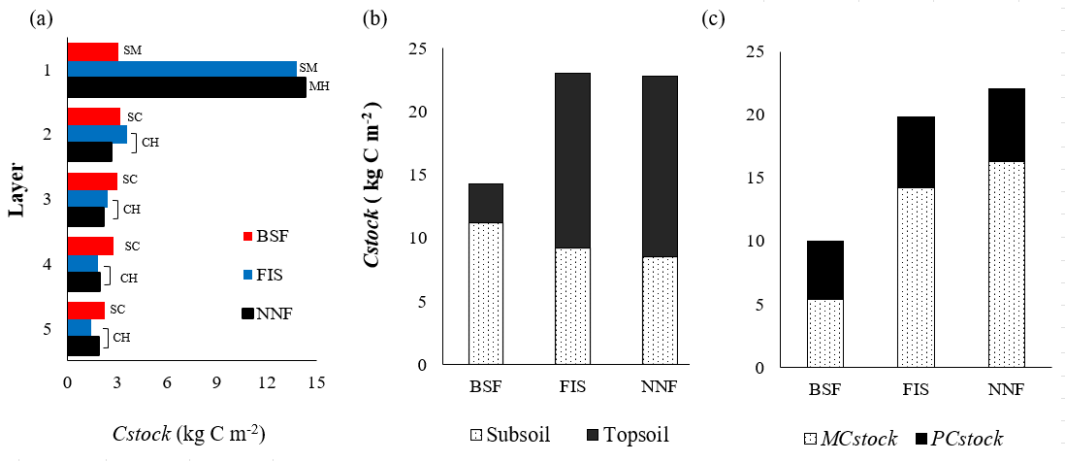

Figure 13. SOC stock results. a) Soil organic carbon stock (kg C m^{-2}) in the areas BSF, FIS and NNF from layers 1 to 5, including at the top of the bar, the type of soil in the respective layer: silty sand (SM), high plasticity silt (MH), clayey sand (SC) and high plasticity clay (CH); b) Soil organic carbon stock in the topsoil (0 – 20 cm) and in the subsoil (20 – 100 cm) and c) Soil organic carbon stock in the MAOM fraction (*MCstock*) and in the POM fraction (*PCstock*) in the three classes of land cover

3.4. Discussion

3.4.1. Soil properties

Urban soil is a distinct material resulting from direct or indirect anthropogenic influences. Along with urbanization, soil may be transported, sealed, compacted, cultivated, leveled, landfilled, or removed, which alters soil properties and results in significant heterogeneity at small scales (Trammel et al. 2018).

The three surveyed classes of land use and cover are located at a short distance, suggesting that they would present similar properties in their natural state. Nevertheless, comparing a more preserved area, NNF, with the reforested area (FIS) and the backfilled area (BSF), the results of soil physical, chemical and mineralogical characterization indicate levels of anthropogenic disturbance.

For instance, the grain size distribution of the areas reflects textural differences between classes. In the BSF area, the gravelly topsoil (~ 34%), associated with the large fraction of sand (~ 70 %) and the lowest fraction of clay (~ 13 %) in the subsoil, confirms the backfilled features of the BSF (Figure 9). On the other hand, the contrast of the fine content, as well as of the Atterberg limits, in the topsoil of the areas FIS and NNF suggests the occurrence of some distinct management practices affecting the topsoil of these areas. This, however, is not observed along their subsoil profiles, which show similar textures.

Further distinctions among the areas are provided by ρ_s, which shows a clear difference between the topsoil of the three areas, while it presents a similar magnitude in their subsoil layers (Figure 11a). Additionally, *e* in the topsoil of area NNF is some ~37% higher than in the areas BSF and FIS. However, in the subsoil, while it is similar in the areas FIS and NNF, it is some 14% smaller in the area BSF.

Chemical and mineralogical parameters also point out the distinction between classes of land use and cover. The average values of Mn, Mg and K in the profile drastically separate the BSF area from FIS and NNF area; however, in terms of Fe concentration, NNF holds about 1.6 times the content of it in BSF and FIS. The diversity of mineralogy in the BSF area, compared to the stable pattern of that in the areas FIS and NNF, also contributes to establishing physicochemical and mineralogical dissimilarities between areas.

Corroborating the above geotechnical analysis, multivariate statistical analysis, considering non-collinear and statistically significant variables (fines

content, pH, OM, Fe, Mg, Mn, K, Kln, Fsp and Qz), shows a clear differentiation among the areas, as illustrated in Figure 14.

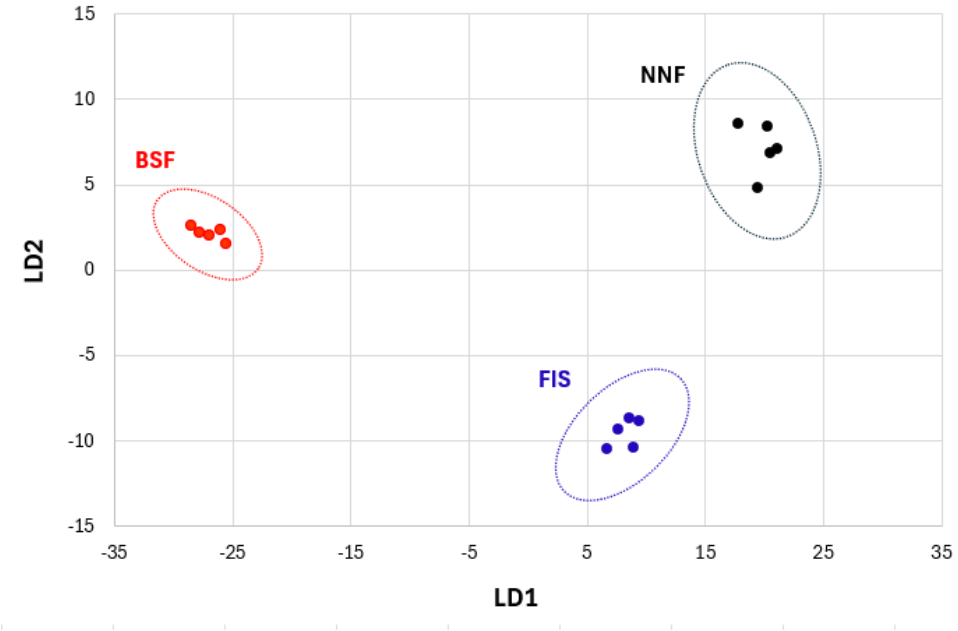

Figure 14. Linear Discriminant Analysis (LDA) for the three areas.

3.4.2. SOC stock in the profiles

As defined earlier, *Cstock* is a parameter expressed in mass per area, given by the product of *OC* content, the dry density of fines and the layer thickness (e.g., Peoplau et al, 2017). Bearing in mind that, the C*stocks* within the whole 1 m deep soil profile in the vegetated areas (NNF and FIS) are ~ 38% higher than in the landfilled area BSF (Figure 13a). This is supported by the higher content of soil OC in layer 1 along the profiles in the green areas (Table 5).

Unexpectedly, the *Cstock* in the mature non-native forest area (NNF), with the richest organic matter (OM) topsoil, is nearly the same as that in the reforested FIS area, which is in an initial vegetation stage. This can be explained by analyzing layers 1 and 2 of both profiles. While the content of *OC* in layer 1 of the NNF area is ~ 27% higher than that in the same layer of the FIS area, the respective dry density of fine earth fraction is ~ 32% smaller in NNF (1.02 g cm^{-3}) than in the FIS (1.35 g cm^{-3}). In this case, the *Cstock* in the topsoil of NNF is only 3.3% higher than in the FIS.

On the other hand, considering layer 2, the OC content is ~ 31% higher in the FIS area than in NNF, while the dry density of fine soil in the FIS area remains nearly the same (1.37 g cm^{-3}), it increases by ~ 30% in the NNF area (1.45 g cm^{-3}). This implies a ~ 28% higher *Cstock* in layer 2 of the FIS area than in the NNF one. As the *Cstock* in the underlying layers (3 to 5) of both areas is about the same, the differences in *OC* and $\rho_{dfine\ earth}$ in layers 1 and 2 explain the similar *Cstock* found for the whole profile of areas FIS and NNF.

Another unexpected result occurs between layers 3 to 5 of the landfilled area (BSF), where the *Cstock* is ~ 25% higher than that in the vegetated areas (FIS and NNF). In this profile section, this pattern also replicates for *OC* (~ 29 % higher) and for the average dry density of fines (~5 % higher). This is probably due to the occurrence of OM fragments such as leaves and branch litter in the landfilled material, which does not occur in the subsoil of the FIS and NNF areas.

It is interesting to note here that, as shown in Figure 15 if, instead of considering a layer thickness of 1m, it was adopted the standard thickness of 30 cm depth considered by FAO (2019), it would be obtained similar *Cstock*s for the vegetated areas NNF and FIS (~15.60 kgC m^{-2} and 15.62 kgC m^{-2}, respectively), while BSF would store 4.64 kgC m^{-2}. Authors such as Pouyat et al. (2006), Lorenz and Lal (2015), Cambou et al. (2018), V. Vasenev & Kuzyakov (2018), Zhang et al. (2021) and H. Guo et al. (2024) provide values of *Cstock* for distinct urban areas around the world. However, comparisons are difficult due to differences in land-cover and use classifications, as well as adopted layer thickness.

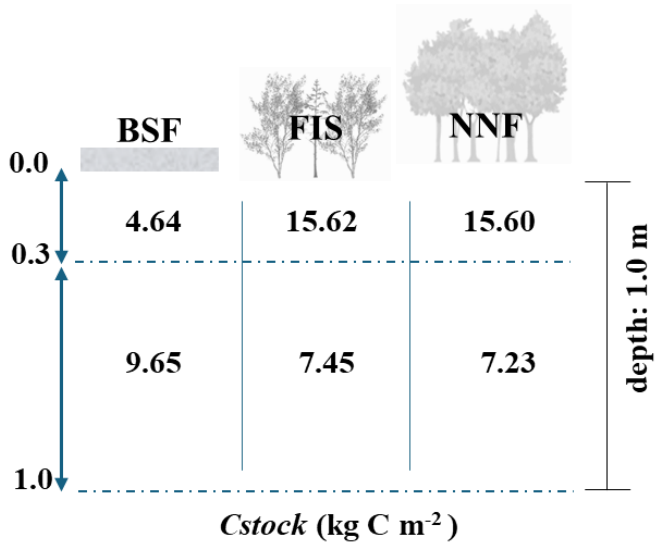

Figure 15. Cstock in the BSF, FIS and NNF areas by thickness of 0 to 30 cm, and the section of 30 to 100 cm depth

3.4.3. SOM fraction dynamics on SOC stocks

Beyond the analysis of total SOC stock, the quantified OC stocks in the SOM fraction provide evidence on the dynamics of SOM in terms of its turnover time, functioning, and formation (Cotrufo et al., 2019). While the MAOM fraction comprises the stabilized OC in soil, which is associated with the soil matrix (organo-mineral complexes and fines aggregates), the POM fraction encompasses the free OM compounds, more vulnerable to land-use changes (Lavallee et al., 2019).

In this study, the amount of mineral-associated organic carbon fraction, expressed by *MCstock,* is higher than the particulate OM stock, *PCstock,* in the three urban soil profiles. The *PCstock* has a similar magnitude in the three areas (*mean* = 5.33 kg C m^{-2}, *SD* = 0.63). In contrast, *MCstock* is ~ 63 % higher than *PCstock* in the green areas (FIS and NNF), while it is only ~ 15% higher in the BSF soil profile (Figure 13c).

Analyzing the dynamics of SOM fractions in layers 1 and 2, *MCstock* is ~73 % lower than *PCstock* in the BSF area. In the vegetated areas, *MCstock* is ~ 67 % higher than *PCstock* in the NNF area, while it is ~ 52 % in the FIS area. Thus, even though the *Cstocks* for total soil in the green areas are nearly the same, the NNF top layers retain more organic carbon in stabilized form than in the FIS area.

From layers 3 to 5, *MCstock* is 81.8% and 56.8% higher than *PCstock* in the FIS and NNF areas, respectively, which comprises ~61% of mass in the grain size range of MAOM (Figure 9). In the BSF area, unexpectedly, *MCstock* is 60.4% higher than *PCstock*, despite the low content of MAOM soil fraction (~25 %) in this profile section.

As mentioned before, *MCstock* is associated with the dry soil density of fines and with the *MOC* content, which is given by the product of *OC* content in the MAOM fraction and the percentage of soil mass in the grain size range of MAOM. Thus, an explanation for the obtained result of *MCstock* in the above-mentioned BSF area would be the high content of *OC* encountered in the MAOM fraction, which is 2 times higher than the *OC* in the MAOM fraction of the FIS and NNF areas, resulting in similar content of *OC* in the MAOM fraction (*MOC*) of the three areas (Table 5).

This higher content of *OC* in the MAOM fraction of layers 3 to 5 of the BSF area may be related to their mineralogical and soil chemical composition characteristics. As shown in Table 4, apart from exhibiting higher pH values, the BSF area contains higher concentrations of Feldspar and metals such as Mn, Mg, and K than the other two areas. As reported by Behera & Shukla (2015), Khaledian et al. (2017), L. Xiao et al. (2016), Brüggenwirth et al. (2024), Dhaliwal et al. (2024) and Montgomery et al. (2025), and also it will be seen next, there are positive correlations between these variables and the soil organic carbon (*OC*).

3.4.4. Soil properties correlations with *OC* and *Cstock*

In this study, Spearman´s correlation was employed to evaluate the connection between the geotechnical parameters and soil properties with the soil *OC* and *Cstock*. For that, the soil data were unified without division between areas, depth, and type of soil. It was considered a single sample dataset.

Initially, correlations were performed for all soil samples (n = 15), which included results from the five layers of the three areas (Figure 16). Afterward, correlations were made in a sample dataset considering only the subsoil (n =12) (Figure 17).

Correlations considering the whole soil samples (n = 15) present a high number of strong significant correlations. Moderate significant correlations with soil *OC* occur with *pH*, *Fe, Mn,* Kaolinite and Quartz (> 0.5 and < - 0.5, $p \leq 0.05$), while the strong ones occur for the metals Mg and K ($p \leq 0.01$). These significant correlations also happen with Cstock in the whole soil, except for the minerals *Kln* and *Qz*. These findings are supported by results put forward by Montgomery et al. (2025).

Despite the strong correlations of the chemical and mineralogical variables considering the whole sample dataset, geotechnical parameters, such as *fines, Ac,* ρ_d, void ratio *(e), EC and OM*, do not present significant correlations with soil *OC* and *Cstock,* besides the weak correlation for fines (-0.45; $p > 0.05$).

In the analysis of the correlations for the subsoil sample dataset *(n* =12), the correlation between *OC* and *Cstock* with *Mg* ($p \leq 0.001$) and K ($p \leq 0.01$) presents strong significance, while the correlations with pH are moderate. In contrast, the other metals and minerals show non-significant and weak correlations ($0.3 < r < 0.6$ and $-0.4 > r > -0.6$, $p > 0.05$). On the other hand, among geotechnical variables,

void ratio (*e*) has a significant negative correlation with Cstock ($p \leq 0.05$), while it is non-significant but moderate with OC. The correlations between ρ_d and *EC* with *OC* and *Cstock* are also non-significant but moderate ($0.4 < r < 0.6$ and $-0.4 < r < -0.6$, $p > 0.05$).

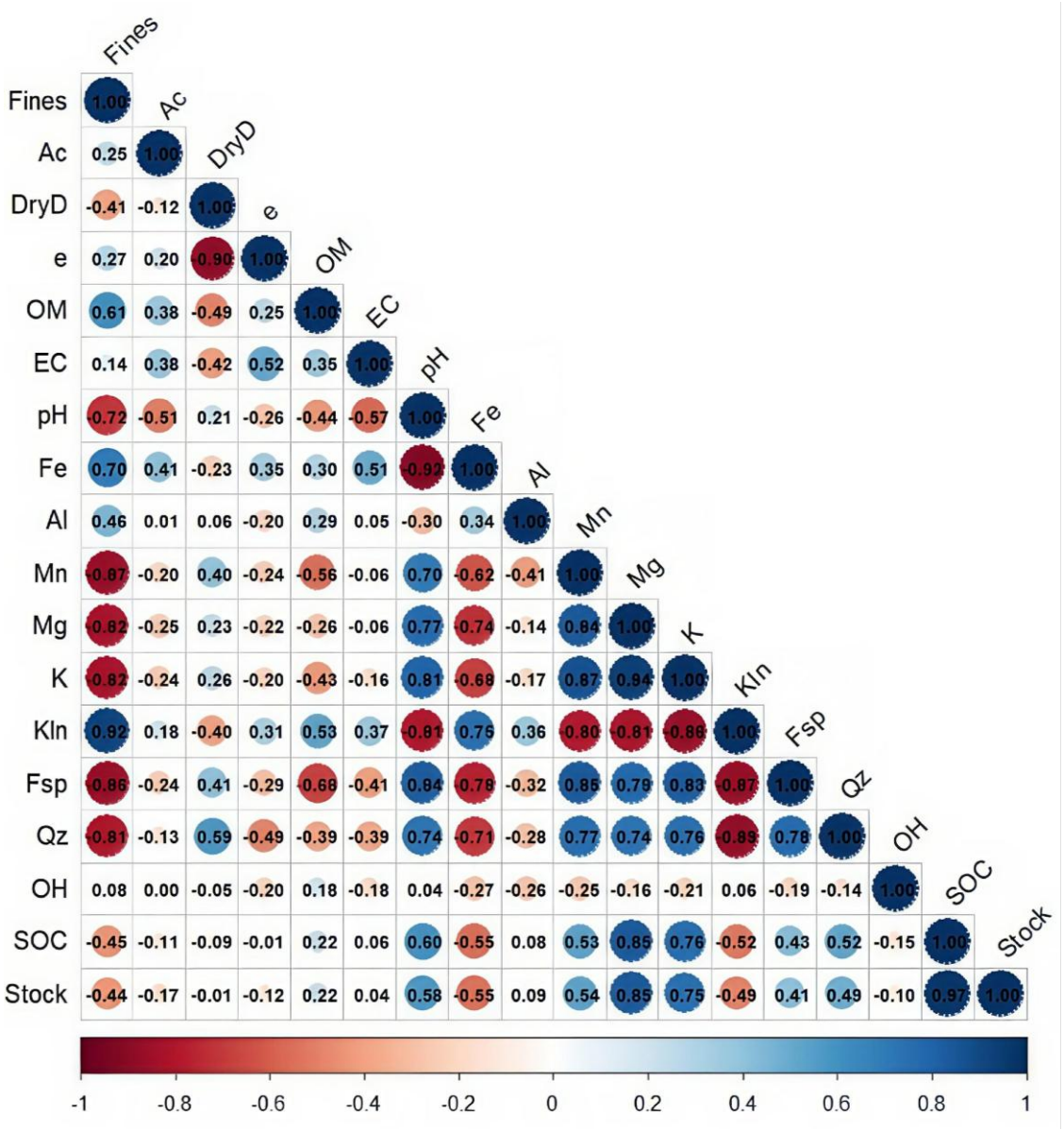

Figure 16. Correlation between soil properties and SOC stock (n=15) for the data of the three soil profiles.

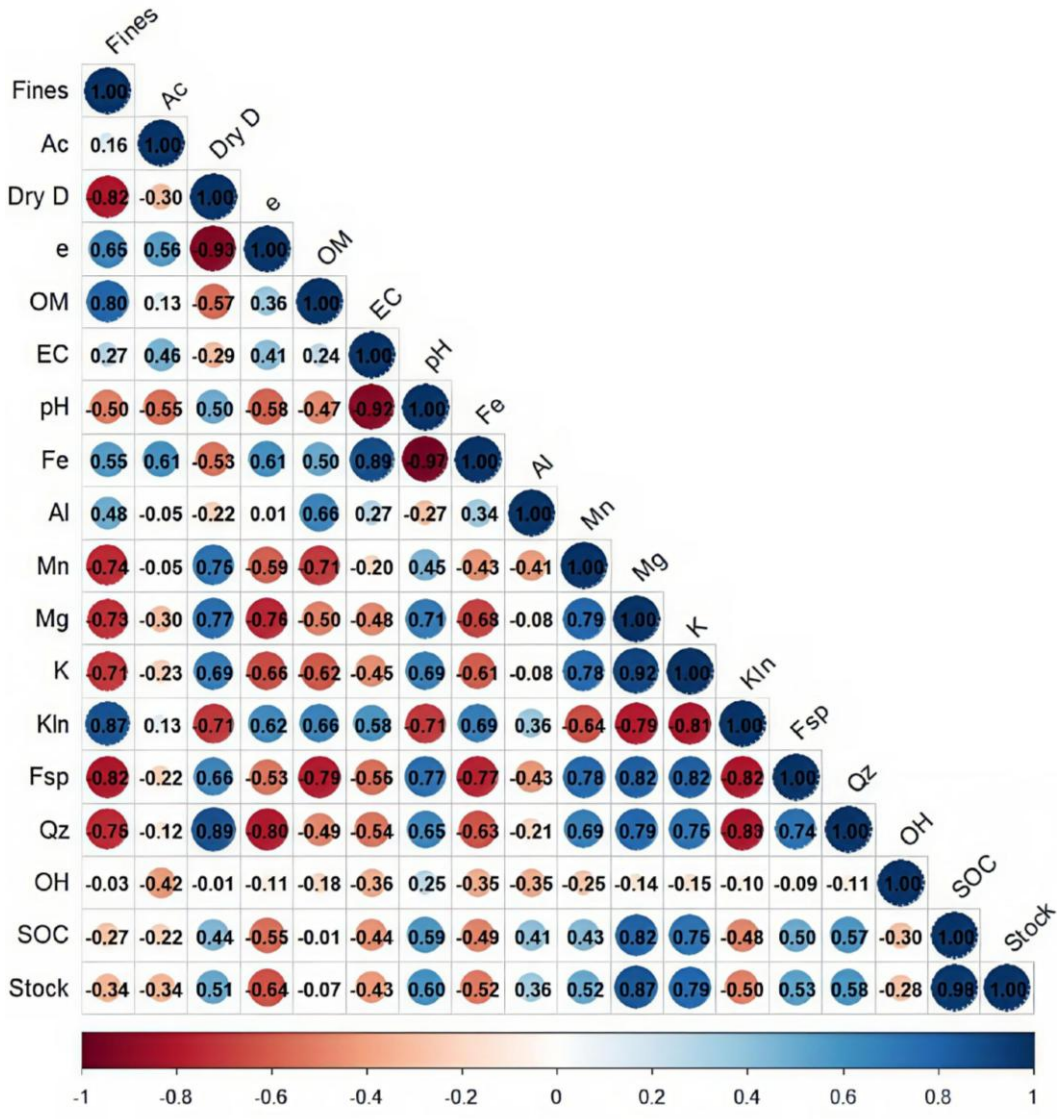

Figure 17. Correlation between soil properties and SOC stock (n=12) for the data of the subsoil of the three soil profiles.

It is interesting to note that the better correlations found for geotechnical variables with *OC* and *Cstock* in this last analysis (n = 12) are supported by the fact that the absence of topsoil data imposes less variation in the sample dataset, which enhances the accuracy of statistical analyses. Indeed, this finding is related to the natural differences in soil properties between the topsoil and subsoil of the profiles. Finally, as it can be seen in the last lines of Figures 16 and 17, the correlations of variables follow nearly the same pattern for OC and Cstock.

By comparing Figures 16 and 17, it is also interesting to note that better correlations among the metal elements (*Fe, Al, Mn, Mg* and *K*) and minerals (*Kln, Fsp* and *Qz*) with geotechnical variables (*Dry D, e, OM* and *EC*) are observed when

the top soil layer is not considered in the sample dataset, which imply in having a more homogeneous material.

Statistical correlations for each land-use and cover class profile, or for the type of soil, were not performed due to the small number of samples.

3.5. Conclusion

This study evaluated the *Cstock* for three classes of land use and cover in the city of Rio de Janeiro. The *Cstocks* in the two green-cover classes are similar, while in the bare landfilled area, it is much lower. Nevertheless, the analysis of SOC fractions stocks highlights that the more preserved green area in urban soil holds a high amount of *Cstock* in the protected form of organic carbon (MAOM).

Organic matter inputs in the soil surface of the green cover areas enrich the *Cstocks* in the topsoil. On the other hand, the OM matter added in the landfilled material, associated to the presence of Feldspar and metals such as Mn, Mg, and K, enhanced *Cstock* in the subsoil. Nonetheless, the soil dry density exhibits a high influence on the *Cstock* in all situations.

Soil organic carbon and *Cstock* variables do not statistically differentiate the three areas. However, the soil physico-chemical and mineralogical properties of the soil profiles showed differences between classes. This was also statistically confirmed

Cstock correlations with geotechnical parameters are expressive in the more homogenous subsoil of the three areas. In here, it would be expected to have better correlations with fines content and soil activity. However, the analysis indicated that only the void ratio showed a significant correlation. A possible explanation for that may be related to the available dataset sample size.

3.6. References

Alvares CA, Stape JL, Sentelhas PC, Gonçalves JLM, Sparovek G. Köppen's climate classification map for Brazil. Meteorol Z. 2013; 22: 711-728. https://doi.org/10.1127/0941-2948/2013/0507

American Society for Testing and Materials – ASTM. D2487-25: Standard Practice for Classification of Soils for Engineering Purposes (Unified Soil Classification System), ASTM International, West Conshohocken, PA, 2025. DOI: 10.1520/D2487-25.

Associação Brasileira de Normas Técnicas – ABNT. Norma Brasileira -.NBR 6459: Soil – Liquid limit determination. Rio de Janeiro: ABNT; 2016a.

Associação Brasileira de Normas Técnicas – ABNT. Norma Brasileira -. NBR 7180: Soil – Plasticity limit determination. Rio de Janeiro: ABNT; 2016b.

Associação Brasileira de Normas Técnicas – ABNT. Norma Brasileira -NBR ISO 6502: Soils and Rocks: Terminology. Rio de Janeiro: ABNT; 2022a.

Associação Brasileira de Normas Técnicas – ABNT. Norma Brasileira -. NBR 13600: Soil – Determination of organic material content by burning at 440°C. Rio de Janeiro: ABNT; 2022b.

Associação Brasileira de Normas Técnicas – ABNT. Norma Brasileira -NBR 6457: Soils - Preparation of samples for compaction tests, characterization and determination of moisture content. Rio de Janeiro: ABNT; 2024.

Associação Brasileira de Normas Técnicas – ABNT. Norma Brasileira -. NBR 7181: Soil-granulometric analysis. Rio de Janeiro: ABNT; 2025a.

Associação Brasileira de Normas Técnicas – ABNT. Norma Brasileira -. NBR 6458: Soils — Determination of the specific mass of solids, the apparent specific mass and the water absorption of the fraction retained in the 2,0 mm aperture sieve. Rio de Janeiro: ABNT; 2025b.

Baer SG, Birgé HE. Soil ecosystem services: an overview. 2018. p. 17-38. https://doi.org/10.19103/as.2017.0033.02

Batjes NH. Mitigation of atmospheric CO2 concentrations by increased carbon sequestration in the soil. Biol Fertil Soils. 1998;27:230-5. https://doi.org/10.1007/s003740050425

Behera SK, Shukla AK. Spatial Distribution of Surface Soil Acidity, Electrical Conductivity, Soil Organic Carbon Content and Exchangeable Potassium, Calcium and Magnesium in Some Cropped Acid Soils of India. Land Degrad Dev. 2015;26:71-9. https://doi.org/10.1002/ldr.2306

Brüggenwirth L, Behrens R, Schnee LS, Sauheitl L, Mikutta R, Mikutta C. Interactions of manganese oxides with natural dissolved organic matter: Implications for soil organic carbon cycling. Geochim Cosmochim Acta. 2024;366:182-200. https://doi.org/10.1016/j.gca.2023.12.016

Burghardt W, Morel JL, Zhang GL. Development of the soil research about urban, industrial, traffic, mining and military areas (SUITMA). Soil Sci Plant Nutr. 2015;61:3-21. https://doi.org/10.1080/00380768.2015.1046136

Burgos Hernández TD, Slater BK, Shaffer JM. Characterizing Minimally Disturbed Soils in a Highly Disturbed Urban Environment. Agrosystems, Geosciences and Environment. 2019;2:1-13. https://doi.org/10.2134/age2019.07.0053

Cambou A, Chevallier T, Barthès B, Derrien D, Cannavo P, Bouchard A, Allory V, Schwartz C, Beaudet LV. The impact of urbanization on soil organic carbon stocks

and particle size and density fractions. J Soils Sediments. 2023;2023. https://doi.org/10.1007/s11368-022-03352-3ï

Cambou A, Shaw RK, Huot H, Vidal-Beaudet L, Hunault G, Cannavo P, Nold F, Schwartz C. Estimation of soil organic carbon stocks of two cities, New York City and Paris. Science of the Total Environment. 2018;644:452-64. https://doi.org/10.1016/j.scitotenv.2018.06.322

Charzynski P, Galbraith J, Tech V, Kabala C. Classification of urban soils. 2017.

Chien SC, Krumins JA. Natural versus urban global soil organic carbon stocks: A meta-analysis. Science of the Total Environment. 2022;807. https://doi.org/10.1016/j.scitotenv.2021.150999

Clayton CRI, Matthews MC, Simons NE. Site Investigation. Second Edition. Cambridge: Department of Civil Engineering, University of Surrey, USA; 1995.

Corwin DL, Lesch SM. Apparent soil electrical conductivity measurements in agriculture. Comput Electron Agric. 2005; 46: 11-43. https://doi.org/10.1016/j.compag.2004.10.005

Costa JR, Pedron F de A, Dalmolin RSD, Schenato RB. Field description and identification of diagnostic qualifiers for urban soils in Brazil. Rev Bras Cienc Solo. 2019;43. https://doi.org/10.1590/18069657rbcs20180121

Cotrufo MF, Ranalli MG, Haddix ML, Six J, Lugato E. Soil carbon storage informed by particulate and mineral-associated organic matter. Nat Geosci. 2019;12:989-94. https://doi.org/10.1038/s41561-019-0484-6

Dhaliwal SS, Dubey SK, Kumar D, Toor AS, Walia SS, Randhawa MK, Kaur G, Brar SK, Khambalkar PA, Shivey YS. Enhanced Organic Carbon Triggers Transformations of Macronutrients, Micronutrients, and Secondary Plant Nutrients and Their Dynamics in the Soil under Different Cropping Systems-A Review. J Soil Sci Plant Nutr. 2024. https://doi.org/10.1007/s42729-024-01907-6

De Campos, T. C. P. Relatório NIMA/PUC-RIO 201113: diagnóstico das presentes condições da estação Gávea do metrô do Rio de Janeiro e alternativas para minimização de riscos associados. Submitted to the Government of the Rio de Janeiro State by the Interdisciplinary Center for Environment in the Pontifical Catholic University of Rio de Janeiro, November 2020.

Doebelin N, Kleeberg R. Profex: A graphical user interface for the Rietveld refinement program BGMN. J Appl Crystallogr. 2015;48:1573-80. https://doi.org/10.1107/S1600576715014685

Dupla X, Bonvin E, Deluz C, Lugassy L, Verrecchia E, Baveye PC, Grand S, Boivin P. Are soil carbon credits empty promises? Shortcomings of current soil carbon quantification methodologies and improvement avenues. Soil Use Manag. 2024;40. https://doi.org/10.1111/sum.13092

Food and Agriculture Organization of the United Nations - FAO. Standard operating procedure for soil electrical conductivity, soil/water, 1:5. Rome: 2021a.

Food and Agriculture Organization of the United Nations - FAO. Standard operating procedure for soil pH determination. Rome: 2021b.

Food and Agriculture Organization of the United Nations - FAO. Measuring and modeling soil carbon stocks and stock changes in livestock production systems: Guidelines for assessment. 2019.

Feng L, Jiang J, Hu J, Chen T. Predicting the impact of dynamic global urban expansion on urban soil organic carbon. Sci Rep. 2025;15:1949. https://doi.org/10.1038/s41598-025-85753-1

Friedlingstein P, O'Sullivan M, Jones MW, Andrew RM, Hauck J, Olsen A, Peters GP, Peters W, Pongratz J, Sitch S, Le Quéré C, Canadell JG, Ciais P, Jackson RB, Alin S, Aragão LEOC, Arneth A, Arora V, Bates NR, Becker M, Benoit-Cattin A, Bittig HC, Bopp L, Bultan S, Chandra N, Chevallier F, Chini LP, Evans W, Florentie L, Forster PM, Gasser T, Gehlen M, Gilfillan D, Gkritzalis T, Gregor L, Gruber N, Harris I, Hartung K, Haverd V, Houghton RA, Ilyina T, Jain AK, Joetzjer E, Kadono K, Kato E, Kitidis V, Korsbakken JI, Landschützer P, Lefèvre N, Lenton A, Lienert S, Liu Z, Lombardozzi D, Marland G, Metzl N, Munro DR, Nabel JEMS, Nakaoka SI, Niwa Y, O'Brien K, Ono T, Palmer PI, Pierrot D, Poulter B, Resplandy L, Robertson E, Rödenbeck C, Schwinger J, Séférian R, Skjelvan I, Smith AJP, Sutton AJ, Tanhua T, Tans PP, Tian H, Tilbrook B, Van Der Werf G, Vuichard N, Walker AP, Wanninkhof R, Watson AJ, Willis D, Wiltshire AJ, Yuan W, Yue X, Zaehle S. Global Carbon Budget 2020. Earth Syst Sci Data. 2020;12:3269-340. https://doi.org/10.5194/ESSD-12-3269-2020

Furquim SAC, Almeida ÍS. Urban soils in Brazil: A review. Rev Bras Cienc Solo. 2022;46. https://doi.org/10.36783/18069657rbcs20210124

Gauthier TD. Detecting trends using Spearman's rank correlation coefficient. Environ Forensics. 2001;2:359-62. https://doi.org/10.1006/enfo.2001.0061

Gozukara G, Hartemink AE, Zhang Y. Factors driving inorganic carbon levels in the soils of the conterminous USA. Catena (Amst). 2025;252. https://doi.org/10.1016/j.catena.2025.108841

Guo H, Du E, Terrer C, Jackson RB. Global distribution of surface soil organic carbon in urban greenspaces. Nat Commun. 2024;15. https://doi.org/10.1038/s41467-024-44887-y

Guo Y, Han J, Bao H, Wu Y, Shen L, Xu X, Chen Z, Smith P, Abdalla M. A systematic analysis and review of soil organic carbon stocks in urban greenspaces. Science of the Total Environment. 2024;948. https://doi.org/10.1016/j.scitotenv.2024.174788

Hu S, Yang Z, Galindo Torres SA, Wang Z, Han H, Wada Y, Wanger TC, Li L. Statistical Distribution of Urban Area Reveals a Converging Trend of Global Urban Land Expansion. Earths Future. 2025;13. https://doi.org/10.1029/2024EF005130

Huang L, Zhou M, Lv J, Chen K. Trends in global research in forest carbon sequestration: A bibliometric analysis. J Clean Prod. 2020;252:119908. https://doi.org/10.1016/j.jclepro.2019.119908

Intergovernmental Panel on Climate Change - IPCC. Summary for Policymakers. In: Climate Change 2023: Synthesis Report. Contribution of Working Groups I, II and III to the Sixth Assessment Report of the Intergovernmental Panel on Climate Change. Geneva, Switzerland: 2023. https://doi.org/doi:10.59327/IPCC/AR6-9789291691647.001

IUSS Working Group WRB. World reference base for soil resources 2014, update 2015: International soil classification system for naming soils and creating legends for soil maps. Rome: Food and Agriculture Organization of the United Nations; 2015. (World Soil Resources Reports, 106).

Janzen HH. Carbon cycling in earth systems—a soil science perspective. Agric Ecosyst Environ. 2004;104:399-417. https://doi.org/10.1016/J.AGEE.2004.01.040

Jobbágy EG, Jackson RB. The vertical distribution of soil organic carbon and its relation to climate and vegetation. Ecological Applications. 2000;10:423-36. https://doi.org/10.1890/1051-0761(2000)010[0423:TVDOSO]2.0.CO;2

Khaledian Y, Pereira P, Brevik EC, Pundyte N, Paliulis D. The Influence of Organic Carbon and pH on Heavy Metals, Potassium, and Magnesium Levels in Lithuanian Podzols. Land Degrad Dev. 2017;28:345-54. https://doi.org/10.1002/ldr.2638

Kopittke PM, Berhe AA, Carrillo Y, Cavagnaro TR, Chen D, Chen QL, Román Dobarco M, Dijkstra FA, Field DJ, Grundy MJ, He JZ, Hoyle FC, Kögel-Knabner I, Lam SK, Marschner P, Martinez C, McBratney AB, McDonald-Madden E, Menzies NW, Mosley LM, Mueller CW, Murphy D V., Nielsen UN, O'Donnell AG, Pendall E, Pett-Ridge J, Rumpel C, Young IM, Minasny B. Ensuring planetary survival: the centrality of organic carbon in balancing the multifunctional nature of soils. Crit Rev Environ Sci Technol. 2022;52:4308-24. https://doi.org/10.1080/10643389.2021.2024484

Lal R. Soil carbon sequestration to mitigate climate change. Geoderma. 2004;123:1-22. https://doi.org/10.1016/j.geoderma.2004.01.032

Lal R, Negassa W, Lorenz K. Carbon sequestration in soil. Curr Opin Environ Sustain. 2015;15:79-86. https://doi.org/10.1016/j.cosust.2015.09.002

Lambe TW; Whitman RV. Soil Mechanics. New York: Wiley, 1969.

Lavallee JM, Soong JL, Cotrufo MF. Conceptualizing soil organic matter into particulate and mineral-associated forms to address global change in the 21st century. Glob Chang Biol. 2019;26:261-73. https://doi.org/10.1111/gcb.14859

Legg TA, Hodges C. Toward a community-engaged framework for urban soil research. Soil Science Society of America Journal. 2024. https://doi.org/10.1002/saj2.20776

Lehmann J, Kleber M. The contentious nature of soil organic matter. Nature. 2015;528:60-8. https://doi.org/10.1038/nature16069

Leuthold S, Lavallee JM, Haddix ML, Cotrufo MF. Contrasting properties of soil organic matter fractions isolated by different physical separation methodologies. Geoderma. 2024;445. https://doi.org/https://doi.org/10.1016/j.geoderma.2024.116870

Lorenz K, Lal R. Managing soil carbon stocks to enhance the resilience of urban ecosystems. Carbon Manag. 2015;6:35-50. https://doi.org/10.1080/17583004.2015.1071182

Lorenz K, Lal R, Ehlers K. Soil organic carbon stock as an indicator for monitoring land and soil degradation in relation to United Nations' Sustainable Development Goals. Land Degrad Dev. 2019;30:824-38. https://doi.org/10.1002/ldr.3270

Lumbreras JF, Gomes JBG. Mapeamento pedológico e interpretações úteis ao planejamento ambiental do Município do Rio de Janeiro. Sergipe: Embrapa Tabuleiros Costeiros; Rio de Janeiro: Embrapa Solos, 2004.

Martinelli LA, Ometto JPHB, Ferraz ES, Victoria RL, Camargo PB, Moreiras MZ. Desvendando questões ambientais com isótopos estáveis. São Paulo: Oficina de Textos, 2009.

Millennium Ecosystem Assessment - MEA. Ecosystems and Human Well-Being: a Framework for Assessment. 2003.

Minasny B, Malone BP, McBratney AB, Angers DA, Arrouays D, Chambers A, Chaplot V, Chen ZS, Cheng K, Das BS, Field DJ, Gimona A, Hedley CB, Hong SY, Mandal B, Marchant BP, Martin M, McConkey BG, Mulder VL, O'Rourke S, Richer-de-Forges AC, Odeh I, Padarian J, Paustian K, Pan G, Poggio L, Savin I, Stolbovoy V, Stockmann U, Sulaeman Y, Tsui CC, Vågen TG, van Wesemael B, Winowiecki L. Soil carbon 4 per mille. Geoderma. 2017;292:59-86. https://doi.org/10.1016/j.geoderma.2017.01.002

Mitchell JK, Soga K. Fundamentals of soil behavior. Third edition. New Jersey: John Wiley & Sons; 2005.

Montgomery A, Herndon E, Jagadamma S. Linking Manganese Fractions and Organic Carbon in Soils of Contrasting Land Use Systems. ACS Agricultural Science and Technology. 2025. https://doi.org/10.1021/acsagscitech.4c00546

Morel JL, Chenu C, Lorenz K. Ecosystem services provided by soils of urban, industrial, traffic, mining, and military areas (SUITMAs). J Soils Sediments. 2015;15:1659-66. https://doi.org/10.1007/s11368-014-0926-0

O'Riordan R, Davies J, Stevens C, Quinton JN, Boyko C. The ecosystem services of urban soils: A review. Geoderma. 2021;395:115076. https://doi.org/10.1016/J.GEODERMA.2021.115076

Orlova KS, Savin IY. Ecosystem Services Provided by Urban Soils and Their Assessment: A Review. Eurasian Soil Science. 2024;57:1072-83. https://doi.org/10.1134/S1064229324600155

Poeplau C, Vos C, Don A. Soil organic carbon stocks are systematically overestimated by misuse of the parameters bulk density and rock fragment content. SOIL. 2017;3:61-6. https://doi.org/10.5194/SOIL-3-61-2017

Pouyat R, Groffman P, Yesilonis I, Hernandez L. Soil carbon pools and fluxes in urban ecosystems. Environmental Pollution. 2002;116:S107-18. https://doi.org/10.1016/S0269-7491(01)00263-9

Pouyat R V., Yesilonis ID, Nowak DJ. Carbon Storage by Urban Soils in the United States. J Environ Qual. 2006;35:1566-75. https://doi.org/10.2134/jeq2005.0215

R Core Team. (2024). R: A Language and Environment for Statistical Computing. R Foundation for Statistical Computing, Vienna, Austria. Available: https://www.R-project.org/

Rio de Janeiro (2022) Monitoramento da cobertura vegetal e do uso das terras do município do rio de janeiro – DATA.RIO, available: SIG Floresta.

Sanderman J, Hengl T, Fiske GJ. Soil carbon debt of 12,000 years of human land use. 2017. https://doi.org/10.7910/DVN/QQQM8V

Santos HG, Jacomine PKT, Anjos LHC, Oliveira VA, Lumbreras JF, Coelho MR, Almeida JA, Araújo Filho JC, Lima HN, Marques FA, Oliveira JB, Cunha TJF. Sistema Brasileiro de Classificação de Solos. 6. ed. rev. e ampl. Brasília, DF: Embrapa; 2025.

Scharenbroch B, Day S, Trammell T, Pouyat R. Urban Soil Carbon Storage. In: Lal R., Stewart BA. Urban Soils: Advances in Soil Science. Boca Raton: Taylor & Francis; 2018. p.137-154

Skempton AW, Northey RD. The sensitivity of clays. Géotechnique, Vol.3 (1); 1953.

Stevenson A, Hartemink AE. Sampling soils in urban ecosystems: a review. Advances in Agronomy. 2024.

Tagiverdiev SS, Gorbov SN, Bezuglova OS, Skripnikov PN. The content and distribution of various forms of carbon in urban soils of southern Russia on the example of Rostov agglomeration. Geoderma Regional. 2020;21. https://doi.org/10.1016/j.geodrs.2020.e00266

Tiema A, Gasiorek M. Urban soils organic carbon: A review. Samsun. 2024.

Trammell TLE, Day S., Pouyat RV, Rosier C, Scharenbroch B, Yesilonis I. Drivers of urban soil carbon dynamics. In: Lal R., Stewart BA. Urban Soils: Advances in Soil Science. Boca Raton: Taylor & Francis; 2018. p. 93-120.

United Nations Population Division (via World Bank) (2025) – processed by Our World in Data. "Urban" [dataset]. UN Population Division (via World Bank), "World Development Indicators" [original data]. Available in: https://ourworldindata.org/urbanization#all-charts. Accessed in 2025 03 27.

Vasenev V, Kuzyakov Y. Urban soils as hot spots of anthropogenic carbon accumulation: Review of stocks, mechanisms and driving factors. Land Degrad Dev. 2018;29:1607-22. https://doi.org/10.1002/ldr.2944

Vasenev VI, Stoorvogel JJ, Dolgikh AV, Ananyeva ND, Ivashchenko K, Valentini R. Changes in Soil Organic Carbon Stocks by Urbanization. In: Lal R., Stewart BA. Urban Soils: Advances in Soil Science. Boca Raton: Taylor & Francis; 2018; 61-92

Vasenev VI, Stoorvogel JJ, Leemans R, Valentini R, Hajiaghayeva RA. Projection of urban expansion and related changes in soil carbon stocks in the Moscow Region. J Clean Prod. 2018;170:902-14. https://doi.org/10.1016/j.jclepro.2017.09.161

Xiao L, Sun Q, Yuan H, Li X, Chu Y, Ruan Y, Lu C, Lian B. A feasible way to increase carbon sequestration by adding dolomite and K-feldspar to soil. Cogent Geosci. 2016;2:1205324. https://doi.org/10.1080/23312041.2016.1205324

Yu L, Zhang W, Liu J, Sun W, Zhang Q. Potential for soil carbon sequestration under conservation agriculture in a warming climate. Sci Bull (Beijing). 2024;69:2030-3. https://doi.org/10.1016/j.scib.2024.03.021

Zhang P, Wang Y, Sun H, Qi L, Liu H, Wang Z. Spatial variation and distribution of soil organic carbon in an urban ecosystem from high-density sampling. Catena (Amst). 2021;204. https://doi.org/10.1016/j.catena.2021.105364

Zhao M, Cheng C, Zhou Y, Shen S, Song C. A global dataset of annual urban extents (1992-2020) from harmonized nightime lights. Earth Syst Sci Data. 2022:517-34

4. SOC stock and physical-hydric analysis

This chapter addresses the investigation of the physical-hydric properties (soil-water retention curves and the soil-pore distribution) and their correlations with C stocks in the three soil profiles. It describes the materials and methods employed for these laboratory tests and presents and discusses the obtained results.

4.1. Materials

The results presented in this section also refer to the studied materials collected from three urban soil profiles under different land-use and cover classes in the city of Rio de Janeiro, Brazil, as described in Section 3.2.1. The sampling procedure for undisturbed samples also followed the description in item 3.2.3.

The physicochemical and mineralogical characterization of the studied materials and the quantification of SOC stocks were presented in sections 3.2.4, 3.2.5, and 3.2.6. In this section, Table 6 shows the average results of soil characterization, index properties, and SOC stock quantification by area and study layer, which contribute to the physical-hydric analysis and correlations.

Table 6. Soil data resume: WL: Liquid Limit; PI: plasticity index; Gs: specific gravity of grains; ρd: soil dry density; e: void ratio; n: porosity; Cstock: organic carbon stock in total soil; PCstock: organic carbon stock in the POM fraction; and MCstock: organic carbon stock in the MAOM fraction.

Area-Layer	Gravel (%)	Sand (%)	Silt (%)	Clay (%)	W_L (%)	PI (%)	G_s	ρ_d ($g\,cm^{-3}$)	e	*n*	*Cstock* ($kgC\,m^{-2}$)	*Pcstock* ($kgC\,m^{-2}$)	*Mcstock* ($kgC\,m^{-2}$)
BSF-1	33.6	53.9	8.6	3.8	-	-	2.666	1.4	0.9	47.0	3.0	1.0	0.9
BSF-2	7.3	74.5	15.4	2.8	26.9	8.0	2.689	1.6	0.7	41.3	3.2	2.2	0.9
BSF-3	6.8	67.6	12.4	13.2	28.4	12.4	2.714	1.5	0.9	46.3	3.0	0.5	1.2
BSF-4	5.1	68.9	9.6	16.4	26.2	11.5	2.693	1.5	0.8	43.6	2.8	0.6	1.2
BSF-5	2.1	70.9	6.8	20.2	25.3	10.2	2.683	1.6	0.6	38.6	2.3	0.3	1.2
FIS-1	4.4	62.7	20.2	12.7	40.7	11.9	2.564	1.4	0.8	44.6	13.8	4.4	7.3
FIS-2	3.1	30.6	7.2	59.1	76.0	41.0	2.615	1.4	0.8	45.8	3.6	0.5	2.8
FIS-3	2.2	35.1	7.1	55.6	69.6	38.3	2.628	1.4	0.8	44.9	2.4	0.3	1.7
FIS-4	2.2	32.4	8.0	57.4	75.2	40.9	2.652	1.4	0.9	47.1	1.8	0.2	1.5
FIS-5	5.5	35.5	14.8	44.2	68.1	34.7	2.639	1.4	0.9	47.4	1.4	0.2	1.0
NNF-1	4.1	46.8	17.9	31.2	57.7	23.1	2.508	1.1	1.4	57.7	14.3	3.6	10.1
NNF-2	1.5	42.3	7.9	48.3	65.4	38.5	2.664	1.5	0.8	44.5	2.6	0.5	1.9
NNF-3	2.5	38.5	10.7	48.3	74.8	44.3	2.681	1.5	0.8	45.2	2.2	0.4	1.4
NNF-4	1.5	36.8	11.1	50.6	81.2	46.7	2.697	1.4	0.9	46.5	1.9	0.8	1.3
NNF-5	1.1	35.9	12.6	50.4	75.4	44.0	2.686	1.4	0.9	46.6	1.8	0.6	1.5

The studied soil layers were classified into four soil groups according to the Unified Soil Classification System (USCS) (ASTM, 2025). As shown in Table 7, the soil may be assembled into layer groups and material groups, such as sandy and clayey, according to the soil type.

Table 7. Studied soil arrangements.

Area-Layer	Depth (m)	Profile-group	Soil Classification	Layer-group	Material-group
BSF-1	0.0 - 0.2	Topsoil	Silt Sandy (SM)	BSF-1	Sandy
BSF-2	0.2 - 0.4	Subsoil	Clayey sand (SC)	BSF 2-5	Sandy
BSF-3	0.4 - 0.6	Subsoil	Clayey sand (SC)		
BSF-4	0.6 - 0.8	Subsoil	Clayey sand (SC)		
BSF-5	0.8 - 1.0	Subsoil	Clayey sand (SC)		
FIS-1	0.0 - 0.2	Topsoil	Silt Sandy (SM)	FIS-1	Sandy
FIS-2	0.2 - 0.4	Subsoil	High plastcity clay (CH)	FIS 2-5	Clayey
FIS-3	0.4 - 0.6	Subsoil	High plastcity clay (CH)		
FIS-4	0.6 - 0.8	Subsoil	High plastcity clay (CH)		
FIS-5	0.8 - 1.0	Subsoil	High plastcity clay (CH)		
NNF-1	0.0 - 0.2	Topsoil	High plasticity silt (MH)	NNF-1	Silty
NNF-2	0.2 - 0.4	Subsoil	High plastcity clay (CH)	NNF 2-5	Clayey
NNF-3	0.4 - 0.6	Subsoil	High plastcity clay (CH)		
NNF-4	0.6 - 0.8	Subsoil	High plastcity clay (CH)		
NNF-5	0.8 - 1.0	Subsoil	High plastcity clay (CH)		

4.2. Methods

4.2.1. Pore size distribution

Mercury Intrusion Porosimetry (MIP) tests were conducted using the Poresizer 9320 equipment from Micromeritics Instrument Corporation. Undisturbed soil samples were shaped with a 15 mm diameter and 25 mm height. Specimens were air-dried and subjected to a cycle of mercury intrusion and exclusion under varying pressure stages.

There are multiple approaches to detect lower and upper boundary limits for pore diameters (e.g., Lopes et al., 2014; Delcourt et al., 2022). In this study, the quantification of micropore, mesopore, and macropore bands assumes that pore diameters are proportional to grain diameter. The quantification was based on the

assumption that pore diameters are 10 times smaller than grain diameters (e.g., Lamb and Whitman, 1979; Mitchell and Soga, 2005). Based on ABNT (2022), it was assumed that micropore diameters are related to clay fraction (< 0.002 mm), the mesopore diameter is related to silt fraction (0.002mm < ϕ < 0.06 mm), and the macropore diameter correlates to sand fraction (> 0.06 mm).

Micro, meso, and macropores were quantified as a percentage of the total pore volume. It also quantified the free and the occluded porosity of the specimens.

According to Romero et al. (1999), the mercury intrusion identifies the total pore size distribution by filling accessible, interconnected pores. During extrusion, only mercury from non-constricted or interconnected pores is released, which defines the volume of free or intra-aggregate pore space. The difference between intrusion and extrusion cumulative pore volume cycles reveals the entrapped or constricted pores, corresponding to inter-aggregate pore space.

In this context, the percentage of free pore porosity (FP) is defined as the ratio of the difference between intrusion (V_I) and extrusion (V_E) cumulative pore volume per total specimen volume, while the occluded porosity (OP) is the ratio between the extrusion (V_E) cumulative pore volume and the total soil volume (e.g., Delcourt et al., 2022). Figure 18 shows an example of the intrusion and extrusion paths by cumulative pore volume per pressure of the area NNF, layer 2. It indicates the respective free and occluded pore space zones.

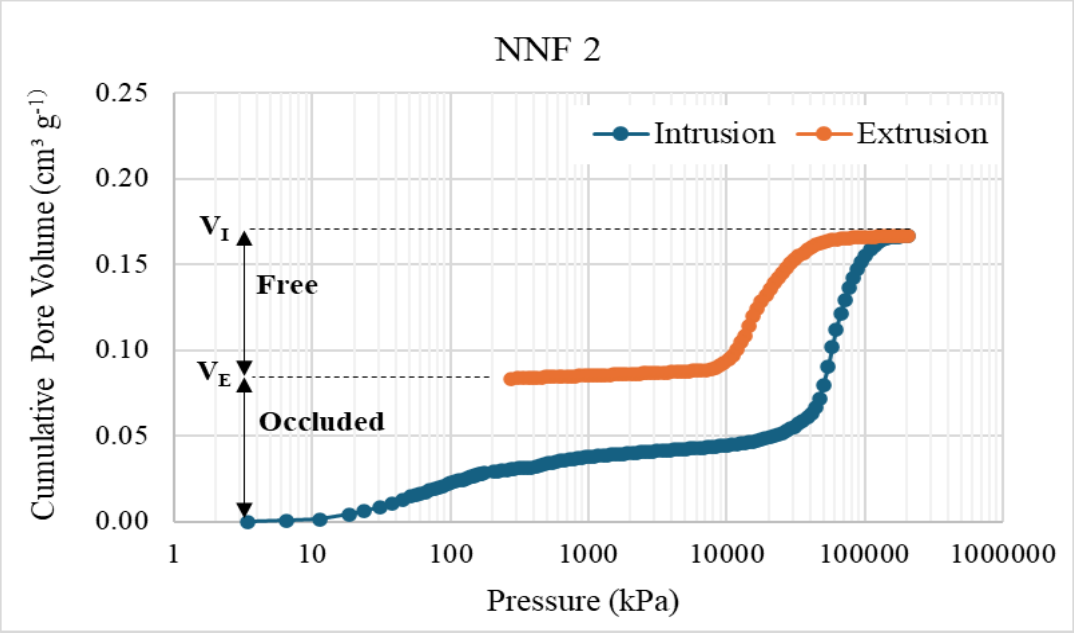

Figure 18. Intrusion and extrusion paths of the porosimetry test.

4.2.2. Soil water retention curve

Drying and wetting soil water retention curves (SWRC) were obtained using the filter paper technique (ASTM, 2016a) and the dewpoint potentiometer WP4C equipment from the Meter Group (ASTM, 2016b). Curves were attained for soil materials of five layer-groups (BSF 2-5, FIS 1, FIS 2-5, NNF 1 and NNF 2-5).

In the drying path of the filter paper technique, undisturbed specimens were initially saturated by capillarity and subsequently air-dried until a required total mass, corresponding to a desired moisture content. In the wetting path, undisturbed specimens were initially air-dried until constant mass and subsequently carefully moistened by dropping water until reaching the required total mass.

For both paths, the Whatman n° 42 filter paper was placed in direct contact with the soil. The specimens were placed in sealed, airtight, containers and kept at a constant temperature for a minimum of seven days to reach equilibrium. Subsequently, the mass of filter paper was determined, and the suction of the specimen was obtained through the calibration suction-water content curve proposed by Chandler and Gutierrez (1986).

Air-dried or forced-dried samples were used to measure the soil water potential using the instrument WP4C. The water-retention curve was fitted using the Van Genuchten (VG) model following Equation 5 (Van Genuchten, 1980):

$$\frac{\theta - \theta_r}{\theta_b - \theta_r} = \left(\frac{1}{1 + |ah|^n}\right)^m \quad \text{(Eq. 5)}$$

where θ is the volumetric water content ($cm^3\ cm^{-3}$), θ_r is the residual water content ($cm^3\ cm^{-3}$), θ_b is the saturated water content ($cm^3 cm^{-3}$), h is the pressure head (cm), and m, n, α are model parameters, with m = 1 – 1/n.

4.2.3. Correlation analysis

The correlation analysis was carried out between carbon parameters such as the concentration of organic carbon in total soil (TOC), concentration of organic carbon in the particulate organic matter (POC), concentration of organic carbon in the mineral-associated organic matter (MOC), total organic carbon stock *(Cstock*), organic carbon stock in the POM fraction (*PCstock*) and organic carbon stock in the MAOM fraction (*MCstock*), with porosimetry parameters such as total porosity (P), percentage of macropores, mesopores, micropores, occluded pores and free

pores. The carbon parameters were also correlated with the fitting parameters from the SWRCs.

The correlations were performed for different datasets of the three areas, as follows: total soil layers (n= number of data pairs =14), sandy material-group (n=5) and clayey material-group (n=8). Correlations were also developed considering only the natural profiles of the FIS and NNF areas. In the case of porosity parameters correlations, it corresponds to n = 10, and in the case of SWRC parameters, n=4. The coefficient of determination (R^2) was obtained using the Pearson correlation for a linear relationship.

4.3. Results and discussion

4.3.1. Poro size distribution

Table 8 shows the results for total porosity (%), micropores volume (%), mesopores volume (%), macropores volume (%), occluded pores porosity (%) and free pores porosity (%). The average porosity of the soil profile obtained by the mercury intrusion porosimetry tests in the areas BSF, FIS and NNF is 27.87 %, 32.05 % and 33.24 % respectively.

Table 8. Pore size distribution results.

Area-Layer	Porosity (%)	Micropores (< 0.2 μm) (%)	Mesopores (0.2 - 6 μm) (%)	Macropores (> 6 μm) (%)	Free pores (%)	Occluded pores (%)
BSF 2	29.94	36.18	41.73	22.09	4.56	25.38
BSF 3	28.43	36.97	11.93	51.10	7.63	20.80
BSF 4	26.63	33.04	8.78	58.19	6.44	20.19
BSF 5	26.48	25.13	7.94	66.93	4.92	21.56
FIS 1	33.07	18.59	19.35	62.06	4.50	28.57
FIS 2	26.69	57.26	8.42	34.33	10.94	15.75
FIS 3	32.23	73.53	6.47	20.00	16.05	16.18
FIS 4	35.44	87.55	3.87	8.58	21.29	14.15
FIS 5	32.80	81.39	6.52	12.10	16.98	15.82
NNF 1	30.58	70.75	7.17	22.07	15.02	15.56
NNF 2	30.70	74.16	8.29	17.55	15.46	15.24
NNF 3	35.02	73.26	5.69	21.05	17.83	17.19
NNF 4	35.28	80.03	5.63	14.33	19.46	15.82
NNF 5	34.60	77.93	7.22	14.85	18.52	16.08

As shown in Figure 19, the porosities obtained from the MIP tests shown in Table 8 by layers do not agree with the porosities resulting from the physical indices (Table 6). A possible explanation for such a difference is the occurrence of non-connected pores in the soil specimens, which are not filled by mercury in the MIP tests (Romero et al., 1999).

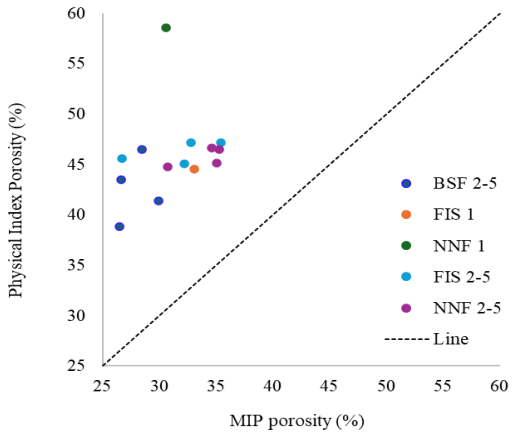

Figure 19. Porosity differences from MIP and Physical indices.

Figure 20 shows the results of the porosimetry tests by the incremental volume of pores (ml g^{-1}) per pore diameter (µm). The tests were carried out on each of the materials in the BSF, FIS, and NNF areas by layers. By exception, the data from the topsoil of the BSF (0 – 0,20 m) area was not obtained due to difficulties in molding this specific soil specimen.

The results of the subsoil profile of the landfilled area (BSF) demonstrated that layer 2 presents a distinct pore size distribution in terms of macro and mesopores from layers 3, 4, and 5 (Figure 20a). While layer 2 holds a large percentage of pore volume in the mesopore band (41.73%), in layers 3, 4, and 5, it is on average ~9.5%. On the other hand, macropores represent 22.0% of the total pores in layer 2, while the average of macropores in layers 3, 4, and 5 is about 58%.

Regarding the results of the FIS area (Figure 20b), it can be observed that layers 1 and 2 hold particular pore distributions, while layers 3, 4, and 5 have similar characteristics. In the topsoil, the majority of the pores are in the macropore region (62.06%), while the percentage of meso and micropores is similar (~18%). In contrast, layer 2 has a large percentage of pores in the micropore region (57.26%), followed by macropores (34.33%) and mesopores (8.42%). Considering layers 3,

4, and 5, despite the percentage of macropores in layer 3 being a little higher than in layers 4 and 5, their pore size distribution is similar.

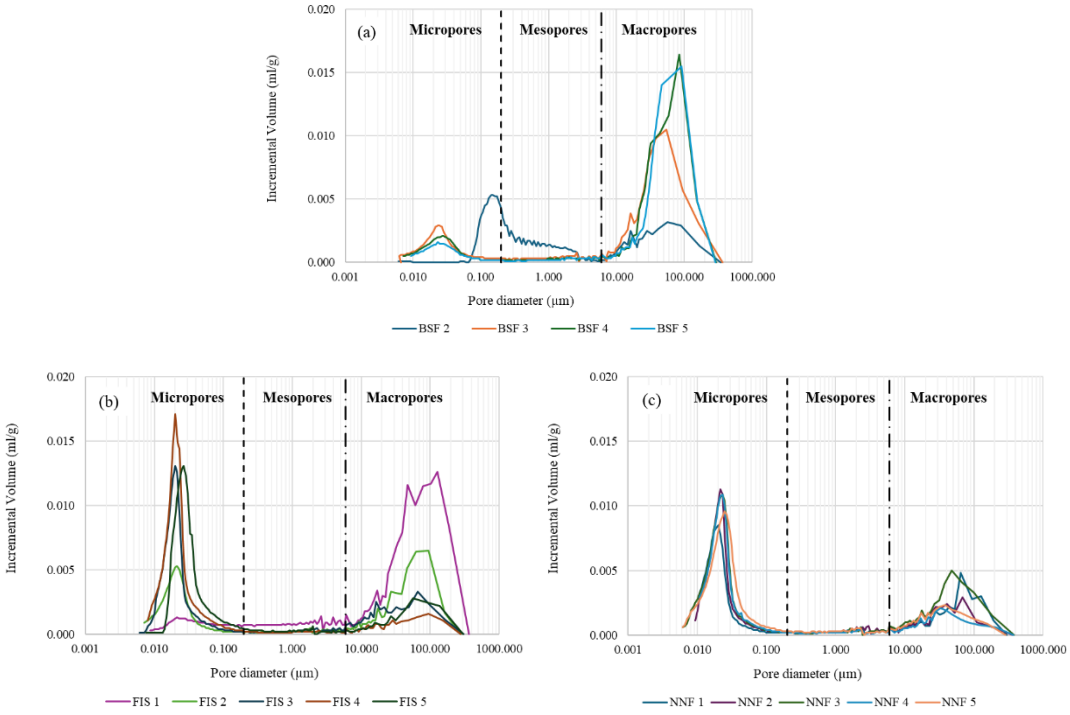

Figure 20. Porosimetry test results in the areas by layers: (a) BSF, (b) area FIS and (c) NNF.

Regarding the results of the NNF area, all layers throughout the profile show a similar pore size distribution (Figure 20c).

Figure 21 presents comparative results of the total porosity (%), micropores volume (%), mesopores volume (%), macropores volume (%), occluded pores porosity (%) and free pores porosity (%) among soil profiles in the three areas.

The results demonstrated that the most preserved area, the NNF, presents less porosity and pore size distribution variation along the profile. In contrast, the FIS area shows the most apparent variation between layers throughout the profile, mainly in the percentage of occluded and free pores and in the distribution of micro and macropores. However, both areas embrace similar porosity patterns in their subsoils.

As expected, the sandy subsoil of the BSF area presents a distinct pore size distribution from the clayey subsoil of the green areas. Although the BSF exhibits a lower percentage of total porosity, occluded pores, and micropores compared to the other areas, it contains a higher proportion of free pores and macropores.

Finally, the three areas present clear differences among them in terms of pore size distribution.

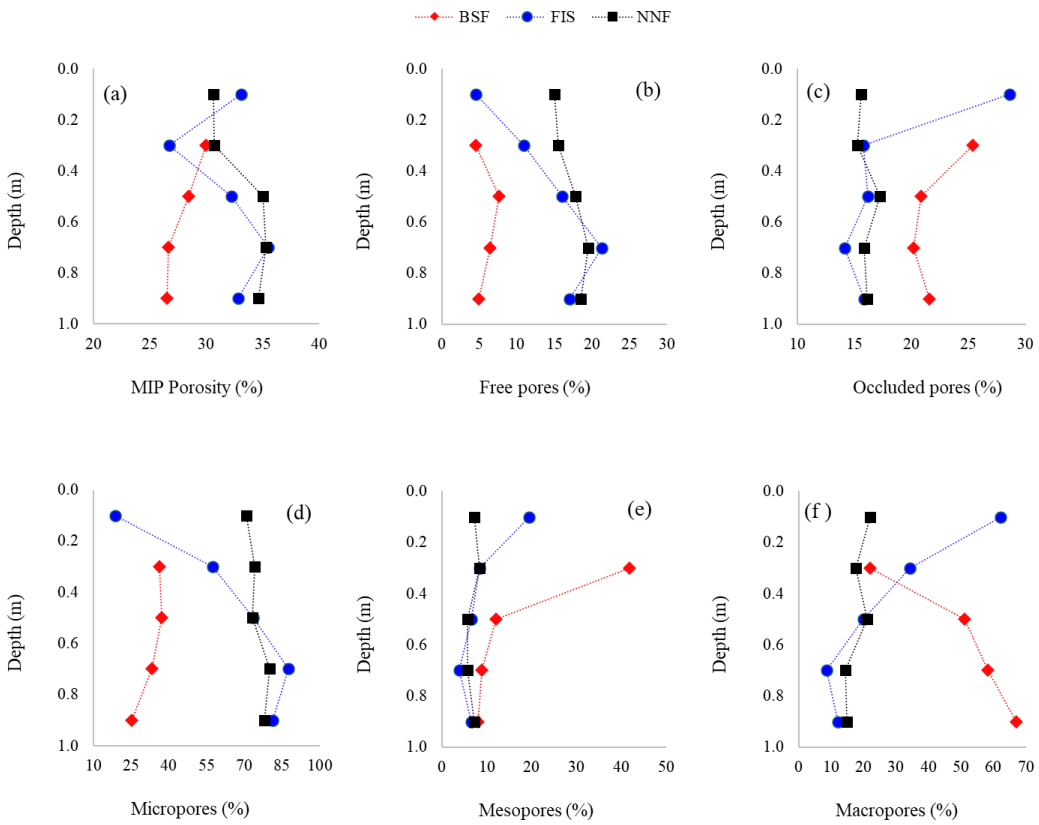

Figure 21. Pore size distribution along the profiles of the areas BSF, FIS, and NNF by layers.

Observing the interactions between the percentage of the micro and macropore bands and the total porosity obtained by MIP, it is noted that there is an inverse distribution between micro and macropores concerning the total porosity magnitude: as porosity increases, macropores decrease and micropores increase, and vice versa (Figure 22).

A similar pattern also occurs in the correlation between the occluded porosity and free porosity with the percentage of micropore and macropore volume (Figure 23). The free porosity increases, and the occluded porosity decreases as the micropore volume increases. The opposite pattern occurs in the correlation with macropore volume.

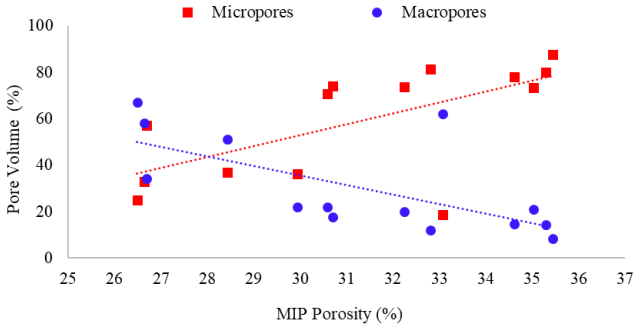

Figure 22. Comparison of the pore band distribution with the total porosity.

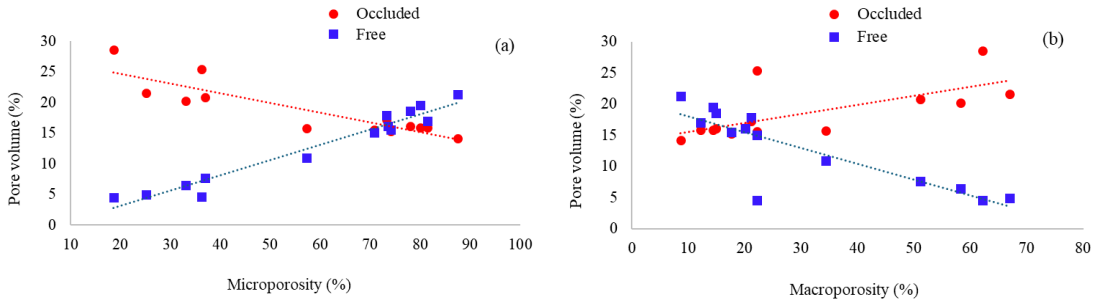

Figure 23. (a) Occluded and free pore distribution under microporosity and (b) under macroporosity.

4.3.2. Soil water retention

Figure 24 shows soil-water retention curves (SWRC) plotted for the volumetric water content for the five-layer-grouped materials. The blue plain dots represent the wetting path obtained by the filter paper method, while the red plain squares represent the drying path carried out using both the filter paper method and the WP4C equipment. The plain green circle dots depict the results of the filter paper tests on specimens at the field moisture content, which are considered representative of soil drying conditions.

All voids in a saturated specimen are filled with water. Based on that, the volumetric water content at 0.1 kPa suction on the drying curve was taken as the average initial porosity of the saturated specimens tested with the filter paper. Considering the Van Genuchten model, the blue and red plain lines in Figure 24 correspond to the fitted curves for the wetting and drying paths, respectively.

Taking into account only the experimental data points in Figure 24, the data from the wetted and dried specimens in the subsoil of the three areas are in close

agreement, suggesting that there is no apparent hysteresis in the SWRCs of the respective materials (Figures 24a, 24d, and 24e). Hysteretic behavior is, however, evident in the topsoil of the FIS and NNF areas (Figures 24b and 24c). On the other hand, the obtained curves that fit best the Van Genuchten model indicate that hysteresis occurs in all cases.

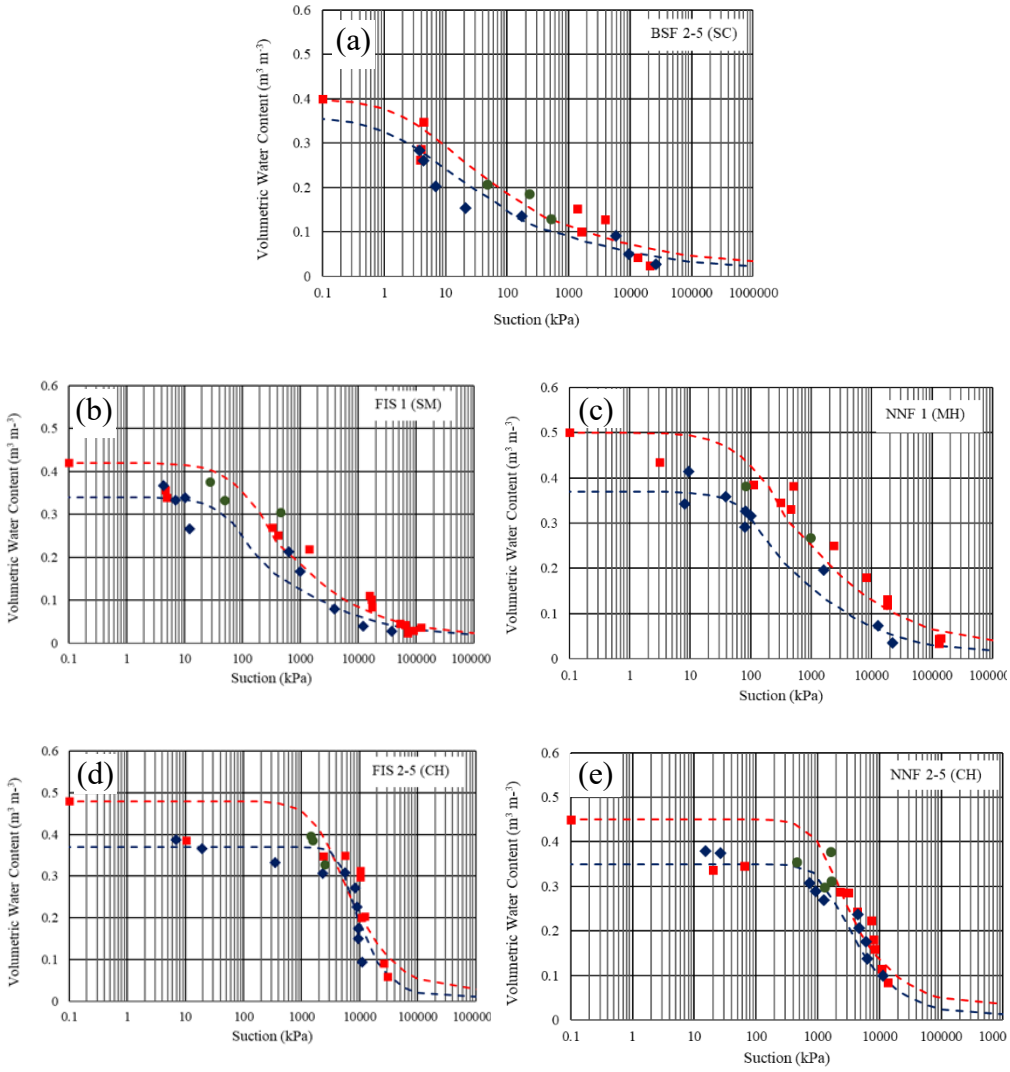

Figure 24. Soil water retention curves for the five-layer group materials.

The hysteresis between the drying and wetting curves in Figure 24 becomes evident due to the inclusion of the average volumetric water content of the materials under saturated conditions (points corresponding to suction of 0.1 kPa) in the drying curves. Such hysteresis is usually expected because micro and, eventually, meso pores (not necessarily interconnected) are not filled with water when wetting a soil

specimen from its air-dried condition, implying a lower volumetric moisture content in the specimens under a given suction.

The lack of agreement between the theoretical drying curves and the respective experimental data points (all in red in Figure 24), particularly below a suction of circa 100 kPa, may be due to: the filter paper technique may not be accurate for suctions below 50 kPa (e.g., Marinho and Oliveira, 2006), and/or, the saturation procedure employed for the specimens of all tested materials (saturation by capillarity) did not work as expected. Indeed, considering this later aspect, it is worth mentioning that the initial saturation degree of the specimens used to follow the drying path ranged from 85% to 90%. Besides filter paper, a suction-controlled pressure plate type of equipment (e.g, de Campos and Vargas Jr, 1991; Fredlund et al., 2012) would be desirable to overcome such potential experimental setbacks.

Figure 25 presents parameters related to the drying path of the SWRC, such as θ_b (volumetric water content at the air entry suction value, Figure 25a), θ_r (residual volumetric water content, Figure 25b), Ψ_b (air entry suction value, Figure 25c), Ψ_{res} (residual suction, Figure 25d), and *n* (Van Genuchten model parameter, which is related to the declivity of the SWRC within the air entry and residual suction values, Figure 25e).

It can be seen in Figures 24d and 24e and in Figure 25c that, as expected, the highest air entry suction values were related to the clayey materials (FIS 2-5 and NNF 2-5). Also, Figure 25d shows that lower residual suction occurs in the sandy materials (BSF 2-5, FIS 1 and NNF 1).

Figure 26 depicts the relationship between air entry and the residual suctions with clay content for all layer groups. The best-fit curve for these relationships, with strong correlation, was found to be exponential.

Attempts to correlate SWRCs parameters with pore size distribution parameters only provided moderate linear correlations for macro, micro, occluded and free pore volume percentage. Table 9 shows the correlation coefficient R^2 and the linear regression equations obtained.

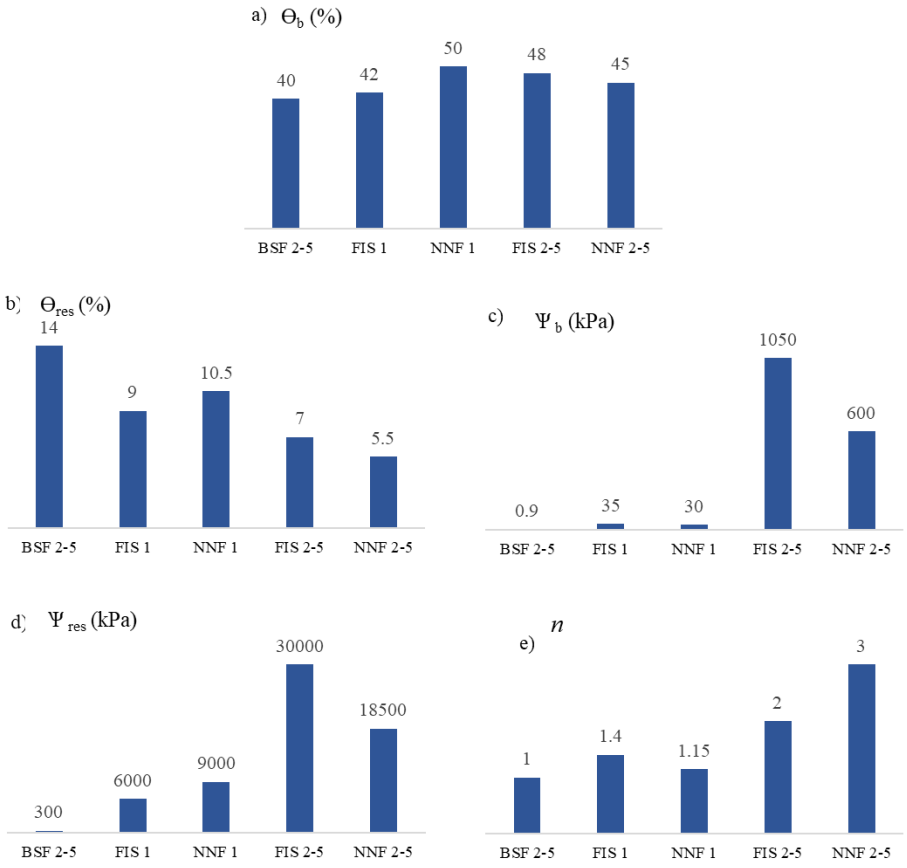

Figure 25. Soil water retention curve results.

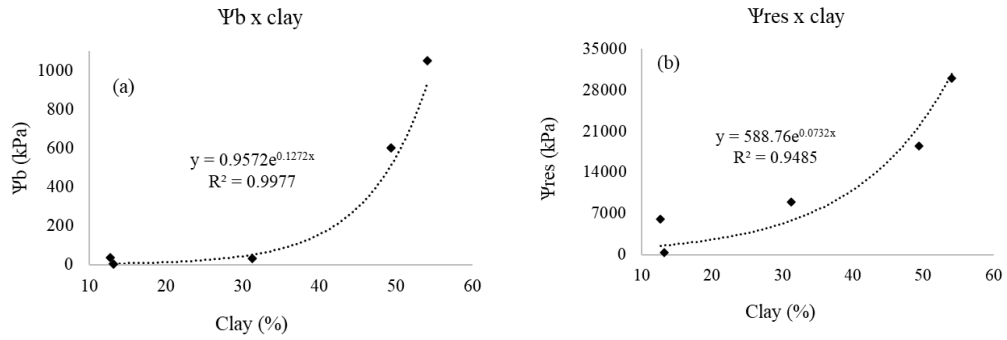

Figure 26. Correlations of SWRC parameters: a) air entry value suction (b) residual suction.

Table 9. Linear regression equation from SWRC and pore size distribution correlations.

n = 5	*Micro*	*Macro*	*Free*	*Occluded*
ψ_b	0.438	0.435	0.471	0.326
	y = -11.45x -283.72	y = -14.97x + 850.75	y = 51.55x -271.24	y = -46.55x + 1252.6
ψ_{res}	0.543	0.530	0.590	0.386
	y = 318.5x - 4658.7	y = -412.66x + 26741	y = 1439.7x - 4384.9	y = -1263.3x + 37436

4.3.3. Correlation analysis

4.3.3.1. Carbon parameters and porosimetry

Table 10 shows the R^2 coefficient of determination encountered for the correlation between porosimetry parameters, which are shown in the first vertical column, with the carbon parameters, shown in the first horizontal row. The analyses were performed for the total soil dataset (number of samples, n=14), natural soil dataset (n=10), material groups dataset of the clayey layers (n=8) and sandy layers (n=5).

Table 10. Correlations of carbon parameters and pore size distribution parameters.

n = 14	*TOC*	*POC*	*MOC*	*Cstock*	*PCstock*	*MCstock*	*n = 10*	*TOC*	*POC*	*MOC*	*Cstock*	*PCstock*	*MCstock*
P	0.001	0.001	2.00E-05	0.001	0.001	2.00E-05	P	0.074	0.024	0.103	0.065	0.001	0.103
Micro	0.005	0.097	0.003	0.101	0.163	0.015	Micro	0.312	0.405	0.181	0.478	0.553	0.313
Meso	0.012	0.138	0.001	0.030	0.226	2.00E-05	Meso	0.287	0.405	0.155	0.452	0.566	0.278
Macro	0.039	0.036	0.006	0.084	0.061	0.018	Macro	0.311	0.394	0.185	0.473	0.536	0.314
FP	0.040	0.093	0.003	0.081	0.150	0.003	FP	0.321	0.370	0.209	0.463	0.481	0.332
OP	0.069	0.211	0.005	0.151	0.344	0.024	OP	0.230	0.366	0.102	0.389	0.537	0.102
n = 8	*TOC*	*POC*	*MOC*	*Cstock*	*PCstock*	*MCstock*	*n = 5*	*TOC*	*POC*	*MOC*	*Cstock*	*PCstock*	*MCstock*
P	0.765	0.014	0.739	0.717	0.016	0.739	P	0.782	0.931	0.708	0.778	0.928	0.709
Micro	0.825	0.027	0.701	0.830	0.030	0.717	Micro	0.565	0.360	0.636	0.584	0.340	0.658
Meso	0.378	0.056	0.362	0.390	0.061	0.383	Meso	0.010	0.210	0.001	0.011	0.241	1.00E-04
Macro	0.833	0.012	0.696	0.836	0.022	0.710	Macro	0.065	0.008	0.116	0.066	0.016	0.125
FP	0.726	0.001	0.633	0.704	0.002	0.633	FP	0.174	0.353	0.162	0.192	0.375	0.162
OP	0.000	0.078	0.018	0.004	0.097	0.010	OP	0.698	0.931	0.637	0.709	0.944	0.637

Best-fitting curves were linear, and the colored cells demonstrate the strength of the respective Person´s correlation. The green cells represent very strong correlations (0.9 to 1.0), the blue cells characterize strong correlations (0.7 to 0.89), and the grey cells represent moderate correlations (0.40 to 0.69). The colorless cells denote weak correlations (0.0 to 0.39).

Analyzing Table 10, correlations between porosimetry parameters and carbon parameters are significant only for the soil material group (clayey/n=8 and sandy/ n=5). As observed in the clayey materials correlations (n=8), total porosity, micropores, macropores, and free pores exhibit strong and moderate correlations with TOC, MOC, Cstock and *MCstock*. Conversely, in the sandy material (n=5), both porosity and occluded porosity exhibit moderate to strong correlations with

carbon parameters, showing very strong associations with POC and *PCstock* (> 0.9).

Figure 27 shows the linear relationship and the regression equations for the very strong correlations in the porosimetry x carbon parameters analysis.

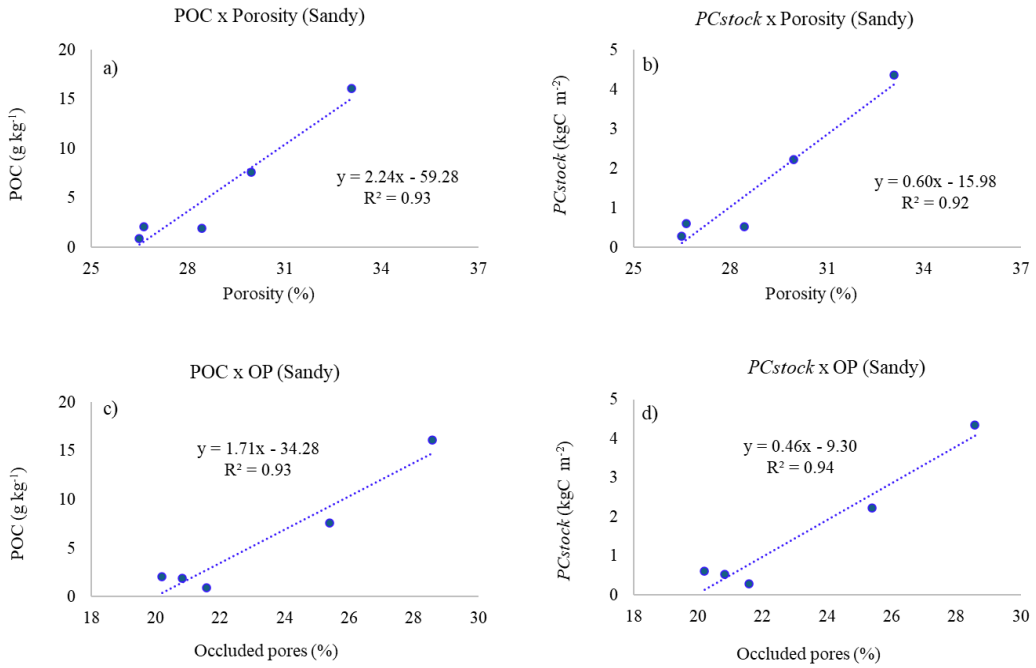

Figure 27. Linear regression equations of the porosimetry correlations.

4.3.3.2. Carbon parameters and SWRC

Bearing in mind that SWRC was obtained for the layer groups, five pairs of data were available for correlations. As shown in Table 11, correlations between carbon parameters and SWRC parameters were carried out based on the layer group dataset (n=5) and in the natural soil profile dataset of the areas FIS and NNF (n=4). The values adopted for carbon parameter correlations in the layer group FIS 2-5 and NNF 2-5 correspond to the average value of the respective layers.

Table 11.Correlations of the carbon parameters and SWRC parameters.

n = 5	*TOC*	*POC*	*MOC*	*Cstock*	*PCstock*	*MCstock*	*n = 4*	*TOC*	*POC*	*MOC*	*Cstock*	*PCstock*	*MCstock*
Θ_b	0.131	0.041	0.2636	0.047	0.001	0.178	Θ_b	0.025	0.001	0.1232	0.003	0.060	0.342
Θ_{res}	0.045	0.084	0.028	0.038	0.005	0.020	Θ_{res}	0.928	0.853	0.906	0.864	0.719	0.933
ψ_b	0.365	0.453	0.269	0.396	0.471	2.95E-01	ψ_b	0.800	0.885	0.679	0.853	0.873	0.784
ψ_{res}	0.156	0.237	0.088	0.191	0.272	0.106	ψ_{res}	0.691	0.812	0.547	0.784	0.850	0.671
n	0.272	0.285	0.216	0.272	0.268	0.216	*n*	0.755	0.713	0.695	0.753	0.643	0.757

The correlations on the layer group dataset (n=5), which comprises the four types of soils (SC, SM, MH and CH) from the three areas, do not present significant correlations between SWRC and carbon parameters. In contrast, the correlation analyses with the dataset comprised by the materials from the topsoil and the subsoil of the green areas, only FIS and NNF, present several strong and very strong linear correlations. Figure 28 presents the equations and linear relationship related to the very strong correlations.

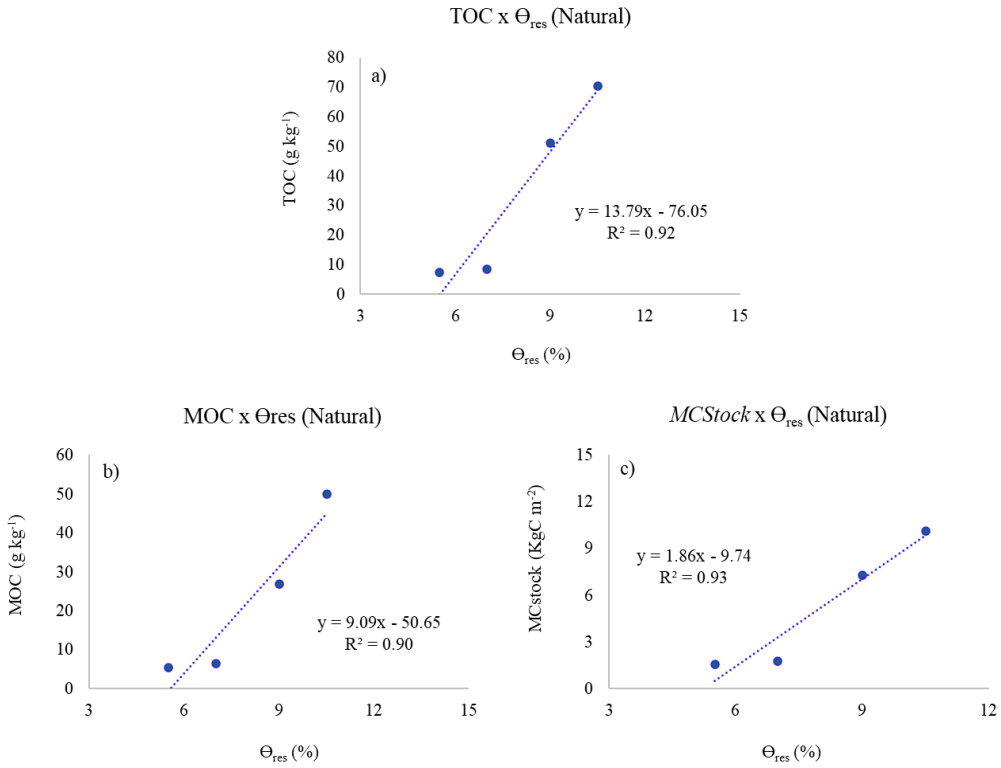

Figure 28. Linear regression equations of the SWRC correlations.

4.3.4. SOC stock regression equations

Besides the linear regression equations shown in Figures 27 and 28 for the very strong correlation, a series of strong linear correlations between pore size distribution and water retention curve with carbon parameters were obtained. Table 12 presents the strong linear regression equations, according to the soil group dataset, encountered for the *Cstock* correlation.

Table 12. Linear regression equations for Cstock correlations.

Method	Soil dataset	Correlation coefficient	x	Linear regression equation Cstock = ax ± b
SWRC	Natural profile	0.864	Θ_{res}	y = 2.90 x - 15.00
	Natural profile	0.853	Ψ_b	y = - 0.013 x + 13.64
	Natural profile	0.784	Ψ_{res}	y = -0.0006x + 17.04
	Natural profile	0.753	n	y = -7.22x + 21.75
MIP	Clayey	0.717	P	y = -0.185x + 8.33
	Clayey	0.830	Micro	y = -0.068x + 7.35
	Clayey	0.836	Macro	y = 0.077x + 0.84
	Clayey	0.704	FP	y = -0.178x + 5.26
	Sandy	0.778	P	y = 1.599x - 41.23
	Sandy	0.709	OP	y = 1.165x -22.13

5. Synthesis and integrated discussion

This study aimed to evaluate SOC Stock, physicochemical, mineralogical and physical-hydric properties in the soil profile of three different classes of land use and cover in the urban area of the Rio de Janeiro city to understand the interactions between land use and cover characterization with soil profile characteristics.

To do so, it was determined soil organic carbon stocks in the total soil (*Cstock*) and the soil organic matter fractions (particulate organic matter, POM – *PCstock* - and mineral-associated organic matter, MAOM – *MCstock*), and measured physico-chemical, mineralogical, and physical-hydric (pore size distribution and soil-water retention) properties to characterize the soil profiles under the land and use classes of: non-native vegetation forest (NNF), dense ombrophylous forest in the initial stage (FIS), and bare soil fill (BSF). The study undertook soil sections of 20 cm (0 - 0.2 m, 0.2 - 0.4 m, 0.4 - 0.6 m, 0.6 - 0.8 m, and 0.8 - 1.0 m) to a depth of 1 m in the soil profile.

At the beginning of the research, a critical literature review was carried out to synthesize concepts of SOC dynamics under a cross-disciplinary approach, to analyze research opportunities, and to examine sustainable applications of the *Cstock* indicator under environmental engineering. It supports synthesizing concepts encompassing SOC stock from the elementary aspects of the carbon biogeochemical cycle to the detailed mechanisms of SOC storage and retention. In this review, aspects of soil type or land use and cover were not considered.

The literature review was presented in the article: *Antunes, M. C.; De Campos, T. M. P.; Araruna, J. T. "Soil carbon storage and retention: a critical synthesis on concepts, research opportunities and environmental engineering sustainable application".* Results pointed out the conceptual advances in organic matter stabilization in soil and highlighted the research gap on the dynamics of the SOC and soil water flux within structured soil profiles, which may be explained through geotechnical engineering concepts.

Considering the overall scope of this research, the critical literature review contributed to *i*) overcoming the multidisciplinary nature of concepts and definitions in soil carbon sequestration (SCS); *ii*) evaluating the investigation methods and protocols usually employed to determine and monitor SOC sequestration, and *iii*) identifying research opportunities through the lens of

geotechnics. Finally, it discusses the employment of the SOC stock indicator in engineering projects

From this literature insight, a research framework was built to link the SOC stock and properties research questions in this project with geotechnical investigation method responses (Figure 29), where the results and analysis stage (2) was split into two blocks of results and analysis to be correlated with Carbon parameters. The first one, the Physical-chemical, and the second one, the Physical-hydric (sections 3 and 4).

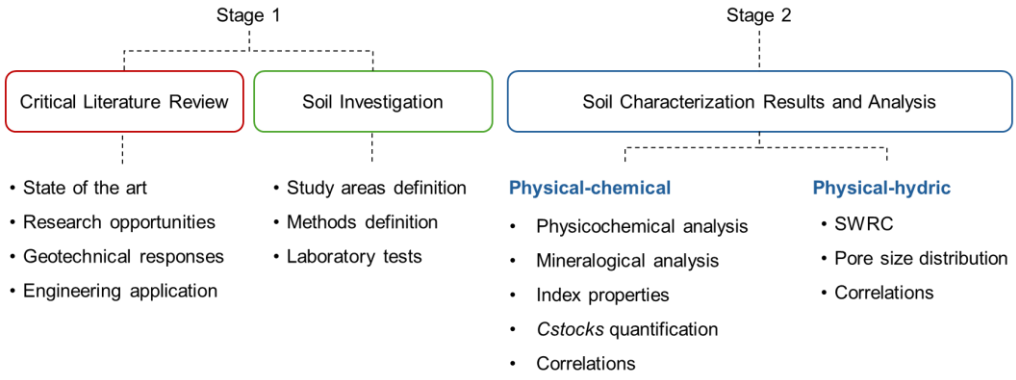

Figure 29. Research framework

The physical-chemical and carbon parameters investigation was presented in section 3 in the article: *Antunes, M. C.; De Campos, T. M. P.; Araruna Jr., J.T.; Sartori, R. A. Soil organic carbon stock: a case study under different land use and cover classes in Rio de Janeiro, Brazil*, which was developed according to the standards of Brazilian Journal of Soil Science (e-ISSN 1806-9657, Qualis A3. It presented the study area and the methodology applied for sampling and assessing soil properties and consolidated results of the physico-chemical, mineralogical properties, soil physical index, and Cstocks quantification. At the end, the article presents the correlations between carbon parameters and soil properties and a discussion about the similarities and dissimilarities between soil profiles in each land use and cover class.

Section 4 addressed the physical-hydric results, carbon parameters correlations and analysis and discussions. It also described the material and methods for water retention analysis and porosimetry tests. At the end, it brought correlations between physical-hydric parameters and carbon parameters.

The results revealed that C*stock* within the 1 m deep profile in the vegetated areas (NNF and FIS) are similar and nearly 38% higher than in the landfilled area (BSF) due to the deposition of organic matter on their surface. In contrast, the Technosol profile (BSF) presented a higher *Cstock* in the subsoil due to the organic matter added into the landfilled material.

The amount of *MCstock* is higher than the *PCstock* in the three urban soils. The natural profile of the preserved green-cover class (NNF) exhibited the highest amount of the persistent form of SOC (*MCstock)*. *PCstocks* have a similar magnitude in the three areas; however, in the BSF area, it represents ~3% of the total Cstock, while in the FIS and NNF, it is around 25%.

The soil dry density has a high influence on the *Cstock* and must be carefully determined in highly heterogeneous urban soil profiles. The horizon's thickness must also be precisely determined due to the influence of the variations of the SOC concentrations and dry soil density along the profile in the quantification of *Cstock* until 1 m depth.

Cstocks do not statistically differentiate the three areas. However, the soil physicochemical and mineralogical properties statistically confirmed the differences.

Cstock correlations with geotechnical parameters are expressive in the more homogenous subsoil of the three areas. In here, it would be expected to have better correlations with fines content and soil activity. However, the analysis indicated that only the void ratio showed a significant correlation. A possible explanation for that may be related to the available dataset sample size.

Pore size distributions differ in the three areas. Macropores prevail in area BSF and in the topsoil of area FIS, while micropores prevail in the subsoil of the FIS and in the NNF areas.

Based on the USCS, the materials from the three areas were classified into five groups: two sandy (SC and SM), one silty (MH) and two clayey (CH). The SWRCs under dry and wetting paths corresponding to such groups presented a hysteretic behavior, with distinct patterns of water retention between clayey and sandy materials.

Linear correlations were obtained between carbon parameters (*Cstock, PCstock* and *MCstock*) and pore size distribution and soil water retention parameters. Better correlations were found for the more homogeneous data se

6. Conclusions and recommendations

This research showed that SOC *stocks* throughout profiles (1m) of the urban green areas studied are higher than the bare landfilled profile. However, the SOC stock in the subsoil of the landfilled profile is higher than that in the clayey subsoil of the green areas due to the OM and minerals added to the land material.

Moreover, the SOC stocks in the two green-covered areas are similar despite the class of cover vegetation. Nevertheless, the analysis of SOC stock in the organic matter fractions highlights that the preserved green area holds a high amount of protected form of organic carbon (MAOM).

Soil organic carbon content and *Cstock* variables do not statistically differentiate the three areas, while physico-chemical and mineralogical properties confirmed the statistical differences between soils in the three classes. Pore size distributions and water retention behavior also differ in the three areas. Macropores prevail in the sandy landfilled profile, while micropores prevail in the clayey subsoils of the green areas.

Cstock correlations with geotechnical parameters are expressive in the more homogenous materials dataset. It would be expected to have better correlations; however, a possible explanation for that may be related to the available sample size. Nonetheless, linear correlations were obtained between carbon parameters (*Cstock, PCstock* and *MCstock*) and physico-hydric soil properties, which may be confirmed by increasing the sample dataset through further investigations.

Recommendations for future work:

- Include in the proposed experimental methodology total chemical analysis, evaluation of cation exchange soil capacity and microbiological analyses.
- To further enhance the knowledge on soil organic carbon storage and retention, it would be of interest to include investigations on soil structure by, for instance, computerized microtomography analysis and scanning electrical microscopy.
- Include other types of tests, such as suction and pressure plate tests, to better define the SWRC in the lower suction range.
- Define organic carbon transport parameters in the soil water and perform numerical analysis to investigate SOC retention in soil profile at depth.

- Expand the study area through other typologies of land use and cover classes in Rio de Janeiro (e.g., native forest in an advanced stage and grass composed of green spaces) using the proposed sampling methodology.
- Increase the sample size to enhance statistical analysis of Cstocks quantification in BSF, FIS, and NNF types of land use and cover in urban areas.
- Quantify the carbon storage potential in the land use and cover class typologies by associating the soil organic carbon pool with net primary production (NPP) and standing biomass of C.
- Investigate the SOC stock accrual in green infrastructure projects in long-term experiments.

7. References

ALBRITTON, D. L. et al. Summary for policymakers. IPCC, 2001.

ARIAS ESTÉVEZ, M.; CONDE CID, M.; PARADELO NÚÑEZ, R. Poorly-crystalline components in aggregates from soils under different land use and parent material. *Catena*, v. 144, p. 141–150, 2016. https://doi.org/10.1016/j.catena.2016.05.012.

AMERICAN SOCIETY FOR TESTING AND MATERIALS – ASTM. **D5298-16**: Standard Test Method for Measurement of Soil Potential (Suction) Using Filter Paper (Withdrawn 2025). ASTM International, 2016a.

AMERICAN SOCIETY FOR TESTING AND MATERIALS – ASTM. **D6836-16**: Standard Test Method for Determination of the Soil Water Characteristic Curve for Desorption Using Hanging Column, Pressure Extractor, Chilled Mirror Hygrometer, or Centrifuge. ASTM International, 2016b.

AMERICAN SOCIETY FOR TESTING AND MATERIALS – ASTM. **D2487-25:** Standard Practice for Classification of Soils for Engineering Purposes (Unified Soil Classification System). West Conshohocken, PA: ASTM International, 2025. DOI: 10.1520/D2487-25.

ASSOCIAÇÃO BRASILEIRA DE NORMAS TÉCNICAS – ABNT. **NBR ISO 6502**: Soils and Rocks: Terminology. Rio de Janeiro: ABNT, 2022a.

BISPO, A. et al. Accounting for carbon stocks in soils and measuring GHGs emission fluxes from soils: Do we have the necessary standards? Frontiers in Environmental Science, v. 5, jul. 2017, p. 1–12. Disponível em: https://doi.org/10.3389/fenvs.2017.00041. Acesso em: 1 nov. 2025.

CAMBOU, A. et al. Estimation of soil organic carbon stocks of two cities, New York City and Paris. Science of the Total Environment, v. 644, p. 452–464, 2018. Disponível em: https://doi.org/10.1016/j.scitotenv.2018.06.322. Acesso em: 1 nov. 2025.

CHANDLER, R. J.; GUTIERREZ, C. I. The filter-paper method of suction measurement. Géotechnique, v. 36, n. 2, p. 265–268, 1986. Disponível em: https://doi.org/10.1680/geot.1986.36.2.265. Acesso em: 1 nov. 2025.

DE CAMPO, T. M. P.; VARGAS JR., E. A. Unsaturated soil studies: recent developments at PUC-Rio. In: Unsaturated soils seminar. Brasília: Brasília University, 1991. p. 109–136.

DELCOUT, R. D.; DE CAMPO, T. M. P.; ANTUNES, F. S. Interrelationship among weathering degree, pore distribution and water retention in an unsaturated gneissic residual soil. *Engineering Geology*, v. 299, 2022. https://doi.org/10.1016/j.enggeo.2022.106570.

DON, A. et al. Carbon sequestration in soils and climate change mitigation—Definitions and pitfalls. *Global Change Biology*, v. 30, n. 1, 2024. John Wiley and Sons Inc. https://doi.org/10.1111/gcb.16983.

FAO. *Measuring and modelling soil carbon stocks and stock changes in livestock production systems: Guidelines for assessment*. v. 1. 2019. Disponível em: http://www.fao.org/partnerships/leap/publications/en/.

FRIEDLINGSTEIN, P. et al. Global Carbon Budget 2020. *Earth System Science Data*, v. 12, n. 4, p. 3269–3340, 2020. Disponível em: https://doi.org/10.5194/ESSD-12-3269-2020.

GEORGIOU, K. et al. Global stocks and capacity of mineral-associated soil organic carbon. *Nature Communications*, v. 13, n. 1, 2022. Disponível em: https://doi.org/10.1038/s41467-022-31540-9.

GRANJA DORILÊO LEITE, F. F. et al. Land use change effect on organic matter dynamics and soil carbon sequestration in the Brazilian Cerrado: A study case in Mato Grosso do Sul state (Midwest-Brazil). *Catena*, v. 249, 2025. Disponível em: https://doi.org/10.1016/j.catena.2024.108670.

GUO, H.; DU, E.; TERRER, C.; JACKSON, R. B. Global distribution of surface soil organic carbon in urban green spaces. *Nature Communications*, v. 15, n. 1, 2024. Disponível em: https://doi.org/10.1038/s41467-024-44887-y.

GUO, Y. et al. A systematic analysis and review of soil organic carbon stocks in urban green spaces. *Science of the Total Environment*, v. 948, 2024. Elsevier B.V. Disponível em: https://doi.org/10.1016/j.scitotenv.2024.174788.
Huang, L., Zhou, M., Lv, J., & Chen, K. (2020). Trends in global research in forest carbon sequestration: A bibliometric analysis. Journal of Cleaner Production, 252, 119908. https://doi.org/10.1016/j.jclepro.2019.119908

IPCC. *Summary for Policymakers*. In: Climate Change 2023: Synthesis Report. Contribution of Working Groups I, II and III to the Sixth Assessment Report of the Intergovernmental Panel on Climate Change. P. Arias et al. (Eds.). 2023. DOI: 10.59327/IPCC/AR6-9789291691647.001.

KÖCHY, M.; HIEDERER, R.; FREIBAUER, A. Global distribution of soil organic carbon – Part 1: Masses and frequency distributions of SOC stocks for the tropics, permafrost regions, wetlands, and the world. *SOIL*, v. 1, n. 1, p. 351–365, 2015. DOI: 10.5194/soil-1-351-2015.

LAL, R.; NEGASSA, W.; LORENZ, K. Carbon sequestration in soil. *Current Opinion in Environmental Sustainability*, v. 15, p. 79–86, 2015. DOI: 10.1016/j.cosust.2015.09.002.

LAMBE, T. W.; WHITMAN, R. V. *Soil Mechanics*. New York: Wiley, 1969.

LOPES, B. C. F. L.; TARANTINO, A.; CORDÃO NETO, M. P. An approach to detect micro- and macro-porosity from MIP data. In: *Unsaturated Soils: Research & Applications*, Sydney, 2014.

LORENZ, K.; LAL, R. Managing soil carbon stocks to enhance the resilience of urban ecosystems. *Carbon Management*, v. 6, n. 1–2, p. 35–50, 2015. DOI: 10.1080/17583004.2015.1071182.

LORENZ, K.; LAL, R.; EHLERS, K. Soil organic carbon stock as an indicator for monitoring land and soil degradation in relation to United Nations' Sustainable Development Goals. *Land Degradation and Development*, v. 30, n. 7, p. 824–838, 2019. DOI: 10.1002/ldr.3270.

MARINHO, F. A. M.; OLIVEIRA, O. M. The Filter Paper Method Revisited. *Geotechnical Testing Journal*, v. 29, n. 3, 2006.

MINASNY, B. et al. Soil carbon 4 per mille. *Geoderma*, v. 292, p. 59–86, 2017. DOI: 10.1016/j.geoderma.2017.01.002.

MITCHELL, J. K.; SOGA, K. *Fundamentals of soil behavior*. 3. ed. New Jersey: John Wiley & Sons, 2005.

MOREL, J. L.; CHENU, C.; LORENZ, K. Ecosystem services provided by soils of urban, industrial, traffic, mining, and military areas (SUITMAs). *Journal of Soils and Sediments*, v. 15, n. 8, p. 1659–1666, 2015. DOI: 10.1007/s11368-014-0926-0.

O'RIORDAN, R. et al. The ecosystem services of urban soils: A review. *Geoderma*, v. 395, 115076, 2021. DOI: 10.1016/J.GEODERMA.2021.115076.

PEREIRA, P. et al. Nature-based solutions for carbon sequestration in urban environments. *Current Opinion in Environmental Science and Health*, v. 37, 2024. DOI: 10.1016/j.coesh.2024.100536.

POUYAT, R. et al. Soil carbon pools and fluxes in urban ecosystems. *Environmental Pollution*, v. 116, supl. 1, p. S107–S118, 2002. DOI: 10.1016/S0269-7491(01)00263-9.

POUYAT, R. V.; YESILONIS, I. D.; NOWAK, D. J. Carbon Storage by Urban Soils in the United States. *Journal of Environmental Quality*, v. 35, n. 4, p. 1566–1575, 2006. DOI: 10.2134/jeq2005.0215.

ROMERO, E.; GENS, A.; LLORET, A. Water permeability, water retention and microstructure of unsaturated compacted Boom clay. *Engineering Geology*, v. 54, p. 117–127, 1999. DOI: 10.1016/S0013-7952(99)00067-8.

TAGIVERDIEV, S. S. et al. The content and distribution of various forms of carbon in urban soils of southern Russia on the example of Rostov agglomeration. *Geoderma Regional*, v. 21, 2020. DOI: 10.1016/j.geodrs.2020.e00266.

UNITED NATIONS. *The World's Cities in 2018*. 2019.

VAN GENUCHTEN, M. T. A Closed-form Equation for Predicting the Hydraulic Conductivity of Unsaturated Soils. *Soil Science Society of America Journal*, v. 44, p. 892–898, 1980. DOI: 10.2136/sssaj1980.03615995004400050002x.

VANCE, E. D.; BROOKES, P. C.; JENKINSON, D. S. 1987.

VASENEV, V. I. et al. Projection of urban expansion and related changes in soil carbon stocks in the Moscow Region. *Journal of Cleaner Production*, v. 170, p. 902–914, 2018. DOI: 10.1016/j.jclepro.2017.09.161.

XIAO, C. L. et al. Crop diversity significantly enhances soil carbon sequestration via alleviating soil inorganic carbon decline caused by rhizobium inoculation. *Soil and Tillage Research*, v. 245, 2025. DOI: 10.1016/j.still.2024.106286.

YU, L. et al. Potential for soil carbon sequestration under conservation agriculture in a warming climate. *Science Bulletin*, v. 69, n. 13, p. 2030–2033, 2024. DOI: 10.1016/j.scib.2024.03.021.

ZHANG, P. et al. Spatial variation and distribution of soil organic carbon in an urban ecosystem from high-density sampling. *Catena*, v. 204, 2021. DOI: 10.1016/j.catena.2021.105364.

APPENDIX 1

A 1. Investigation site, sampling procedure and materials

A 1.1 Definition of the studied sites

The definition of the experimental areas was performed in two phases. The first consisted of preliminary soil physical characterization with remolded samples to support the definition of experimental areas. The second phase encompasses undisturbed sample collection for physico-chemical, mineralogical and hydraulic characterization.

The preliminary soil investigation campaign aimed to identify the soil profiles appropriate for the experimental research in each land use and cover class inside the Gávea Campus of the Pontifical Catholic University. To do so, areas with bare soil fill (BSF), dense ombrophylous forest in the initial stage (FIS) and non-native vegetation forest (NNF) cover typologies were previously identified as A1, A2 and A3, respectively, and selected for sampling and physical characterization (Figure A.1).

Figure A. 1. Previously selected classes of land use and cover in the Gávea Campus. The areas identified were A1: BSF, A2: FIS, and A3: NNF.

The preliminary sampling campaign was carried out adopting the Helicoidal Electric Auger. Drilling was performed to a depth of 1.00 m. Samples were collected at different depths, initially targeting intervals were 0.10 to 0.20 m, 0.40

to 0.50 m, and 0.90 to 1.00 m. Figure A.2 shows the fieldwork conducted by the team from the Geotechnical and Environmental Laboratory (LGMA-PUC-Rio).

Figure A. 2. Preliminary investigation in the FIS area. a) Helicoidal Electric Auger and b) Soil sample.

The previous investigation in the BSF area (A1) detected fragments of concrete blocks, pebbles, ceramic materials and typical construction debris until 60 cm. The auger encountered resistance during drilling. It required manual cleaning of the borehole surface. Additionally, the borehole wall collapsed, mixing soil materials of all profile depths which enabling the collection of samples at the intended depths. In this context, this area was not considered in the research e another location in the Campus, with similar land use and cover (BSF), was selected for characterization. It was identified as A1a (Figure A.3).

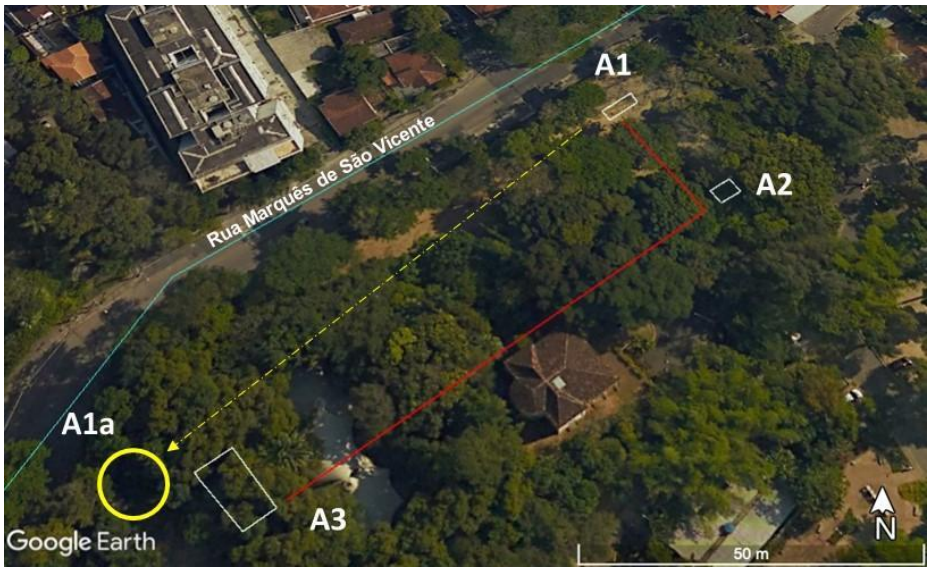

Figure A. 3. Locations of the preliminary investigation campaign. A1) Disposed BSF area; A2) FIS area; A3) NNF area and A1a) New selected BSF area

Figures A.4, A.5 and A.6 present the area and soil surface cover in the three final selected experimental areas located in the Gávea Campus (A1a = BSF, A2 = FIS and A3 = NNF).

Figure A. 4. A1a - BSF experimental area and soil profile investigation site

Figure A. 5. A2 - FIS experimental area and soil profile investigation site.

Figure A. 6.NNF experimental area and soil profile investigation site.

A.1.2 Sampling procedure

The investigation campaign in the selected soil profiles was conducted gradually in each area. It was performed using Geoprobe's Direct Push Subsurface Sampling technology, which is manually operated and utilizes dual tube sampling composed of a soil probe rod (1.75” OD) with a thin wall and a clear PVC liner (1.25” OD) with a 60 cm length.

The probe penetration was carried out using a manual slide hammer (26 k) operated along the guide rod (Figure A.7a). Samples were extracted and stored inside the PVC liners, in which colored caps were used in the liner ends to differentiate the top and bottom (Figure A.7b and A.7c). The cylindrical samples were collected in two consecutive driving stages with 60 cm each to obtain the 1 m soil profile (see Figure A.13). After field collection, the samplers were transferred to the Geotechnical and Environmental Laboratory at PUC-Rio, also located on the Gávea Campus.

Figure A. 7. a) Fieldwork with manual slide hammer; b) Probe extraction and c) Samples stored in the PVC liner

A.1.3 Materials

BSF PROFILE

Figure A.8 shows the investigation hole and the soil obtained at the preliminary investigations as remolded samples in the BSF area. Despite being bare soil, there were fine roots in the top layer. It is also visually detectable the difference between sample colors from the 0.0 to 0.40 m depth section to 0.40 to 1.00 m depth. Figure A.9 presents the 1 m soil profile sample.

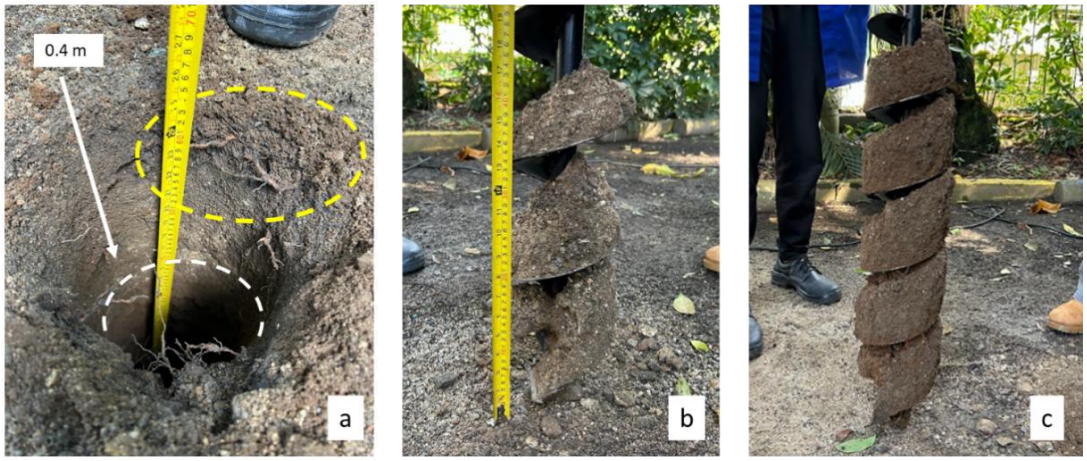

Figure A. 8. Figure 8. a) Borehole top layer with fine roots; b) Remolded sample of the 0.0 to 0.4 m depth and c) remolded sample of the 0.4 to 1.0 m depth.

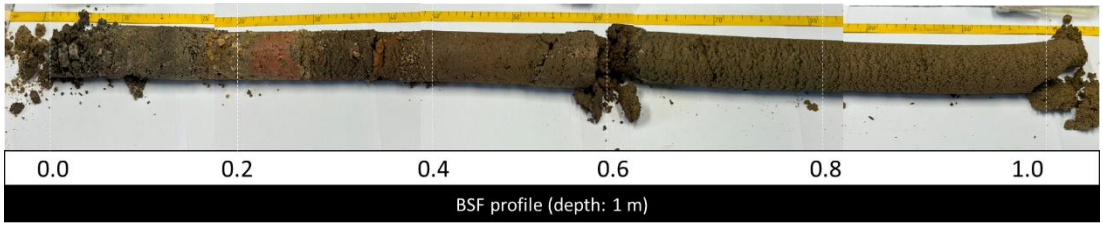

Figure A. 9. The BSF soil profile sample by layers.

FIS PROFILE

Figure A.10 shows the investigation and the remolded samples obtained in the preliminary investigation campaign of the FIS area. It is also detectable presence of fine roots in the topsoil of the FIS area and the difference between colors in subsoil (Figure A.10a and A.10b) and in the topsoil (Figure A.10c). Figure A.11 shows the 1m soil profile sample out of the PVC liner.

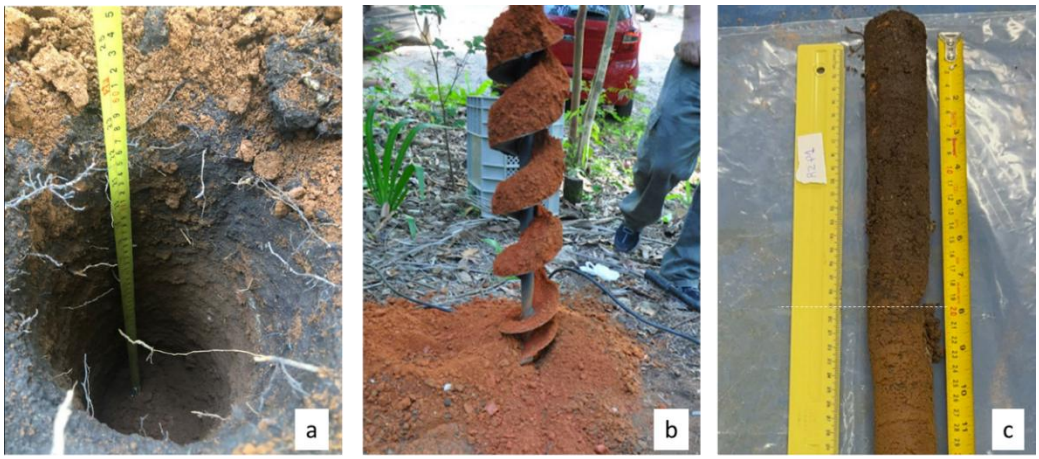

Figure A. 10. a) Top layer of the borehole in the FIS area; b) Remolded samples of the 0.4 to 1.0 profile depth and c) Topsoil sample of the PVC liner.

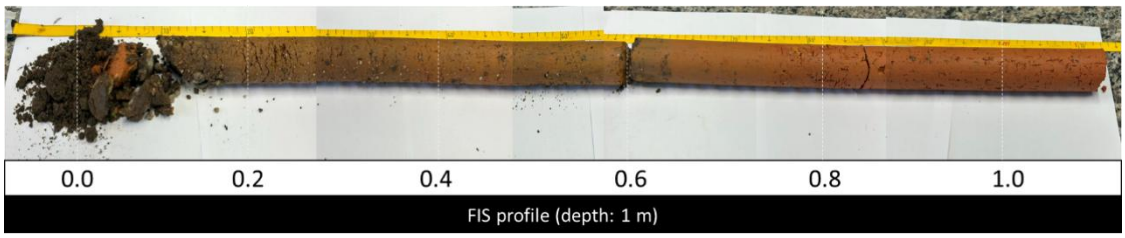

Figure A. 11. The FIS soil profile sample by layer.

NNF PROFILE

Figure A.12 shows the investigation and the samples obtained in the preliminary investigations in the NNF area. It was detected large volume of roots

with a higher diameter than the other areas. The difference between colors in the topsoil sample (Figure A.12b) and in the subsoil sample (Figure A.12c) is also visually recognized. Figure A.13 shows the 1m soil profile sample out of the PVC liner.

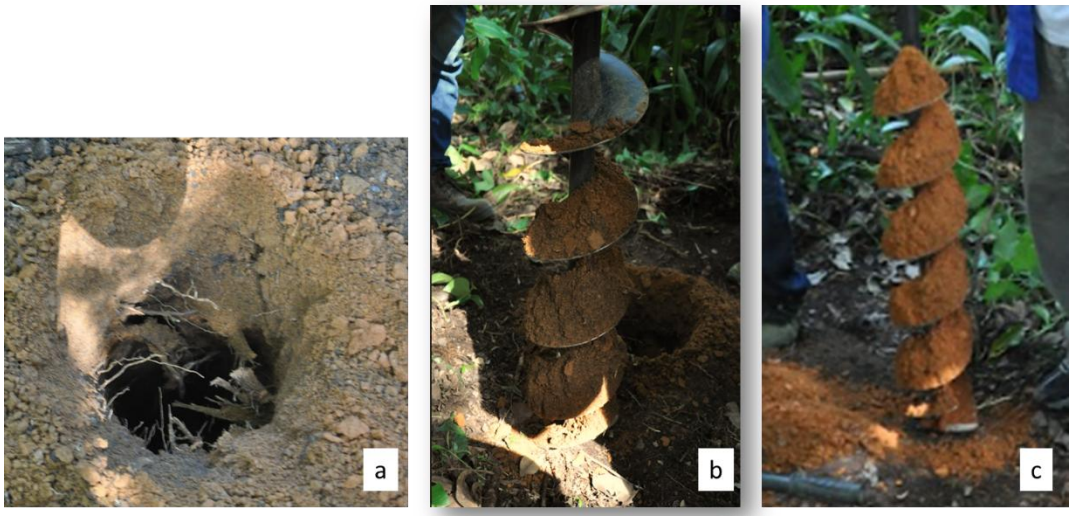

Figure A. 12. a) The NNF borehole with roots; b) Sample of the section 0.0 to 0.20 m depth and c) Sample of the 0.2 to 1.0 m section depth.

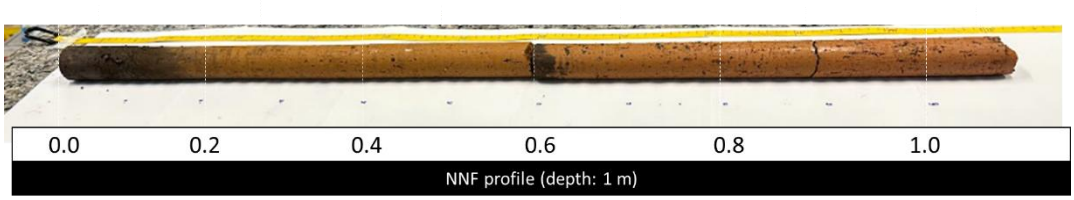

Figure A. 13. The NNF soil profile by layers.

Physical-chemical-mineralogical soil characterization tests were performed in the laboratory on specimens retrieved from investigated layers corresponding to the topsoil (0 – 20 cm) and the subsoil (20 to 40 cm; 40 to 60 cm; 60 to 80 cm and 80 to 100 cm) nominated in this study as layer 1, 2, 3, 4 and 5 from top to bottom.

APPENDIX 2

A.2. Laboratory test methodology and results

A.2.1 Experimental program

Table A. 1 presents the list and quantity of the laboratory tests performed for the characterization of the materials. It is divided into types of characterization: physical, chemical, mineralogical, hydraulic, and microstructural.

Table A. 1. Experimental program

Type	Test	Laboratory
Physical	Grain Size distribution	Laboratory of Geotechnics and Environment (LGMA)
	Atterberg Limits	
	Particle density (Gs)	
	Specific mass of grains	
	Gravimetric water content	
	Total soil density	
	Electrical condutivity	
	Organic matter	
	Organic matter physical fractionation (POM/MAOM)	
Hydrical	Retention curve	
Chemical	pH	
	Metal elements - ICP-OES	Laboratory of Atomic Spectrometry (LABSPECTRO)
	Total C, N and stable isotopes	Laboratory of Marine and Environmental Studies (LabMAM)
	Organic C, N and stable isotopes	
Mineralogical	DRX - X-Ray Difraction	X-Ray Diffraction and Scattering Laboratory (Lab LDRX)
Microstructural	Mercury intrusion and extrusion porosimetry	São Carlos Physics Institute (USP).

A.2.2 Grain size distribution

Grain size distribution was performed by sieving and sedimentation techniques following the Brazilian standard, NBR 7181: Soil-granulometric analysis *(*ABNT,2025a). Grain sizes were defined according to NBR ISO 6502: Soils and Rocks: Terminology. Rio de Janeiro (ABNT, 2022a) as gravel (60 – 2.0 mm), sand (2.0 – 0.06 mm), silt (0.06 – 0.002 mm), and clay (< 0.002 mm).

Figure A.14, A.15, and A.16 present the grain size distribution curves by area (BSF, FIS and NNF) and by layers (1 to 5). Table A.2 presents the numerical results of the grain size distribution with the descriptive statistical analysis of the mean, standard deviation and the coefficient of variation by grain size (gravel, sand, silt and clay) across the profile.

Additionally, Table A.3 and Table A.4 show the results of the descriptive statistical analysis of the Combined Coefficient of Variation (CV-c) in each area, considering all layers and layers 2 to 5, respectively. This analysis consists of the determination of the standard deviation and the coefficient of variation, considering grain size distribution (all sizes) across the profile.

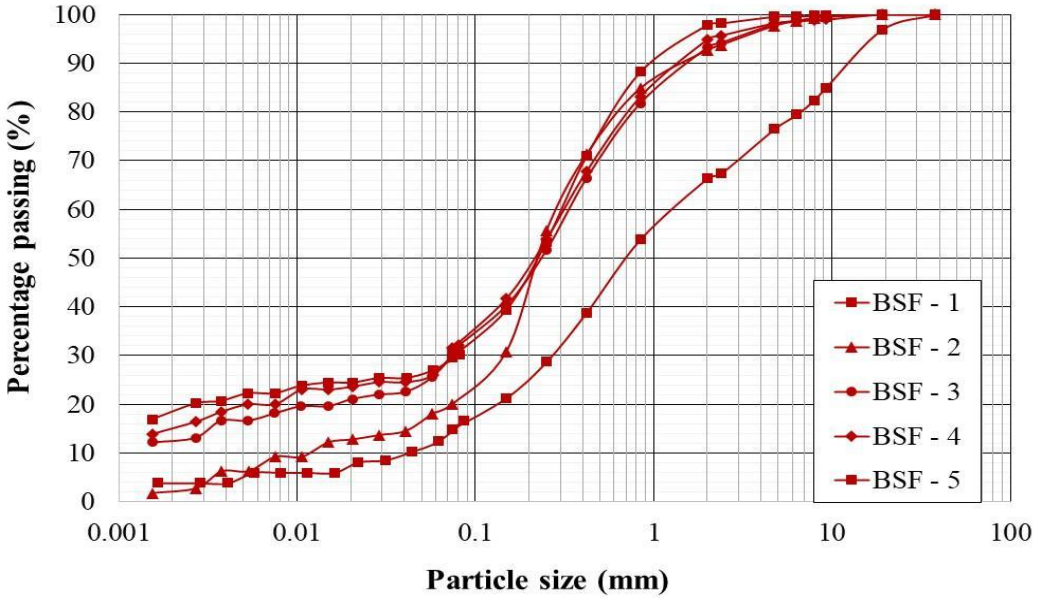

Figure A. 14. Particle size distribution curves of the layers 1 to 5 in the area BSF.

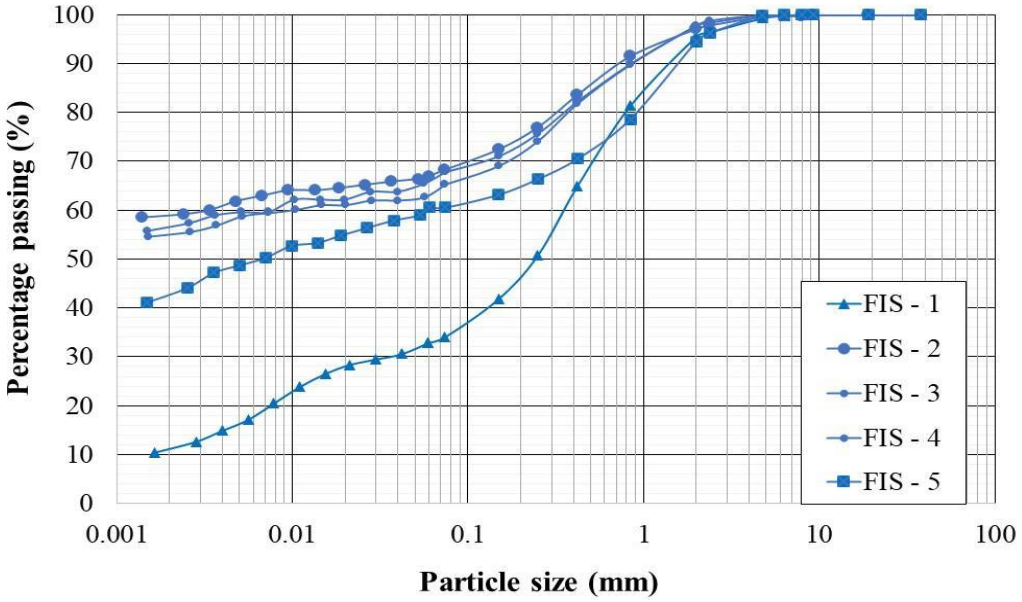

Figure A. 15. Particle size particle distribution curves of the layers 1 to 5 in the area FIS.

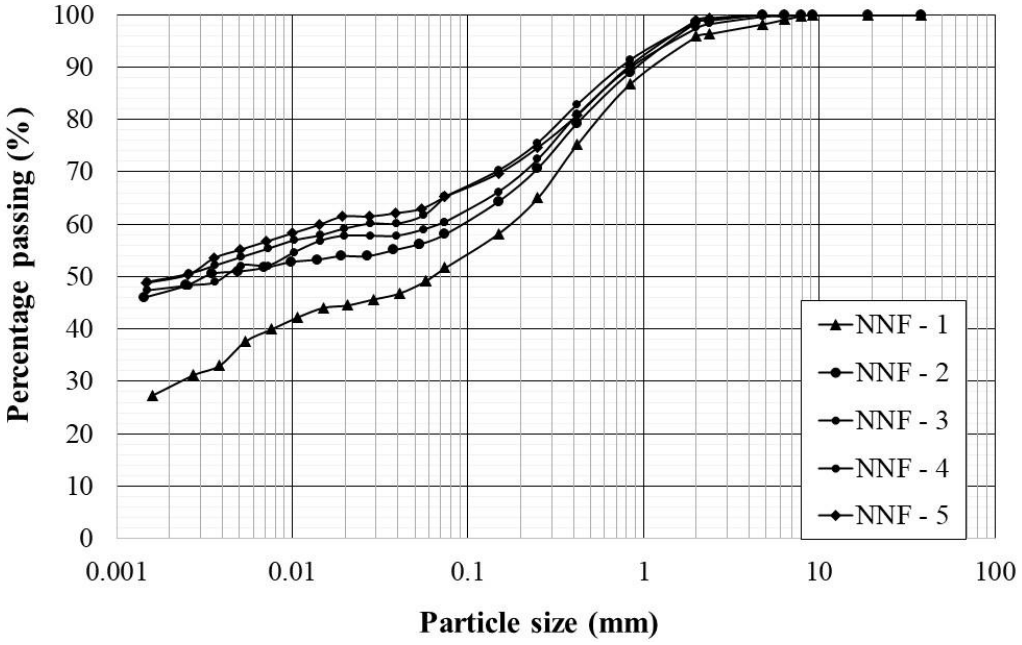

Figure A. 16. Grain size particle distribution curves of the layers 1 to 5 in the area NNF.

Table A. 2. Results of the particle size distribution test.

Land Class	Layer (m)	Code	Particle size distribution (%)			
			Gravel	Sand	Silt	Clay
			mm			
			60.0 - 2.0	2.0 - 0.06	0.06 - 0.002	< 0.002
Bare Soil Fill (BSF)	0.0 - 0.2	BSF-1	33.64	53.93	8.58	3.84
	0.2 - 0.4	BSF-2	7.34	74.53	15.36	2.76
	0.4 - 0.6	BSF-3	6.79	67.62	12.43	13.16
	0.6 - 0.8	BSF-4	5.07	68.89	9.62	16.42
	0.8 - 1.0	BSF-5	2.06	70.93	6.83	20.17
	Average		10.98	67.18	10.56	11.27
	Standard deviation		12.83	7.85	3.36	7.70
	Coefficient of variation (%)		116.89	11.69	31.85	68.29
Dense Ombrophylous Forest in the Initial Stage (FIS)	0.0 - 0.2	FIS-1	4.43	62.71	20.19	12.66
	0.2 - 0.4	FIS-2	3.10	30.56	7.21	59.13
	0.4 - 0.6	FIS-3	2.21	35.12	7.10	55.57
	0.6 - 0.8	FIS-4	2.19	32.39	8.01	57.41
	0.8 - 1.0	FIS-5	5.46	35.54	14.84	44.16
	Average		3.48	39.27	11.47	45.79
	Standard deviation		1.44	13.27	5.85	19.42
	Coefficient of variation (%)		41.37	33.78	50.97	42.42
Non-Native Vegetation Forest (NNF)	0.0 - 0.2	NNF-1	4.08	46.77	17.90	31.25
	0.2 - 0.4	NNF-2	1.52	42.28	7.89	48.30
	0.4 - 0.6	NNF-3	2.49	38.51	10.73	48.27
	0.6 - 0.8	NNF-4	1.48	36.79	11.12	50.60
	0.8 - 1.0	NNF-5	1.08	35.92	12.58	50.42
	Average		2.13	40.06	12.05	45.77
	Standard deviation		1.21	4.48	3.69	8.19
	Coefficient of variation (%)		56.63	11.18	30.61	17.90

Table A. 3. Combined coefficient of variation on profile (layers 1 to 5).

Class	Combined coefficient of variation layer 1-5							
	Size	*Average*	*SD*	*n*	*Average*	*Variance*	*SD*	*CV_c (%)*
BSF	Gravel	10.98	12.83	5	25.00	74.25	8.62	34.47
	Sand	67.18	7.85	5				
	Silt	10.56	3.36	5				
	Clay	11.27	7.70	5				
FIS	Gravel	3.48	1.44	5	25.00	147.36	12.14	48.56
	Sand	39.27	13.27	5				
	Silt	11.47	5.85	5				
	Clay	45.79	19.42	5				
NNF	Gravel	2.13	1.21	5	25.00	25.57	5.06	20.23
	Sand	40.06	4.48	5				
	Silt	12.05	3.69	5				
	Clay	45.77	8.19	5				

Table A. 4. Combined coefficient of variation on subsoil (layers 2 to 5).

Class	Combined coefficient of variation layer 2-5							
	Size	*Average*	*SD*	*n*	*Average*	*Variance*	*SD*	*CV_c (%)*
BSF	Gravel	5.31	2.38	4	25.00	21.06	4.59	18.36
	Sand	70.50	3.02	4				
	Silt	11.06	3.67	4				
	Clay	13.13	7.48	4				
FIS	Gravel	3.24	1.54	4	25.00	16.89	4.11	16.44
	Sand	33.40	2.35	4				
	Silt	9.29	3.72	4				
	Clay	54.07	6.77	4				
NNF	Gravel	1.64	0.60	4	25.00	3.45	1.86	7.43
	Sand	38.38	2.82	4				
	Silt	10.58	1.96	4				
	Clay	49.40	1.29	4				

Grain size distribution was also established according to the grain size ranges applied for organic matter physical fractionation in this study (Cotrufo et al., 2019), which considers Particulate Organic Matter (POM), the organic matter present in the grain size range of 0,053 < ϕ < 2mm, and the Mineral Associated Organic Matter (MAOM), the OM present in the grain size range ϕ < 53 µm. Table A.5 presents the percentages of grain size fractions in the ranges of organic matter

fractions in the total soil (POM, MAOM and coarse grains) and the percentage of POM and MAOM grain size fractions in the fine earth fraction (< 2 mm)

Table A. 5. Grain size distribution according to organic matter fractionation ranges.

Class -Layer	Soil particle size distribution (%)				Fine fraction (%)		
	Coarse	POM	MAOM	Total	Fines	POM	MAOM
	> 2.0 mm	2.0 < φ >0.053	< 0.053 mm		< 2.0 mm	2.0 < φ >0.053	< 0.053 mm
BSF-1	33.64	54.99	11.36	100	66.36	82.88	17.12
BSF-2	7.34	75.48	17.17	100	92.66	81.46	18.54
BSF-3	6.79	68.39	24.82	100	93.21	73.37	26.63
BSF-4	5.07	69.31	25.62	100	94.93	73.01	26.99
BSF-5	2.06	71.38	26.56	100	97.94	72.88	27.12
FIS-1	4.43	63.53	32.04	100	95.57	66.47	33.53
FIS-2	2.84	30.72	66.44	100	97.16	31.62	68.38
FIS-3	2.21	35.26	62.53	100	97.79	36.05	63.95
FIS-4	2.19	32.66	65.15	100	97.81	33.39	66.61
FIS-5	5.46	35.54	59.00	100	94.54	37.59	62.41
NNF-1	4.08	47.39	48.53	100	95.92	49.40	50.60
NNF-2	1.52	42.31	56.17	100	98.48	42.96	57.04
NNF-3	2.49	38.74	58.77	100	97.51	39.73	60.27
NNF-4	1.48	37.08	61.43	100	98.52	37.64	62.36
NNF-5	1.08	35.99	62.92	100	98.92	36.39	63.61

A.2.3 Atterberg Limits and Soil Classification

Table A.6 presents the results of the consistency limits, clay activity and soil classification. Determination of the consistency or Atterberg limits – liquid (w_L) and plasticity (w_P) limits – followed the NBR 6459: Soil – Liquid limit determination (ABNT, 2016a) and NBR 7180: Soil – Plasticity limit determination (ABNT, 2016b), respectively. The materials were tested in the natural humidity. Due to the high organic content of the soil in layer 1 in the NNF area, the liquid limit test was also performed with oven-dried material (100 °C). The results support the soil classification, which was done according to the ASTM. D2487-25: Standard Practice for Classification of Soils for Engineering Purposes (Unified Soil Classification System).

Table A. 6. Consistency Limits, clay activity and soil classification.

Class	Layer (m)	Code	Consistency limits (%)			Clay (%)	Activity IP/clay (%)	Soil Classification
			W_L	W_P	PI			
BSF	0.0 - 0.2	BSF-1	-	-	-	3.84	-	SM
	0.2 - 0.4	BSF-2	26.90	18.90	8.00	2.76	-	SC
	0.4 - 0.6	BSF-3	28.40	16.00	12.40	13.16	0.94	SC
	0.6 - 0.8	BSF-4	26.20	14.70	11.50	16.42	0.70	SC
	0.8 - 1.0	BSF-5	25.30	15.00	10.20	20.17	0.51	SC
	Average		*26.70*	*16.15*	*10.53*	*13.13*	*0.72*	-
	Standard deviation		*1.31*	*1.92*	*1.91*	*7.48*	*0.22*	
FIS	0.0 - 0.2	FIS-1	40.70	28.90	11.90	12.66	0.94	SM
	0.2 - 0.4	FIS-2	76.02	35.03	40.99	59.13	0.69	CH
	0.4 - 0.6	FIS-3	69.60	31.30	38.30	55.57	0.69	CH
	0.6 - 0.8	FIS-4	75.20	34.40	40.90	57.41	0.71	CH
	0.8 - 1.0	FIS-5	68.11	33.43	34.69	44.16	0.79	CH
	Average		*65.93*	*32.61*	*33.36*	*45.79*	*0.76*	-
	Standard deviation		*14.51*	*2.51*	*12.27*	*19.42*	*0.11*	
NNF	0.0 - 0.2	NNF-1	57.73	34.62	23.11	31.25	0.74	MH
	0.2 - 0.4	NNF-2	65.42	26.91	38.51	48.30	0.80	CH
	0.4 - 0.6	NNF-3	74.82	30.52	44.30	48.27	0.92	CH
	0.6 - 0.8	NNF-4	81.20	34.50	46.70	50.60	0.92	CH
	0.8 - 1.0	NNF-5	75.45	31.44	44.01	50.42	0.87	CH
	Average		*70.92*	*31.60*	*39.32*	*45.77*	*0.85*	-
	Standard deviation		*9.30*	*3.19*	*9.55*	*8.19*	*0.08*	

In this system, the topsoil from the NNF area was classified as high-plasticity silt (MH), while that from the BSF and FIS areas were classified as silty sand (SM). Organic classification was excluded by testing the liquid limit values after oven drying. The subsoil from the NNF and FIS areas was classified as high plasticity clay (CH), and that from the BSF as clayey sand (SC). From the viewpoint of Soil Science, the BSF area is classified as Technosol, while the FIS and the NNF areas are classified as Acrisols (Santos et al., 2025; Lumbreras and Gomes, 2004).

It was also computed the Skempton clay activity index, *Ac*, given by the ratio between the plasticity index, $PI = w_L - w_P$, and the percentage by weight of clay (Skempton, 1953).

A.2.4 Particle density, specific mass of grains and physical indexes

The specific mass of grains (ρ_s) followed NBR 6458: Soils — Determination of the specific mass of solids, the apparent specific mass and the water absorption of the fraction retained in the 2,0 mm aperture sieve (ABNT, 2025b). Gravimetric moisture content (w) was determined according to NBR 6457: Soils - Preparation of samples for compaction tests, characterization and determination of moisture content (ABNT, 2024).

Total density, ρ_t, (ratio between the total soil mass, M, and its total volume, V, and dry soil density, ρ_d, (ratio between the oven dried soil mass or mass of solids, M_s, and the total volume of the specimen, V), were determined were retrieved from the liner using a volumetric ring (approximately 11 cm³) with an area ratio of circa of 15 % (Clayton et al., 1995) (Figure A.17).

Figure A. 17. Volumetric ring molding from the PVC liner.

Knowing ρ_s, w and ρ_t, the physical index voids ratio, e, given by V_v/V_s (V_v = volume of voids and V_s = volume of solids) was computed (e.g., Lambe & Whitman, 1969). The mirrored pattern between ρ_d and e results from the inverse relationship between these two physical soil indices, where $e = (\rho_s/\rho_d) - 1$. It was also computed the soil porosity (n) by the index relation where $n = e / (1+e)$. Table A.7 shows the results of the specific mass of grains (ρ_s), particle density (G_s), and physical indexes.

Table A. 7. Results of the specific mass of grains (ρ_s), particle density (G_s), and physical indexes.

Class	Code	ρ_s (g cm^{-3})	G_s	ρ_t (g cm^{-3})	ρ_d (g cm^{-3})	e= (ρ_s/ρ_d) - 1	n = e / (1+e)
Bare Soil Fill (BSF)	BSF-1	2.66	2.666	1.52	1.41	0.89	47.01
	BSF-2	2.68	2.689	1.77	1.57	0.70	41.32
	BSF-3	2.71	2.714	1.62	1.45	0.86	46.31
	BSF-4	2.69	2.693	1.67	1.52	0.77	43.62
	BSF-5	2.68	2.683	1.80	1.64	0.63	38.58
	Average	2.68	2.69	1.68	1.52	0.77	43.37
	SD	0.02	0.02	0.11	0.09	0.11	3.51
	CV (%)	0.65	0.65	6.79	6.16	14.03	8.08
Dense Ombrophylous Forest in the Initial Stage (FIS)	FIS-1	2.56	2.564	1.54	1.42	0.81	44.61
	FIS-2	2.61	2.615	1.71	1.42	0.84	45.76
	FIS-3	2.62	2.628	1.80	1.44	0.82	44.95
	FIS-4	2.65	2.652	1.80	1.40	0.89	47.09
	FIS-5	2.63	2.639	1.78	1.39	0.90	47.39
	Average	2.61	2.62	1.73	1.41	0.85	45.96
	SD	0.03	0.03	0.11	0.02	0.04	1.25
	CV (%)	1.28	1.28	6.38	1.54	5.03	2.71
Non-Native Vegetation Forest (NNF)	NNF-1	2.50	2.508	1.46	1.06	1.36	57.66
	NNF-2	2.66	2.664	1.81	1.47	0.80	44.54
	NNF-3	2.68	2.681	1.82	1.47	0.83	45.25
	NNF-4	2.69	2.697	1.81	1.44	0.87	46.54
	NNF-5	2.68	2.686	1.80	1.43	0.87	46.59
	Average	2.64	2.65	1.74	1.37	0.95	48.11
	SD	0.08	0.08	0.16	0.18	0.23	5.40
	CV (%)	2.98	2.98	8.94	12.85	24.69	11.23

Knowing the total dry density, ρ_d, (ratio between the oven-dried soil mass or mass of solids, M_s, and the total volume of the specimen, V) (Table A.7), and the percentage of the fine earth mass in the total soil (Table A.5) it was computed the dry density of the fine earth, ρ_{dfe} which was employed in the calculation of soil organic carbon stocks (*Cstocks*). Table A.8 shows the results of soil dry density and soil dry density of the fine earth (< 2mm).

Table A. 8. Results of the dry density of the fine earth soil.

Class -Layer	Sample volume	Total soil mass	$\rho_{d\ total}$	Fines content	Fine soil mass	$\rho_{d\ fines}$
	cm^3	g	$g\ cm^{-3}$	(%)	g	$g\ cm^{-3}$
BSF-1	10.68	15.05	1.41	66.36	9.99	0.94
BSF-2	10.67	16.82	1.57	92.66	15.58	1.46
BSF-3	10.44	15.19	1.45	93.21	14.16	1.36
BSF-4	10.78	16.32	1.52	94.93	15.49	1.44
BSF-5	10.68	17.58	1.64	97.94	17.21	1.61
FIS-1	10.82	15.34	1.42	95.57	14.66	1.35
FIS-2	13.04	18.45	1.42	97.16	17.92	1.37
FIS-3	13.14	18.99	1.44	97.79	18.57	1.41
FIS-4	14.19	19.86	1.40	97.81	19.43	1.37
FIS-5	14.24	19.74	1.39	94.54	18.66	1.31
NNF-1	10.73	11.37	1.06	95.92	10.90	1.02
NNF-2	10.73	15.83	1.47	98.48	15.59	1.45
NNF-3	10.98	16.10	1.47	97.51	15.70	1.48
NNF-4	10.62	15.29	1.44	98.52	15.07	1.38
NNF-5	10.94	15.67	1.43	98.92	15.50	1.42

A.2.5 Electrical conductivity, pH and organic matter

Samples for pH and EC were air-dried and sieved (< 2mm). The pH was measured under a 1:25 suspension of soil: water (m:v) using a pHmetro from Hanna Instruments (EDGE HI2002-02) and EC in the soil/water (Mili Q) solution of 1:5 with a conductivity meter Hanna model HI763100. It was reported in dS m^{-1} at 25°C, according to FAO (2021a). Figure A.18a presents an image of the preparation of the soil solution for the EC test, and Figure A. 18 b shows the equipment. While Figure 18. A c shows pH measurement.

Figure A. 18. Electrical conductivity and pH laboratory tests.

Electrical conductivity, *EC*, was determined in soil solution with a conductivity meter, Hanna model HI763100, according to the Food and Agriculture Organization of the United Nations - FAO. Standard operating procedure for soil electrical conductivity, soil/water, 1:5. Rome (FAO, 2021a), while pH was determined according to the Food and Agriculture Organization of the United Nations - FAO. Standard operating procedure for soil pH determination. Rome: 2021b.

Organic matter (*OM*) determination proceeded according to NBR 13600: Soil – Determination of organic material content by burning at 440°C (ABNT, 2022b). Figure A.19 presents stages of the organic matter determination test and Table A. 9 shows the results of pH, EC, and organic matter content.

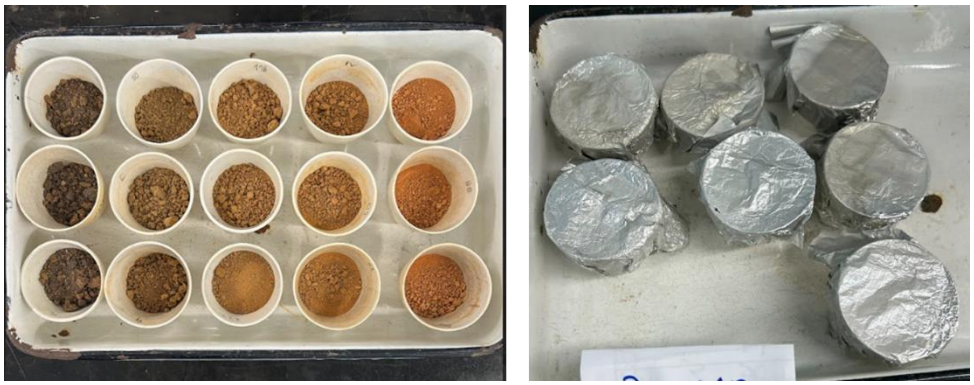

Figure A. 19. Stages of organic matter determination by loss of ignition.

Table A. 9. Results of the pH, EC and OM.

Land class	Depth (m)	Layer (m)	pH	EC (dS m^{-1})	OM (%)
Bare Soil Fill (BSF)	BSF-1	0.0 - 0.2	8.21	0.083	1.72
	BSF-2	0.2 - 0.4	7.70	0.044	1.45
	BSF-3	0.4 - 0.6	7.79	0.030	2.75
	BSF-4	0.6 - 0.8	7.97	0.029	2.00
	BSF-5	0.8 - 1.0	7.89	0.024	1.80
	Average		7.91	0.04	*1.94*
	Standard deviation		0.20	0.02	*0.49*
Dense Ombrophylous Forest in the Initial Stage (FIS)	FIS-1	0.0 - 0.2	7.45	0.087	7.43
	FIS-2	0.2 - 0.4	6.73	0.037	5.10
	FIS-3	0.4 - 0.6	6.01	0.042	4.48
	FIS-4	0.6 - 0.8	4.99	0.043	4.28
	FIS-5	0.8 - 1.0	4.74	0.043	3.45
	Average		5.98	0.05	*4.95*
	Standard deviation		1.15	0.02	*1.51*
Non-Native Vegetation Forest (NNF)	NNF-1	0.0 - 0.2	6.43	0.088	10.57
	NNF-2	0.2 - 0.4	4.44	0.082	4.42
	NNF-3	0.4 - 0.6	4.36	0.092	3.89
	NNF-4	0.6 - 0.8	3.91	0.099	3.46
	NNF-5	0.8 - 1.0	3.82	0.127	4.13
	Average		4.59	0.10	*5.29*
	Standard deviation		1.06	0.02	*2.97*

A.2.6 Organic Matter Fractionation

SOM occurs in various sizes and shapes during different stages of decomposition. Most of them are encountered in two soil fractions: the particulate organic matter (POM), which presents a lower density (<1.60 to 1.85 g cm^{-3}) and larger size (0,053 < ϕ < 2mm), and the mineral-associated organic matter (MAOM), which has higher density (>1.85 g cm^{-3}) and smaller size (< 53 μm). While POM may be free in soil pores or physically protected in soil clusters, MAOM is typically adsorbed in clay minerals (Lavallee et al., 2019).

There are several methods to fractionate the OM in soil by function and formation, which may involve separation by particles based on size, density, or a combination of the two properties. The choice of the fractionation method depends on the goals of the research (Leuthold et al., 2022).

In this study, it was applied the physical fractionation method that is based on the primary particle size. It consists of the separation of sizes ranging between 0,053 and 60 mm as POM and < 0,053 mm as MAOM, following Cotrufo et al. (2019). To do this, bulk soil samples were dispersed in a shaker with glass beads (18 h; ~120 rpm) in a 5 g L^{-1} sodium hexametaphosphate solution. Fractions were separated by sieving and oven-dried (40 ºC). Recovery dry mass must fall between 95% and 105% of the sample mass. This method is relatively simple, requires a low laboratory infrastructure, and has a low cost. Figure A.20 presents the schematic diagram of the physical fractionation method. Table A. 10 shows the mass recovery in the test.

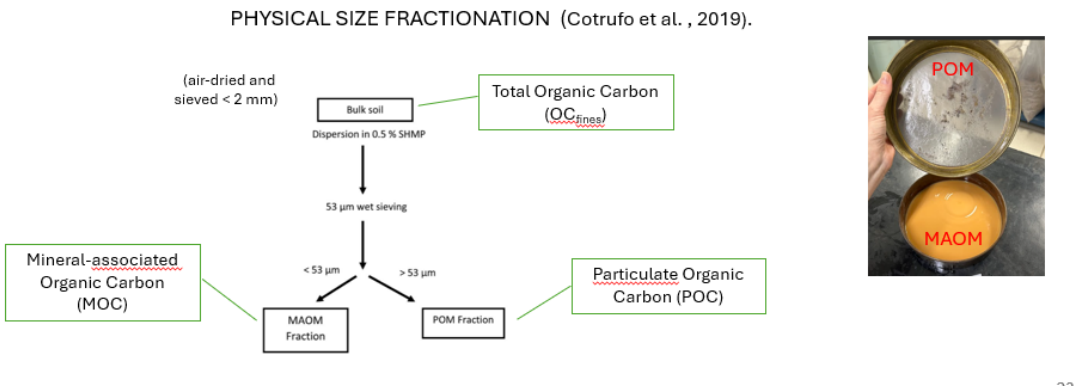

Figure A. 20 Schematic diagram of the physical fractionation method.

A.2.7 Carbon analysis

TC, OC, and stable isotope $\delta^{13}C$ determinations were performed in the bulk soil samples (air-dried and sieved < 2 mm) and in the SOM fractions POM (*POC*) and MAOM (*MOC*), which were obtained using the physical size fractionation method described in the section A.2.

To do this, bulk soil samples were dispersed in a shaker with glass beads (18 h; ~120 rpm) in a 5 g L^{-1} sodium hexametaphosphate solution. Fractions were separated by sieving and oven-dried (40 ºC). Carbon analysis was performed by dry combustion in the Elemental Analyzer coupled to Isotope Ratio Mass Spectrometer

(EA-IRMS), model Focus-Delta V Plus by Thermo Scientific, with a C limit of detection (LOD) of 3 µg. Carbon determinations were performed in the bulk soil sample in quadruplicate, while the SOM fractions (POM and MAOM) were measured in triplicate.

Table A. 10. Mass recovery in the physical OM fractionation test.

Class	Initial soil mass	Mass recovery (g)			Recovery (%)		
	g	POM	MAOM	Total	POM	MAOM	Total
BSF-1	5.38	3.84	1.5	5.34	28.1	71.9	99.3
BSF-2	5.44	3.26	2.43	5.69	42.7	57.3	104.6
BSF-3	5.56	3.72	1.62	5.34	30.3	69.7	96.0
BSF-4	5.36	3.59	1.73	5.32	32.5	67.5	99.3
BSF-5	5.48	3.88	1.32	5.2	25.4	74.6	94.9
FIS-1	5.53	3.57	2.01	5.58	36.0	64.0	100.9
FIS-2	5.52	3.58	1.98	5.56	35.6	64.4	100.7
FIS-3	5.43	3.7	1.78	5.48	32.5	67.5	100.9
FIS-2	5.47	2.4	3.15	5.55	56.8	43.2	101.5
FIS-3	5.44	1.53	3.98	5.51	72.2	27.8	101.3
FIS-4	5.45	1.5	3.98	5.48	72.6	27.4	100.6
FIS-5	5.47	1.52	3.98	5.5	72.4	27.6	100.5
NNF-1	5.05	2.82	1.93	4.75	40.6	59.4	94.1
NNF-2	5.04	2.95	2.14	5.09	42.0	58.0	101.0
NNF-3	5.04	2.02	3.06	5.08	60.2	39.8	100.8
NNF-4	5.08	1.77	3.43	5.2	66.0	34.0	102.4
NNF-5	5.10	1.82	3.25	5.07	64.1	35.9	99.4

A fine powder texture was obtained for the bulk soil and SOM fractions (FAO, 2019). The samples for *OC* quantification were acid-washed with 1 M HCl (hydrochloric acid) to remove inorganic carbon.

Table A.11 presents results of the Total carbon (C), Organic Carbon (OC), total Nitrogen (N), stables isotopes ^{13}C and ^{15}N in the total soil fraction in the bulk soil (< 2mm), Table A.12 presents results of the Total carbon (C), Organic Carbon (OC), total Nitrogen (N), stables isotopes ^{13}C and ^{15}N in the total soil fraction in the POM fraction (0,053 < ϕ < 2mm), and Table A.13 presents the same carbon parameters in the MAOM fraction (< 0,053mm). Table A.14 shows the total recovery rate of the OC concentrations from POM and MAOM.

Table A. 11. Total carbon (C), Organic Carbon (OC), total Nitrogen (N), stables isotopes 13C and 15N in the total soil fraction.

Total Soil (< 2mm)										
Classs - layer	TOTAL CARBON					ORGANIC CARBON				
	$\delta^{15}N$	$\delta^{13}C$	N	C	C/N	$\delta^{15}N$	$\delta^{13}C$	N	OC	C/N
	‰	‰	%	%		‰	‰	%	%	
BSF-1	5.9	-25.2	0.10	1.80	18.46	<LD	-26.5	0.09	1.63	17.50
BSF-2	7.9	-24.5	0.07	1.24	18.16	<LD	-25.4	0.07	1.09	16.36
BSF-3	10.6	-22.5	0.09	1.17	13.44	<LD	-23.0	0.08	1.10	13.68
BSF-4	10.7	-22.3	0.07	1.01	14.04	<LD	-22.8	0.07	0.97	13.93
BSF-5	9.4	-23.0	0.06	0.78	13.42	<LD	-23.4	0.06	0.71	12.76
FIS-1	5.7	-23.6	0.41	5.58	13.61	4.5	-26.2	0.35	5.11	14.80
FIS-2	8.2	-23.6	0.11	1.42	12.63	<LD	-24.6	0.10	1.30	13.04
FIS-3	8.1	-25.1	0.07	0.93	13.54	<LD	-24.9	0.06	0.85	13.40
FIS-4	<LD	-25.7	0.05	0.75	14.70	<LD	-25.5	0.05	0.67	14.00
FIS-5	<LD	-25.6	0.04	0.56	14.80	<LD	-25.5	0.04	0.54	15.22
NNF-1	7.2	-23.6	0.58	8.51	14.79	5.3	-28.2	0.44	7.04	15.83
NNF-2	8.0	-24.3	0.07	0.99	15.06	<LD	-25.7	0.06	0.89	15.55
NNF-3	8.0	-24.3	0.05	0.78	16.46	<LD	-25.5	0.04	0.74	16.74
NNF-4	<LD	-24.3	0.04	0.74	17.14	<LD	-25.9	0.04	0.69	16.73
NNF-5	<LD	-24.1	0.04	0.68	18.12	<LD	-25.9	0.04	0.65	17.06

Note: mean values; $n = 4$

Table A. 12. Total carbon (C), Organic Carbon (OC), total Nitrogen (N), stables isotopes 13C and 15N in the POM soil fraction.

POM FRACTION													
Class -Layer	TOTAL CARBON					ORGANIC CARBON					OC mass correction	
	$\delta^{15}N$	$\delta^{13}C$	N	C	C/N	$\delta^{15}N$	$\delta^{13}C$	N	OC	C/N	POM fraction	OCc
	‰	‰	%	%		‰	‰	%	%		%	%
BSF-1	<LD	-25.8	0.02	0.82	43.16	<LD	-28.06	0.02	0.62	32.2	0.83	0.52
BSF-2	<LD	-27.2	0.03	1.01	32.71	<LD	-28.43	0.03	0.93	31.4	0.81	0.76
BSF-3	<LD	-26.6	<LD	0.32	<LD	<LD	-27.2	<LD	0.3	<LD	0.73	0.19
BSF-4	<LD	-26.4	<LD	0.27	<LD	<LD	-27.1	<LD	0.3	<LD	0.73	0.21
BSF-5	<LD	-26.7	<LD	0.13	<LD	<LD	-27.2	<LD	0.1	<LD	0.73	0.09
FIS-1	<LD	-27.2	0.13	2.75	21.58	<LD	-29.62	0.11	2.42	23.0	0.66	1.61
FIS-2	<LD	-29.6	0.01	0.51	42.29	<LD	-27.94	0.02	0.52	34.8	0.32	0.17
FIS-3	<LD	-29.6	<LD	0.33	<LD	<LD	-27.6	<LD	0.3	<LD	0.36	0.11
FIS-4	<LD	-29.5	<LD	0.27	<LD	<LD	-27.5	<LD	0.2	<LD	0.33	0.08
FIS-5	<LD	-29.4	<LD	0.21	<LD	<LD	-26.7	<LD	0.2	<LD	0.38	0.09
NNF-1	<LD	-24.2	0.19	3.44	18.56	4.9	-29.29	0.17	3.55	21.0	0.49	1.75
NNF-2	<LD	-26.5	0.02	0.42	26.16	<LD	-27.76	<LD	0.36	<LD	0.43	0.16
NNF-3	<LD	-25.5	0.03	0.43	13.45	<LD	-26.96	<LD	0.37	<LD	0.40	0.15
NNF-4	<LD	-23.9	0.21	0.75	3.55	<LD	-26.05	0.02	0.73	45.5	0.38	0.27
NNF-5	<LD	-25.0	<LD	0.60	<LD	<LD	-26.6	0.0	0.6	31.8	0.36	0.22

Note: mean values; Total carbon ($n = 2$) and Organic carbon (n = 3); OCc = Organic Carbon corrected

Table A. 13. Total carbon (C), Organic Carbon (OC), total Nitrogen (N), stables isotopes 13C and 15N in the MAOM soil fraction.

MAOM FRACTION													
Class -Layer	TOTAL CARBON					ORGANIC CARBON					OC mass correction	
	$\delta^{15}N$	$\delta^{13}C$	N	C	C/N	$\delta^{15}N$	$\delta^{13}C$	N	OC	C/N	MAOM fraction	OCc
	‰	‰	%	%		‰	‰	%	%		%	%
BSF-1	4.6	-26.0	0.21	3.06	14.67	5.1	-25.19	0.26	2.93	11.2	0.17	0.50
BSF-2	<LD	-25.3	0.13	1.75	13.69	<LD	-25.09	0.12	1.65	13.9	0.19	0.31
BSF-3	<LD	-25.4	0.1	1.76	12.3	<LD	-23.1	<LD	1.7	<LD	0.27	0.46
BSF-4	<LD	-23.0	0.1	1.52	11.8	<LD	-23.0	<LD	1.5	<LD	0.27	0.40
BSF-5	<LD	-27.1	0.1	1.33	10.6	<LD	-24.9	<LD	1.3	<LD	0.27	0.36
FIS-1	6.8	-20.5	0.65	8.01	12.36	4.1	-28.79	0.58	8.01	13.7	0.34	2.69
FIS-2	<LD	-20.5	0.15	1.63	10.84	<LD	-24.05	0.12	1.50	12.5	0.68	1.03
FIS-3	<LD	-21.8	0.1	1.05	10.9	<LD	-24.3	<LD	0.9	<LD	0.64	0.60
FIS-4	<LD	-22.3	0.1	0.86	11.4	<LD	-24.7	<LD	0.8	<LD	0.67	0.55
FIS-5	<LD	-23.8	0.1	0.60	11.0	<LD	-25.6	<LD	0.6	<LD	0.62	0.37
NNF-1	20.2	-18.5	2.33	9.80	4.20	7.2	-29.26	0.66	9.86	15.0	0.51	4.99
NNF-2	<LD	-27.7	6.65	1.21	0.18	<LD	-26.23	<LD	1.17	<LD	0.57	0.67
NNF-3	<LD	-32.2	13.38	0.84	0.06	<LD	-25.94	<LD	0.79	<LD	0.60	0.48
NNF-4	<LD	-33.3	18.79	0.76	0.04	<LD	-26.07	0.05	0.73	14.6	0.62	0.45
NNF-5	<LD	-32.1	25.2	0.91	0.0	<LD	-26.2	0.1	0.9	15.5	0.64	0.54

Note: mean values; Total carbon ($n = 2$) and Organic carbon (n = 3); OCc = Organic Carbon corrected

Table A. 14. C recovery control of the Particulate Organic Carbon (POC) and Mineral-associated Organic Carbon (MOC).

Class -Layer	OC (%)		POCc (%)		MOCc (%)		POCc + MOCc	C recovery	Average C recovery
	$n = 4$		$n = 3$				%		
	mean	Sd	mean	Sd	mean	Sd			
BSF-1	1.63	0.54	0.52	0.07	0.50	0.01	1.02	62.6	69.26
BSF-2	1.09	0.17	0.76	0.10	0.31	0.00	1.07	97.6	
BSF-3	1.10	0.01	0.19	0.01	0.46	0.01	0.65	59.2	
BSF-4	0.97	0.09	0.21	0.02	0.40	0.01	0.61	62.9	
BSF-5	0.71	0.04	0.09	0.01	0.36	0.00	0.45	64.0	
FIS-1	5.11	2.15	1.61	0.03	2.69	0.07	4.29	84.1	87.42
FIS-2	1.30	0.12	0.17	0.01	1.03	0.05	1.19	91.6	
FIS-3	0.85	0.15	0.11	0.01	0.60	0.03	0.71	82.9	
FIS-4	0.67	0.13	0.08	0.01	0.55	0.02	0.63	94.2	
FIS-5	0.54	0.01	0.09	0.01	0.37	0.01	0.46	84.4	
NNF-1	7.04	1.75	1.75	0.27	4.99	0.02	6.74	95.8	98.99
NNF-2	0.89	0.09	0.16	0.01	0.67	0.04	0.82	91.7	
NNF-3	0.74	0.04	0.15	0.01	0.48	0.01	0.62	84.7	
NNF-4	0.69	0.05	0.27	0.01	0.45	0.00	0.73	105.0	
NNF-5	0.65	0.17	0.22	0.01	0.54	0.01	0.76	117.8	

A.2.8 Metal elements

Samples for heavy metals were treated according to USEPA (1996) in air-dried and sieved (< 2 mm) samples, grounded with a mortar and pestle, and sieved to get a fine powder texture (< 0,15mm). The quantification was performed by inductively coupled plasma optical emission spectrometry (ICP-OES) with Optima DV 4300 (Perkin Elmer, EUA). Table A.15 presents the results of concentration of metal elements: Silica (Si), Manganese (Mn), Magnesium (Mg), Potassium (K), Iron (Fe), Aluminum (Al), Zircon (Zr), Zinc (Zn), Titanium (Ti), Lead (Pb), Nickel (Ni), Molybdenum (Mo), Copper (Cu), Chromium (Cr), Cadmium (Cd) and Bario (Ba).

A.2.9 X-Ray difraction

Mineralogical analysis patterns were carried out with X-ray diffraction by the powder method in air-dried and sieved samples (< 0.053 mm) with a D8 Advance Bruker XRD diffractometer. Qualitative analysis applies Profex and the EVA program by Bruker, and quantitative analysis follows Doebelin & Kleeberg (2015). Table A.16 presents the detailed results of the mineralogical quantities in each layer by area. Figures A.21 to A.35 show the diffractograms of each layer by area.

Table A. 15. Results of the concentration of metal elements: Silica (Si), Manganese (Mn), Magnesium (Mg), Potassium (K), Iron (Fe), Aluminum (Al), Zircon (Zr), Zinc (Zn), Titanium (Ti), Lead (Pb), Nickel (Ni), Molybdenum (Mo), Copper (Cu), Chromium (Cr), Cadmium (Cd) and Bario (Ba).

Land class	Class -Layer	Si	Mn	Mg	K	Fe	Al	Zr	Zn	Ti	Pb	Ni	Mo	Cu	Cr	Cd	Ba
		(mg kg^{-1})															
Bare Soil Fill (BSF)	BSF-1	162.6	341.5	4011.0	5751.5	30495	26230	7.3	148.9	1446.5	58.6	9.0	< 1,0	26.3	21.8	< 0,4	149.2
	BSF-2	188.9	222.9	2235.5	3574.5	33405	27220	6.0	164.2	1221.5	103.4	7.5	< 1,0	29.5	25.3	< 0,4	103.7
	BSF-3	158.3	205.5	947.9	774.9	33405	25710	7.7	72.4	400.1	57.6	6.9	< 1,0	24.5	38.8	< 0,4	52.5
	BSF-4	188.6	245.7	567.2	548.4	31920	21960	6.8	38.9	204.6	29.8	4.2	< 1,0	16.6	36.8	< 0,4	26.2
	BSF-5	64.1	203.8	256.6	220.2	26915	19485	6.5	18.5	111.6	10.2	2.7	< 1,0	12.1	31.5	< 0,4	12.0
	Average	152.5	243.9	1603.6	2173.9	31228.0	24121.0	6.9	88.6	676.8	51.9	6.1		21.8	30.8		68.7
	SD	51.4	57.1	1542.2	2407.1	2697.1	3268.8	0.7	65.2	614.0	35.2	2.6		7.2	7.3		57.0
Dense Ombrophylous Forest in the Initial Stage (FIS)	FIS-1	631.9	100.1	976.2	488.7	28185	27030	8.3	99.4	183.6	63.8	4.8	< 1,0	43.3	24.9	< 0,4	34.2
	FIS-2	279.1	26.6	249.3	188.8	37910	32580	16.5	19.4	91.4	16.3	2.5	< 1,0	9.1	29.9	< 0,4	13.0
	FIS-3	236.3	18.1	127.9	147.4	36830	30735	16.4	10.5	82.6	8.6	2.5	< 1,0	5.7	29.6	< 0,4	6.5
	FIS-4	144.0	14.5	64.8	139.6	39675	26535	12.6	10.2	126.5	11.2	1.8	< 1,0	7.5	26.7	< 0,4	3.9
	FIS-5	1040.5	14.9	65.2	149.9	40640	25070	10.9	9.6	160.6	12.3	1.6	< 1,0	7.6	25.5	< 0,4	3.7
	Average	466.3	34.8	296.7	222.9	36648.0	28390.0	12.9	29.8	128.9	22.4	2.6		14.6	27.3		12.3
	SD	370.4	36.8	387.2	149.8	4958.5	3137.2	3.6	39.1	43.4	23.3	1.3		16.0	2.3		12.8
Non-Native Vegetation Forest (NNF)	NNF-1	452.3	99.6	758.4	405.0	37670	20060	8.5	100.2	136.0	34.3	4.6	< 1,0	29.9	37.8	< 0,4	38.0
	NNF-2	92.3	32.1	164.6	160.5	55835	27710	13.5	15.4	114.8	7.3	2.7	< 1,0	12.5	49.9	< 0,4	4.6
	NNF-3	91.8	29.4	150.9	159.4	55080	27180	13.5	13.7	117.7	7.0	2.6	< 1,0	12.3	49.7	< 0,4	4.1
	NNF-4	121.3	38.8	125.4	160.1	60110	27475	13.2	15.2	168.6	9.4	3.1	< 1,0	15.5	49.8	< 0,4	4.9
	NNF-5	141.4	74.7	127.7	147.3	57485	24620	11.1	15.8	202.6	13.9	3.5	< 1,0	17.7	43.9	< 0,4	10.6
	Average	179.8	54.9	265.4	206.5	53236.0	25409.0	11.9	32.1	147.9	14.4	3.3		17.6	46.2		12.5
	SD	153.7	30.9	276.1	111.1	8912.9	3237.8	2.2	38.1	37.3	11.5	0.8		7.3	5.3		14.5

Table A. 16. Mineralogical phases quantities.

Land class	Depth (m)	Phase Quantity (wt-%)										Total
		Kaolinite	Illite	Mica	Quartz	Feldspar	Óxi-hidróxidos	Sulfatos	Cloritoide	Mulita	Dichromate de potassic	
Bare Soil Fill (BSF)	BSF-1	29.18	18.25	13.46	18.01	21.00	-	-	-	-	-	100
	BSF-2	69.53	-	-	13.05	12.98	2.15	1.99	-	-	-	100
	BSF-3	16.15	-	8.60	23.34	51.41	-	-	-	-	-	100
	BSF-4	67.70	-	-	22.10	5.15	4.35	-	-	-	-	100
	BSF-5	38.73	-	-	41.03	9.65	5.05		4.64	-	-	100
Dense Ombrophylous Forest in the Initial Stage (FIS)	FIS-1	73.45	-	-	14.32	4.22	7.91	-	-	-	-	100
	FIS-2	92.52	-	-	3.54	-	3.20	-	0.44	-	-	100
	FIS-3	92.09	-	-	3.66	-	4.25	-	-	-	-	101
	FIS-4	94.68	-	-	2.89	-	2.44	-	-	-	-	101
	FIS-5	87.81	-	-	1.30	-	10.89	-	-	-	-	101
Non-Native Vegetation Forest (NNF)	NNF-1	86.74	-	-	9.35	-	3.91	-	-	-	-	100
	NNF-2	85.02	-	-	14.98	-	-	-	-	-	-	100
	NNF-3	89.87	-	-	5.77	-	4.36	-	-	-	-	101
	NNF-4	93.07	-	-	3.56	-	1.77	-	-	1.59	-	101
	NNF-5	93.22	-	-	1.72	-	2.05	-	-	-	3.01	101

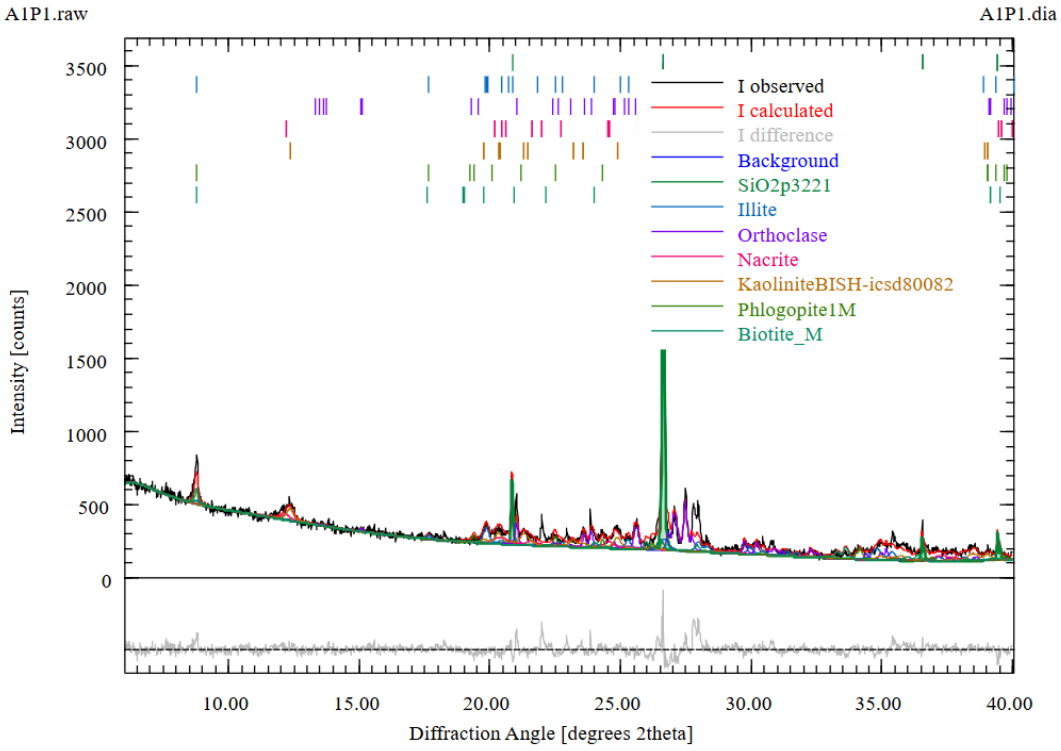

Figure A. 21. DRX pattern of the area BSF, layer 1.

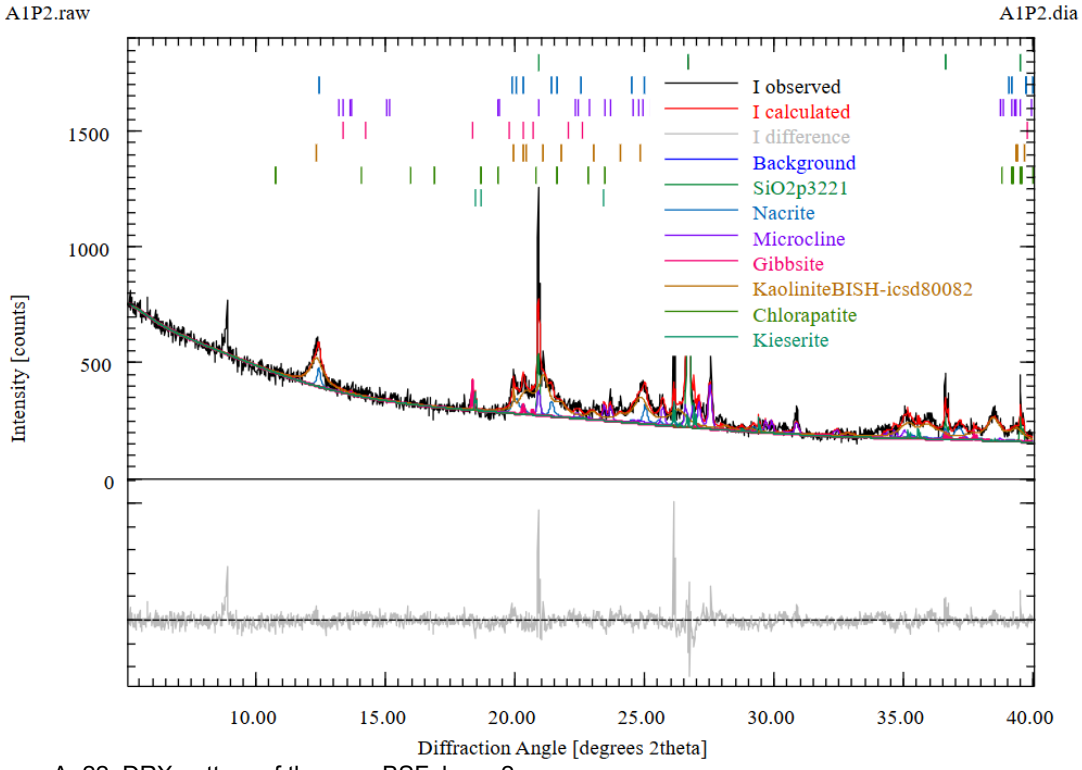

Figure A. 22. DRX pattern of the area BSF, layer 2.

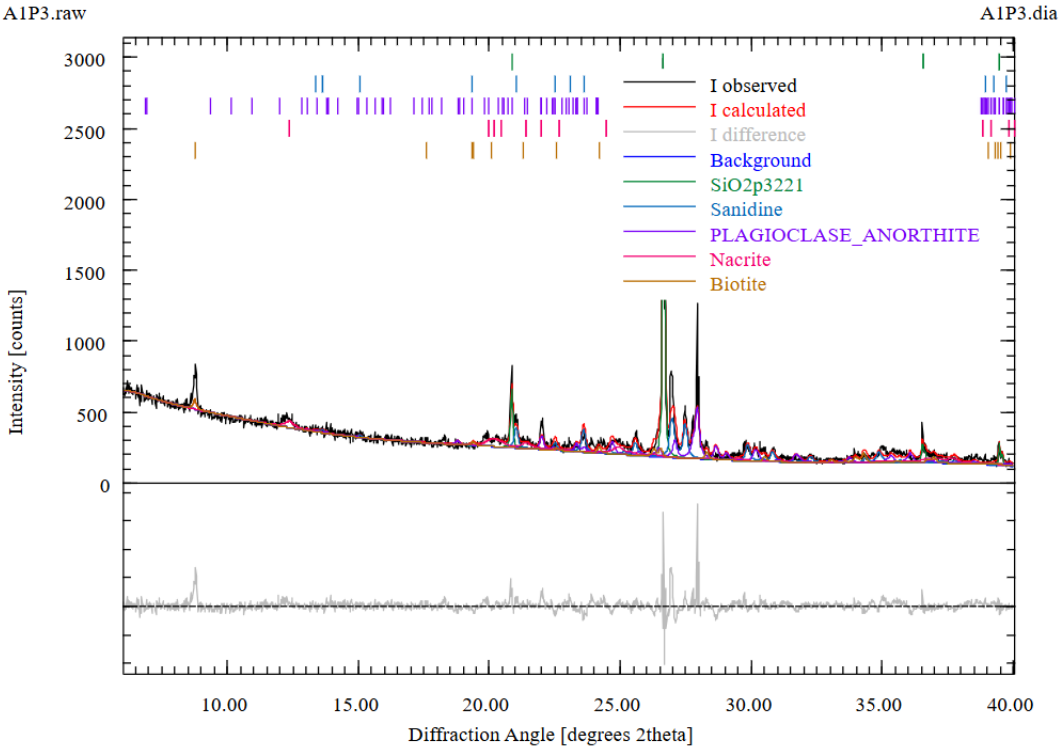

Figure A. 23. DRX pattern of the area BSF, layer 3.

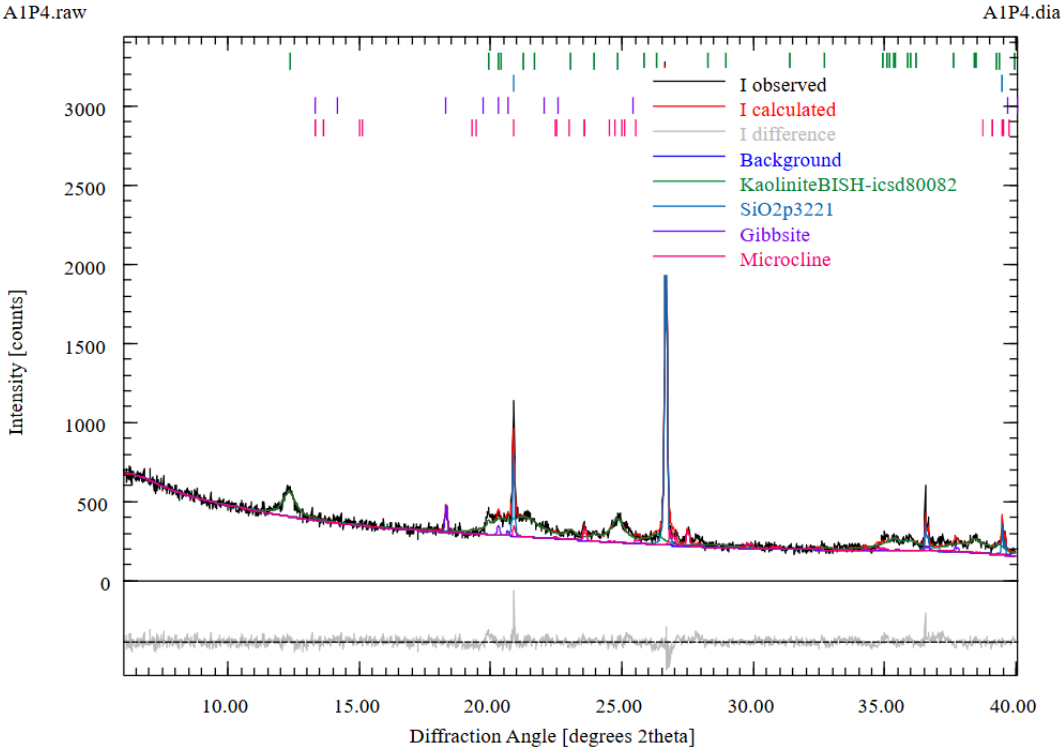

Figure A. 24. DRX pattern of the area BSF, layer 4.

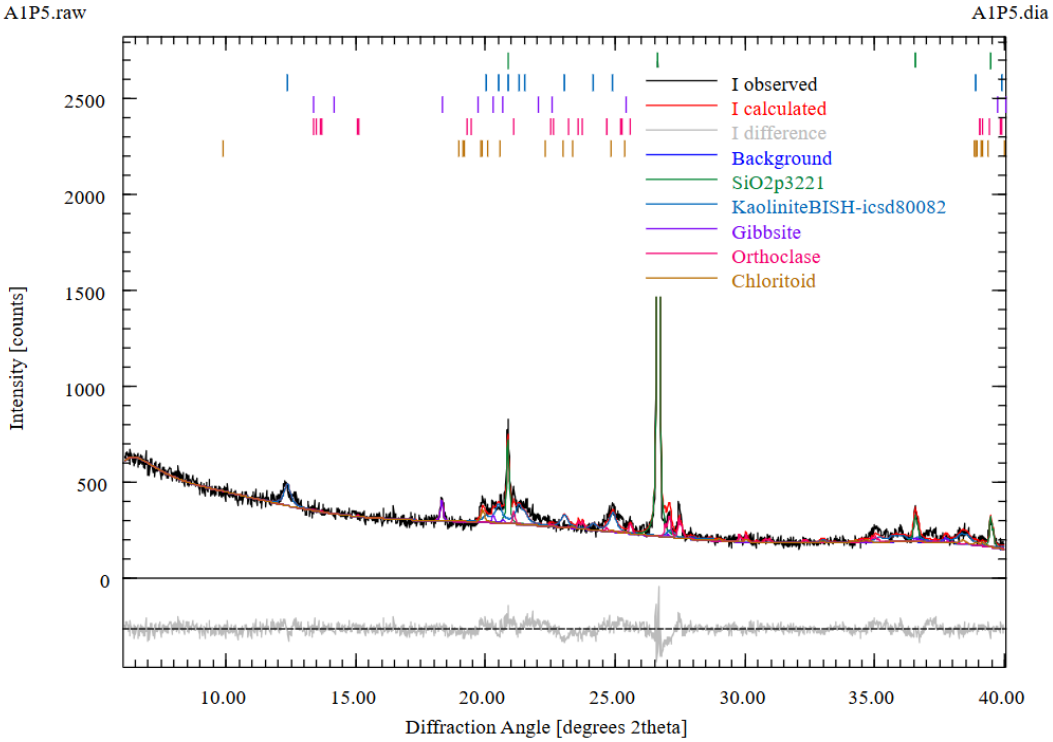

Figure A. 25. DRX pattern of the area BSF, layer 5.

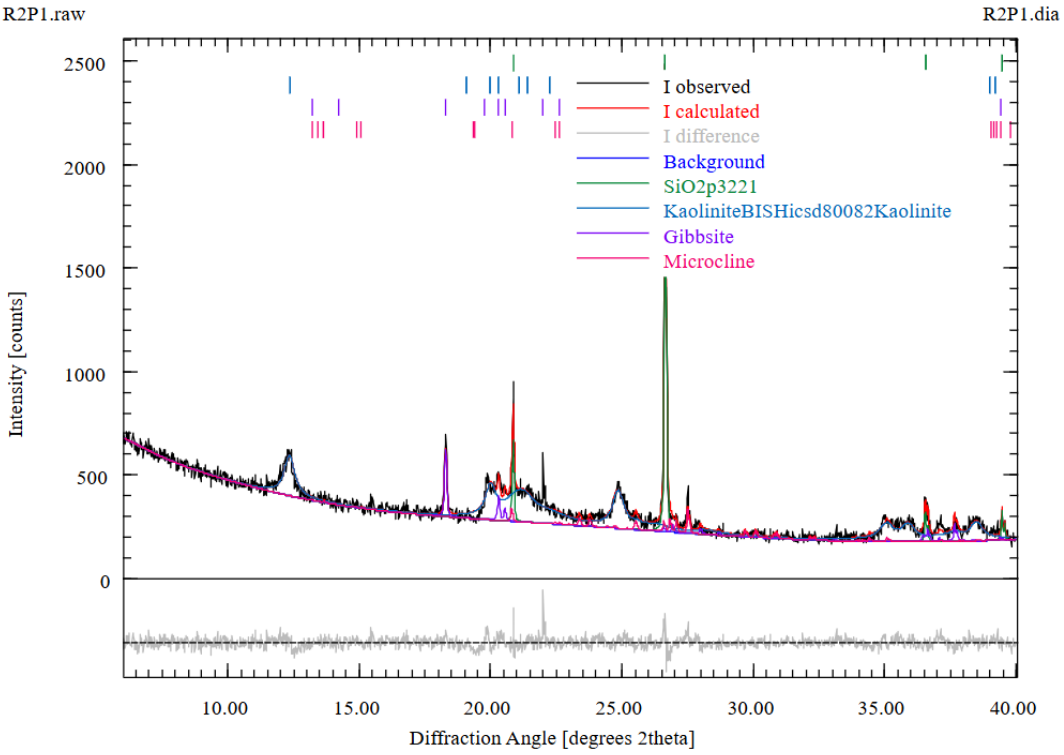

Figure A. 26. DRX pattern of the area FIS, layer 1

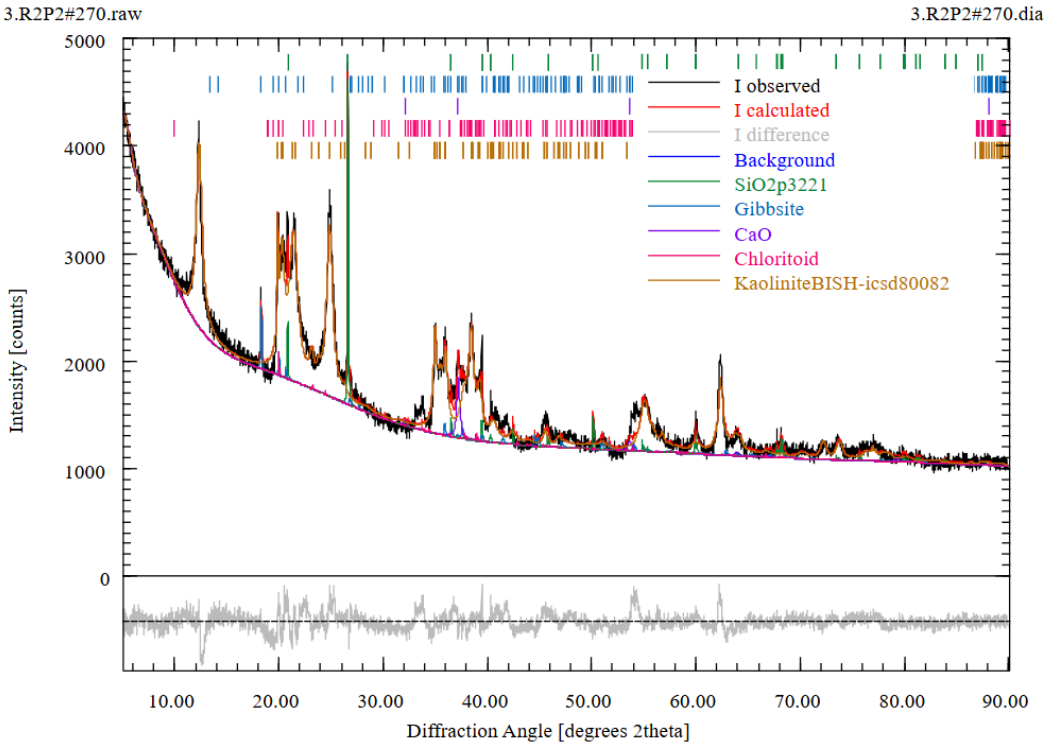

Figure A. 27. DRX pattern of area FIS, layer 2.

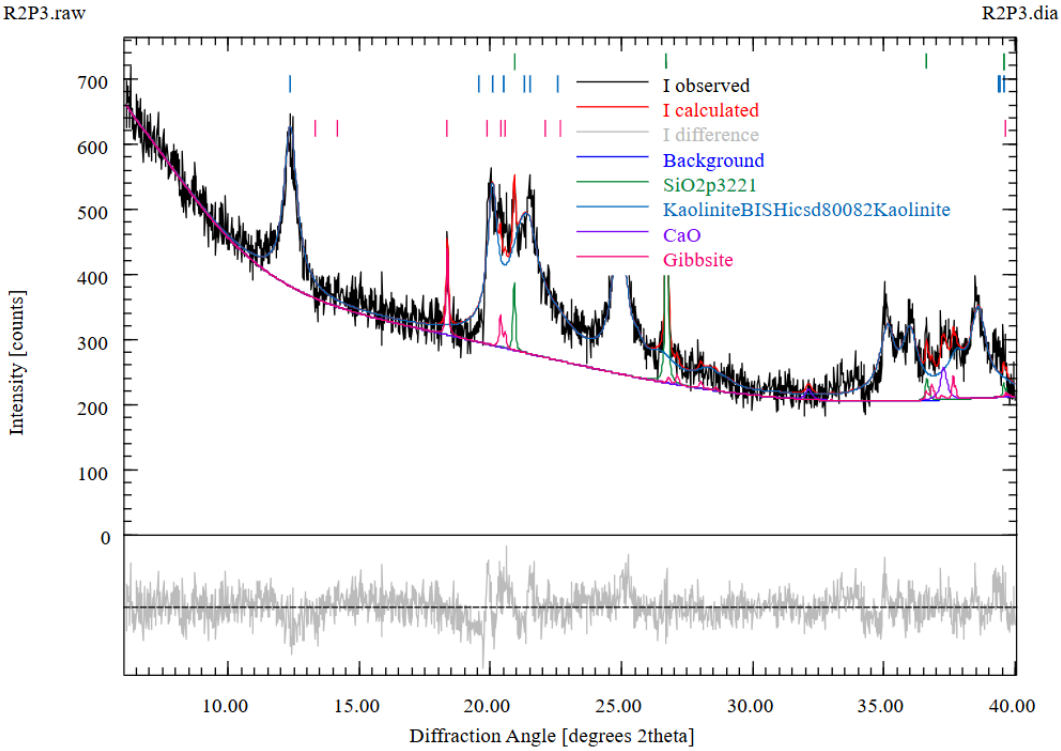

Figure A. 28. DRX pattern of area FIS, layer 3.

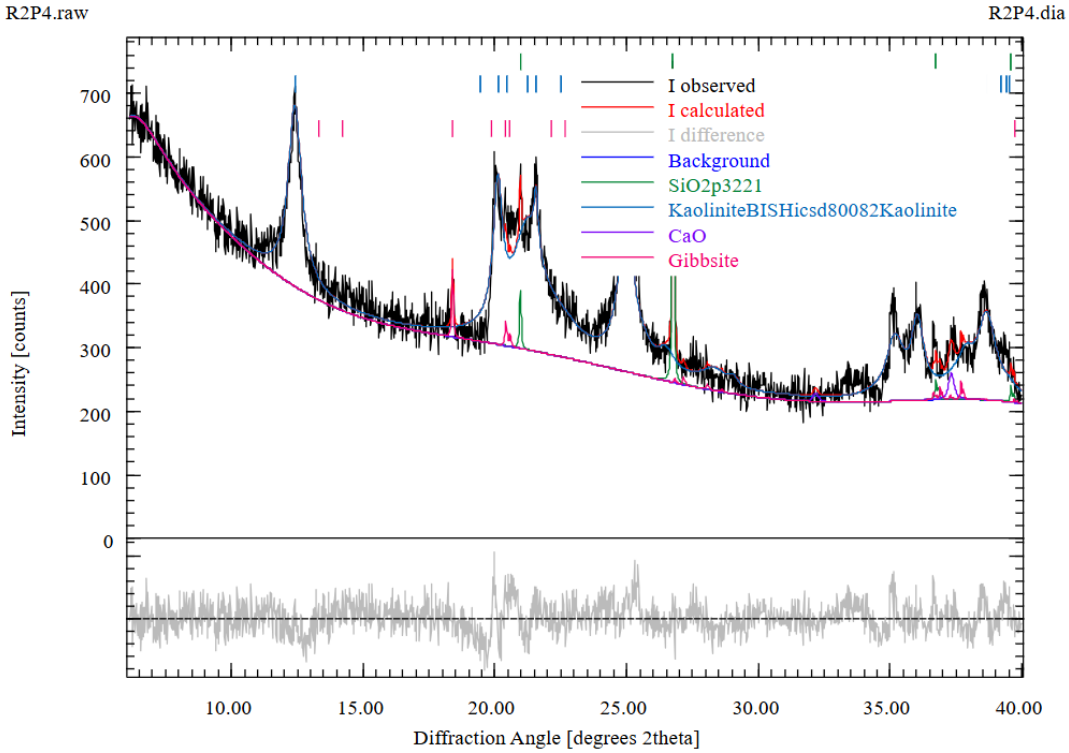

Figure A. 29. DRX pattern of the area FIS, layer 4.

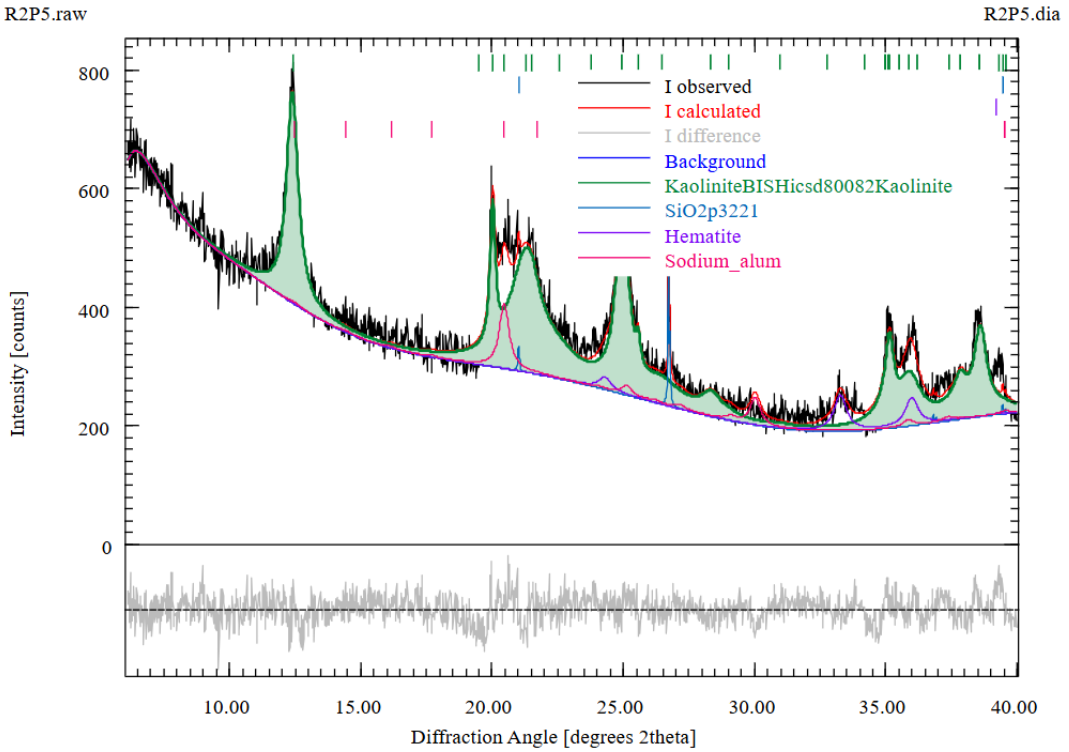

Figure A. 30. DRX pattern of area FIS, layer 5.

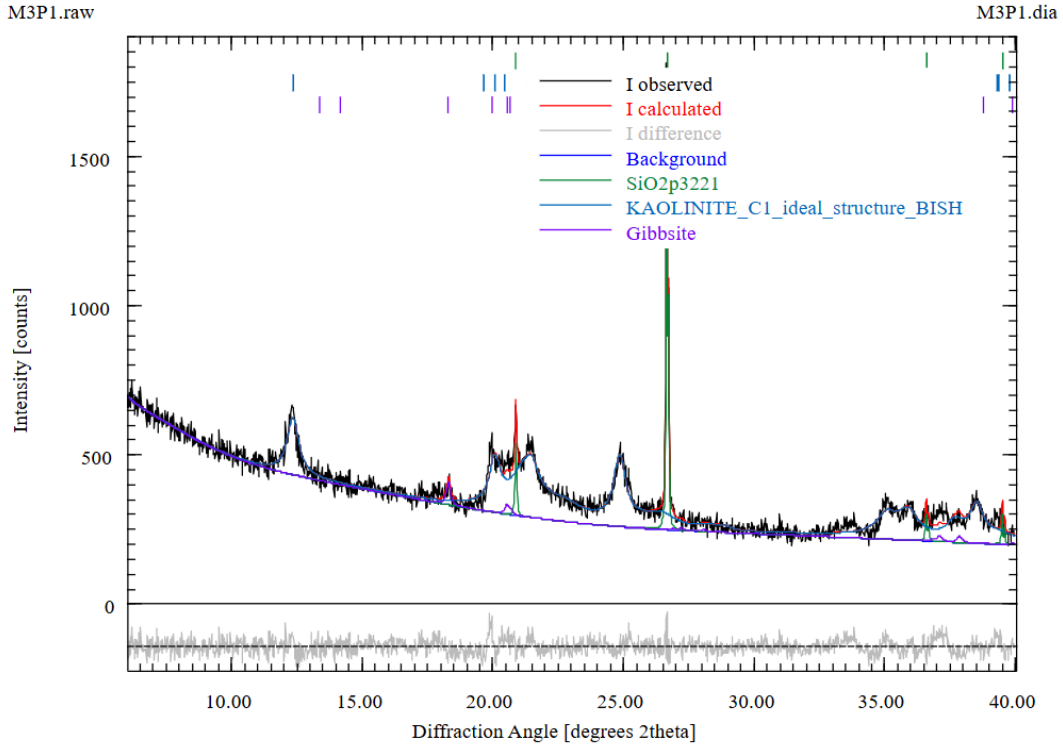

Figure A. 31. DRX pattern of area NNF, layer 1

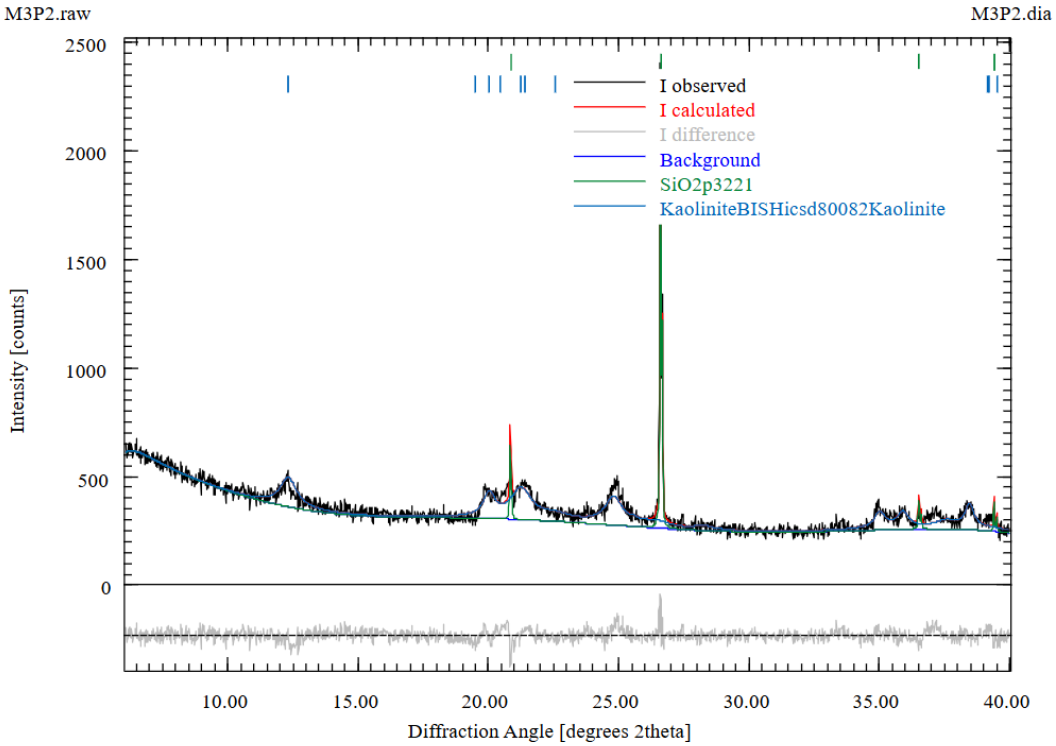

Figure A. 32. DRX pattern of area NNF, layer 2.

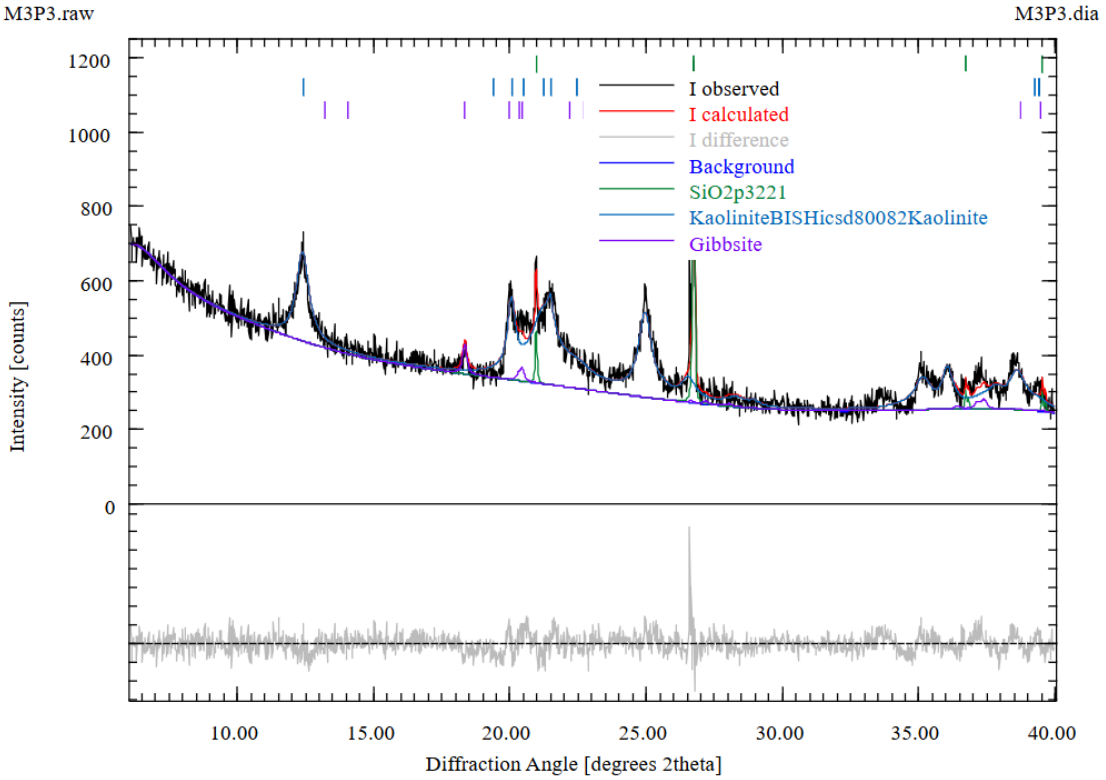

Figure A. 33. DRX pattern of the area NNF, layer 3.

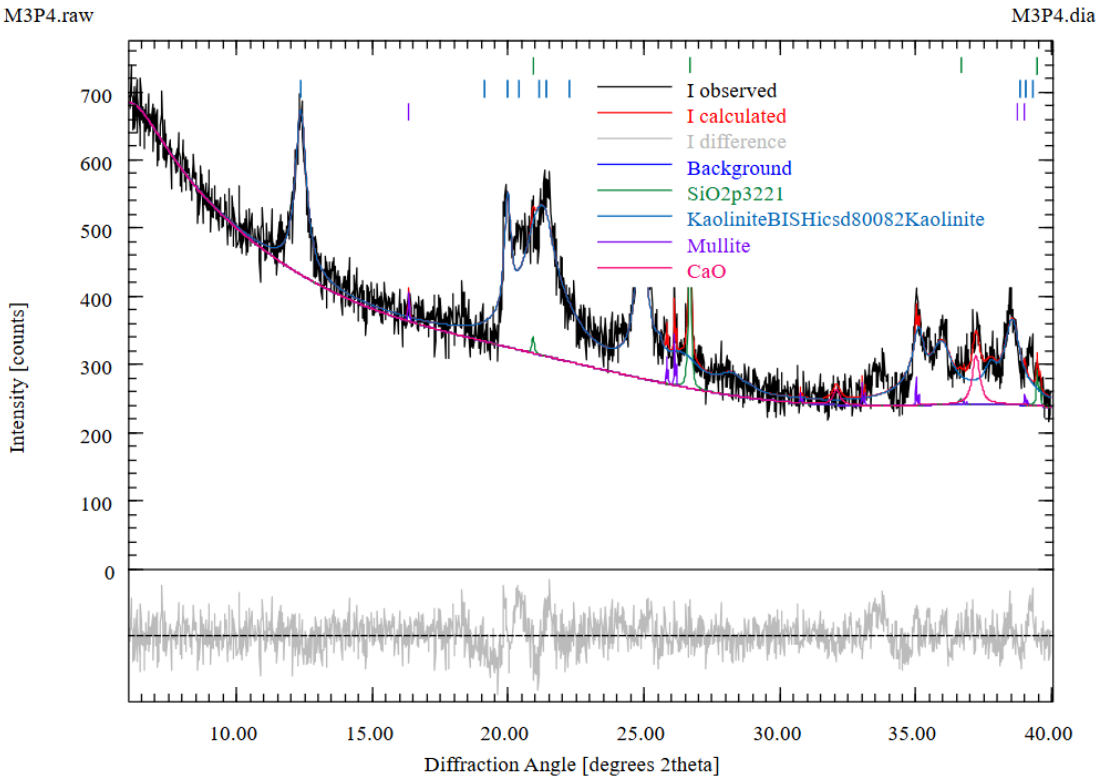

Figure A. 34. DRX pattern of the area NNF, layer 4.

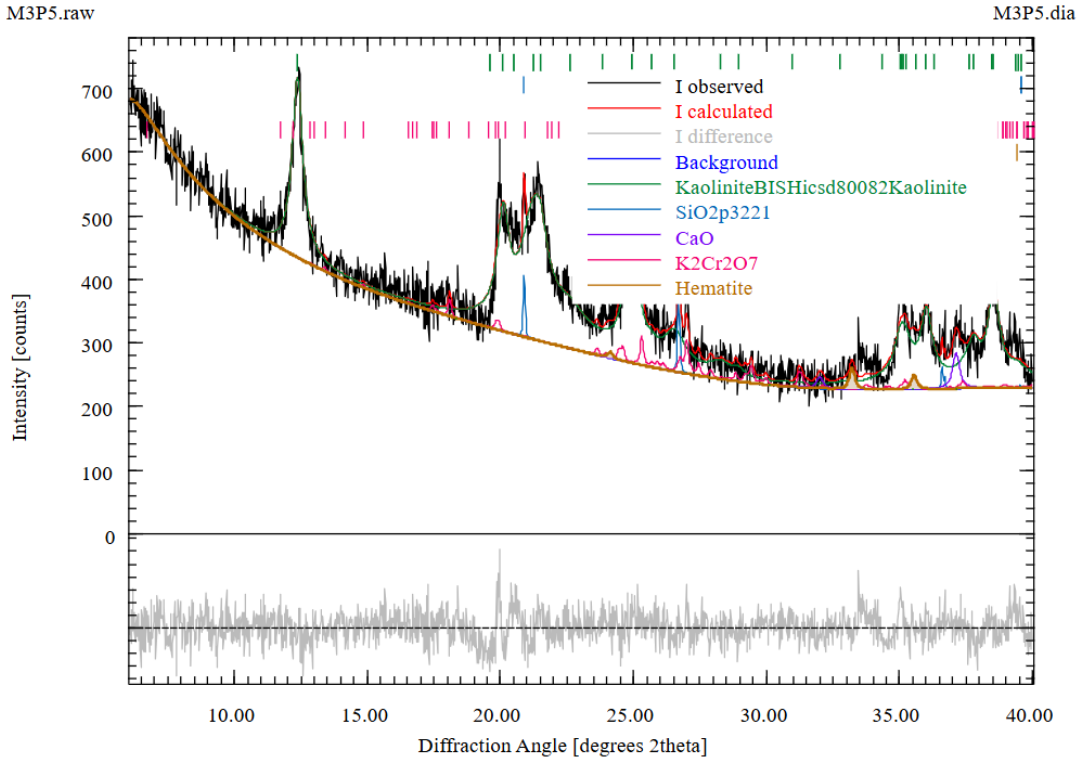

Figure A. 35. DRX pattern of the area NNF, layer 5.

A.2.10 Retention curve

Drying and wetting soil water retention curves (SWRC) were obtained using the filter paper technique, based on ASTM. D5298-16: Standard Test Method for Measurement of Soil Potential (Suction) Using Filter Paper (Withdrawn 2025) (ASTM, 2016a), and also using the dewpoint potentiometer WP4C equipment from the Meter Group, which is based on ASTM. D6836-16: Standard Test Method for Determination of the Soil Water Characteristic Curve for Desorption Using Hanging Column, Pressure Extractor, Chilled Mirror Hygrometer, or Centrifuge. ASTM International, 2016b.ASTM, 2016b). Curves were attained for soil materials of five layer-groups (BSF 2-5, FIS 1, FIS 2-5, NNF 1, and NNF 2-5). Drying and wetting pathways were performed with distinct specimens.

In the drying path of the filter paper technique, undisturbed specimens were initially saturated by capillarity and subsequently air-dried until a required total mass, corresponding to a desired moisture content. In the wetting path, undisturbed specimens were initially air-dried until constant mass and subsequently carefully moistened by dropping water until reaching the required total mass (Figure A.36).

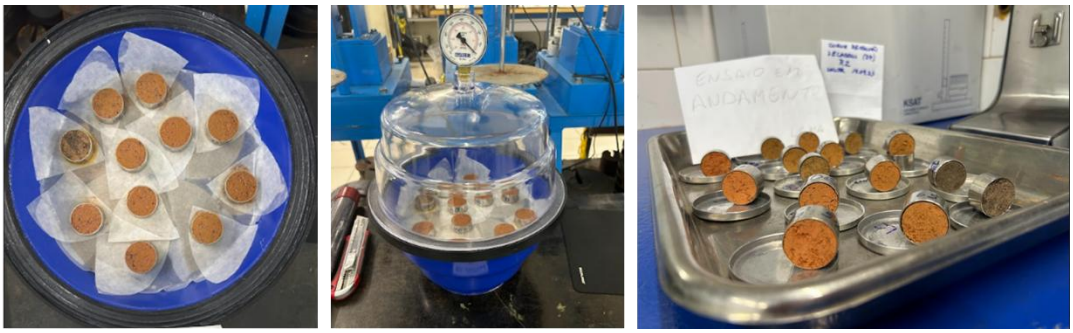

Figure A. 36. Retention curve laboratory test – Wet and Dry pathways.

For both paths, the Whatman n° 42 filter paper was placed in direct contact with the soil. The specimens were placed in sealed, airtight, containers and kept at a constant temperature for a minimum of seven days to reach equilibrium (Figure A.37). Subsequently, the mass of filter paper was determined, and the suction of the specimen was obtained through the calibration suction-water content curve proposed by Chandler and Gutierrez (1986).

Figure A. 37. Filter paper procedure.

Air-dried or forced-dried samples were used to measure the soil water potential using the instrument WP4C. The water-retention curve was fitted using the Van Genuchten (VG) model (Van Genuchten, 1980). Figure A.38 presents the water retention curves, and Table A.17 shows the Van Genuchten parameters.

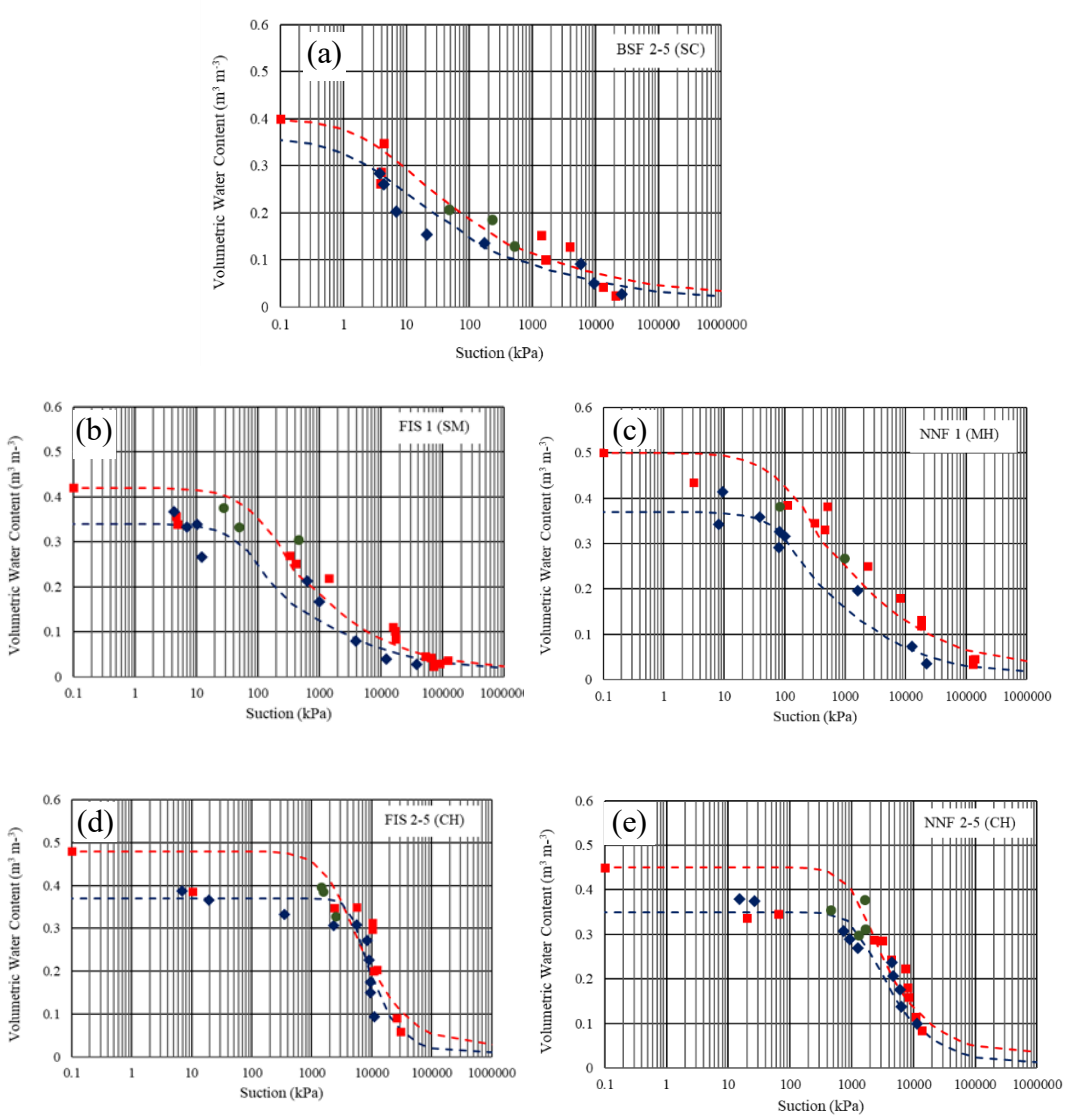

Figure A. 38. Soil water retention curves for the five-layer group materials

Table A. 17. Van Genuchten parameters

Layer-group	Θ_b (%)	Θ_{res} (%)	ψ_b (kPa)	ψ_{res} (kPa)	n
BSF 2-5	40.0	14.0	0.9	300	1.0
FIS 1	42.0	9.0	35.0	6000	1.4
NNF 1	50.0	10.5	30.0	9000	1.2
FIS 2-5	48.0	7.0	1050.0	30000	2.0
NNF 2-5	45.0	5.5	600.0	18500	3.0

A.2.11 Carbon stocks quantification

Soil organic carbon stock was calculated in each 20 cm soil layer for the total soil and the SOM fractions, applying the following equation proposed by Poeplau et al. (2017) and FAO (2019).

$$Cstock_i(kg\ C\ m^{-2}) = OC_{fine\ earth_i}\ x\ \rho_{dfine\ earth_i}\ x\ depth_i$$

where $Cstock_i$ is the SOC stock in the investigated soil layer (i); $OC_{fines\ earth_i}$ is the soil organic carbon content in the fine earth (< 2 mm) in the layer (g kg^{-1}), $depth_i$ is the thickness of the respective layer (m) and $\rho_{dfines\ earth_i}$ is the dry density of the fine soil fraction, given by Equation A.1.

$$\rho_{dfines\ earth_i}\ (g\ cm^{-3}) = \frac{mass_{fine\ earth\ soil}}{volume_{sample}} \quad \text{(Eq. A.1)}$$

For each soil layer, the mass of fine earth soil was obtained by the product of the total dry mass by the percentage of fine earth soil mass with less than 2 mm (obtained from the respective particle size distribution curve) as presented in Table A.8.

The *Cstock* equation was also applied to determine the SOC stock for the POM fraction (*PCstock*) and the MAOM fraction (*Mcstock*). In this case, for each soil layer, the mass of the soil fraction (POM or MAOM) was obtained by the product of the mass of fine earth soil by the percentage of soil mass for POM range and for MAOM range (Table A.5) Additionally, OC content for POM (POC) and MAOM (MOC) was obtained by the OC content in the POM fraction (POC_i) and the MAOM fraction (MOC_i). POC and MOC contents were computed considering the percentage in mass of the respective grain size range - POM (2 mm < ϕ > 0.053 mm) and MAOM (ϕ < 0.053 mm) Then, equation was also applied to determine the SOC stock for the POM fraction (*PCstock*) and the MAOM fraction (*MCstock*).

Table A.18 presents the resultos of *Cstock*, *PCstock* and *MCstock*.

Table A. 18. Quantification of the SOC stock in the total soil fraction (Cstock), in the POM fraction (PCstock) and in the MAOM fraction (MCstock).

Class -Layer	$Depth_i$	ρ_{dfines}	OC_{fines}	Cstock	POC	PCstock	MOC	MCstock
	m	g cm^{-3}	g kg^{-1}	kgC m^{-2}	g kg^{-1}	kg m^{-2}	g kg^{-1}	kgC m^{-2}
BSF-1	0.2	0.94	16.28	3.05	5.17	0.97	5.02	0.94
BSF-2	0.2	1.46	10.92	3.19	7.60	2.22	3.05	0.89
BSF-3	0.2	1.36	11.01	2.99	1.93	0.52	4.59	1.25
BSF-4	0.2	1.44	9.72	2.79	2.09	0.60	4.03	1.16
BSF-5	0.2	1.61	7.05	2.27	0.90	0.29	3.61	1.16
Total	-	-	54.98	14.29	17.69	4.60	20.31	5.40
FIS-1	0.2	1.35	51.06	13.83	16.06	4.35	26.86	7.28
FIS-2	0.2	1.37	13.01	3.58	1.65	0.45	10.26	2.82
FIS-3	0.2	1.41	8.55	2.42	1.07	0.30	6.01	1.70
FIS-4	0.2	1.37	6.65	1.82	0.81	0.22	5.46	1.49
FIS-5	0.2	1.31	5.42	1.42	0.87	0.23	3.71	0.97
Total	-	-	84.69	23.07	20.46	5.56	52.29	14.26
NNF-1	0.2	1.02	70.40	14.30	17.52	3.56	49.91	10.14
NNF-2	0.2	1.45	8.94	2.60	1.55	0.45	6.65	1.93
NNF-3	0.2	1.48	7.37	2.18	1.48	0.44	4.76	1.41
NNF-4	0.2	1.38	6.94	1.91	2.74	0.76	4.55	1.25
NNF-5	0.2	1.42	6.48	1.84	2.20	0.62	5.44	1.54
Total	-	-	100.13	22.83	25.48	5.82	71.30	16.27